Study the Molecular Basis of Interaction of Heat Shock Factor 1 with its Activator Azadiradione

THESIS SUBMITTED FOR THE DEGREE OF DOCTOR OF PHILOSOPHY IN SCIENCE

BY

ANIRBAN MANNA

Index no. 215/18/Life Sc./26

DEPARTMENT OF LIFE SCIENCE AND BIOTECHNOLOGY

JADAVPUR UNIVERSITY

2024

CERTIFICATE FROM THE SUPERVISOR(S)

This is to certify that the thesis entitled **"Study the Molecular Basis of Interaction of Heat Shock Factor 1 with its Activator Azadiradione"** Submitted by Sri **Anirban Manna** who got his name registered on **26.09.2018** for the award of Ph. D. (Science) degree of Jadavpur University, is absolutely based upon his own work under my supervision and that neither this thesis nor any part of it has been submitted for either any degree / diploma or any other academic award anywhere before.

30.4.24

Mahadeb Pal, Ph.D.
Professor
Division of Molecular Medicine
BOSE INSTITUTE
P-1/12, C.I.T. SCHEME VIIM
Kolkata-700 054, India

[Signature of the Supervisor(s) date with official seal]

This work is dedicated to my parents.

Contents

Acknowledgements

Pursuing a Ph.D. and being actively involved in scientific research was a dream I had nurtured since my M.Sc. days. Despite discouragement from some of my peers and certain family members, I stuck to the belief that I could do independent research and contribute to the betterment of society. Mainly because of the encouragement received from my mother, my conviction won over self-doubt, criticism, and occasional ridicule.

The year 2015 was indeed a turning point in my career. I managed to qualify for the JNU entrance examination and interview (on the first attempt) and got admitted as a Ph.D. scholar in the Special Centre for Molecular Medicine (SCMM), JNU, New Delhi; something which I had little expected. I was fortunate enough to gain the opportunity to work under the supervision of Prof. Chinmay Kumar Mukhopadhyay, a person who will forever occupy a special place in my heart. Unfortunately, I could not continue working in his lab for long and had to return to my hometown due to family issues. But I shall forever be grateful to him for accepting me as his Ph.D. student and cherish my time in his lab. Our enriching discussions undoubtedly helped me understand research better. Like a true teacher, he had keenly observed me during my tenure in his lab, understood the problems that I faced, and provided necessary solutions. He arranged for my Ph.D. under the supervision of his friend Prof. Mahadeb Pal in Bose Institute, Kolkata, enabling a seamless transition to a new lab.

It would not be out of place to mention the names of some dear friends I made in JNU. Santosh, the best hostel roommate one could ever have, and his brother (whose name is also Santosh!) were there with me through thick and thin. Our common friend Amita, who has risen from a very humble background and is currently a business owner post-Ph.D., should be an inspiration for all. I was extremely fortunate to have supportive friends like Imran, Anupam, Keshav, Tarkeshwar, Pragya, Shashi, Zille, and Maitrayee in my department. I also acknowledge the help of my JNU lab seniors. I cannot thank you guys enough.

My time with Prof. Mahadeb Pal started in October 2016, to whom I must express my sincerest gratitude. The patience he showed while training me in his lab and his guidance has significantly contributed to my growth as a researcher. He was, and is, always available for my needs, scientific or otherwise. His being hard on me sometimes, as I later realized, was to ensure my betterment as a researcher and a human being. He has, without any doubt, contributed enormously to helping me achieve my dream of a Ph.D.

I wish to thank the Department of Biotechnology (DBT), Govt. of India, for supporting me financially with Junior and Senior Research Fellowships. I take this opportunity to thank Prof. Uday Bandyopadhyay, the present director of our institute, as well as the previous directors Prof. Siddhartha Roy, Prof. Pinak Chakrabarti, and Prof. Sujoy K. Dasgupta, for providing the necessary facilities to conduct my research. I would also like to thank Prof. Anup Kumar Mishra, Dr. Kuladip Jana, Prof. Atin Kumar Mandal, Prof. Tanya Das, Prof. Gaurishankar Sa, Prof. Parames C. Sil, Prof. Tapan Kumar Dutta, Prof. Kaushik Biswas, Prof. Jayanta Mukhopadhyay, Prof. Pallob Kundu, Prof. Ajit Bikram Dutta, Prof. Pinak Chakrabarti, Prof. Gautam Basu, and Dr. Smarajit Polley for allowing me access to the instruments in their respective labs whenever I was in need. Prof. Subrata Sau, my co-supervisor at Bose Institute, has helped me with official matters.

I am indebted to Prof. Gopal Chakrabarti (Dept. of Biotechnology, University of Calcutta) for agreeing to be a member of my Research Advisory Committee (RAC), evaluating my research progress from time to time, and providing valuable suggestions whenever necessary. He also allowed me access to the instruments in his lab for my research.

As my research involved extensive use of the instruments in our Central Instrumentation Facility (CIF), I must express my sincere gratitude to the staff members of the Bose Institute CIF. I am especially grateful to Mr. Dipak Konar, Mr. Swaroop Biswas, Mr. Smriti Ranjan Maji, Mr. Mrinal Das, Mr. Tanmoy Debnath, Mr. Ranjan Kumar Dutta, and Mr. Pallab Chakrabarti for facilitating my work. Prof. Jayanta Mukhopadhyay, the present chairperson of the CIF, and Prof. Sujoy K. Dasgupta, the previous chairperson, have also helped me immensely during my work in the CIF.

Narayan da and Gazi da (Dept. of Microbiology), and Subhash da and Roma di (Dept. of Biochemistry) have also extended a helping hand whenever I needed them. I cannot thank Pradip da and Somnath da (Division of Molecular Medicine) enough for their help in procuring lab consumables and in other office-related matters.

This work would not have been possible without the sincere efforts of Dr. Papri Basak, my senior in the lab. I shall forever be grateful to my guide for involving her in my research project. From standardizing experimental protocols to acquiring and analyzing data and preparing manuscripts, she put in her best efforts for my all-round improvement, besides running a project of her own. Most importantly, she taught me to be self-reliant. I shall never forget her support for my work during the pandemic.

I also thank my other lab seniors, Dr. Vinod K. Nelson, Dr. Asif Ali, Dr. Soumyadip Paul, Dr. Suvranil Ghosh, Dr. Naibedya Dutta, and Dr. Ayan Mondal. Dr. Nelson and Dr. Ali were with me during the initial phase of my work. Of my juniors, Chirantan was with me through thick and thin. I shall never forget our endless tea sessions, scientific (and non-scientific) discussions, and occasional trips to various places in Kolkata from the lab. Hossainoor (the junior most in our lab, whom I teased a lot) and Samhita also deserve mention.

I would also like to acknowledge the help I have received from friends working in other labs at Bose Institute. I received immense support from Satyajit, without whose help I could not have completed my work. Help from Sharmistha, Somesh, Dhiman, Upama, Madhuparna, Debanjana, Alapan, Swarnali, Samrat, Byapti, Troyee, Abhishek, Ellora, Sounak, Subho, Anik, Rahul, Suman, Megha, Rinita, Sourio, Udit, Nilanjana, Madhurima, Mousumi, Manish, Sonal, Ananya, Himadri, Srabani, Shreya, Rohit, Monami, Durba, Sauryadeep, Soham and Tushar also deserve mention. I highly appreciate the help received from seniors in various labs of our institute: Bankim da, Bhavna di, Bijoya di, Dwijit da, Barun da, Ananya di, Nilanjan da, Sharmistha di, Sayantani di, Pritam da, Sumit da, Sarita di, Sayani di, Rishila di, Nibedita di and Poulomi di.

No words are sufficient to describe the contributions of my father and mother, who have sacrificed immensely for their only child all these years. Without their unswerving support, patience, and encouragement, I could never have come this far. I have received endless love and support from many other members of my family as well, especially my paternal aunt, uncle, and cousin.

By the grace of the Almighty, this incredible journey called ‘Ph.D.’ is finally on the verge of conclusion. The person writing this thesis has come a long way from being the shy, introverted boy who had stepped into the world of scientific research all these years ago. I do not wish to end my scientific journey here, however. I firmly believe that, with the experiences gained during my Ph.D., I shall be able to learn more sophisticated techniques, explore uncharted areas of biomedical sciences, and contribute to the betterment of the world in my humble way. As the saying goes, every end is just another beginning.

Anirban Manna

List of Abbreviations

°C	Degree Celsius
µl	Microlitre
µM	Micromolar
AKT	Protein Kinase B
ANOVA	Analysis of Variance
AZD	Azadiradione
ALS	Amyotrophic Lateral Sclerosis
AMP	Adenosine Monophosphate
ATP	Adenosine Triphosphate
BTZ	Bortezomib
DBD	DNA Binding Domain
DEPT	Distortionless Enhancement by Polarization Transfer
DMSO	Dimethyl Sulfoxide
DTT	Dithiothreitol
DTHIB	Direct Targeted HSF1 InhiBitor
DLS	Dynamic Light Scattering
EDTA	Ethylenediaminetetraacetic Acid
FPA	Fluorescence Polarization Assay
HD	Huntington's Disease
HEPES	N-2-hydroxyethylpiperazine-N'-2-ethanesulfonic acid
HPLC	High-Performance Liquid Chromatography
HSE	Heat Shock Element

HSF1	Heat Shock Factor 1
HSP90	Heat Shock Protein 90
HSR	Heat Shock Response
IPTG	Isopropyl β- D-1-thiogalactopyranoside
ITC	Isothermal Titration Calorimetry
kDa	kilodalton
KRIBB11	N2 - (1H-indazole-5-yl)-N6 -methyl-3-nitropyridine-2,6-diamine
LDH	Lactate Dehydrogenase
MEF	Mouse Embryonic Fibroblasts
mM	millimolar
NAD^+	Nicotinamide Adenine Dinucleotide
NTA	Nitrilotriacetic Acid
NMR	Nuclear Magnetic Resonance
nm	nanometre
nM	nanomolar
PD	Parkinson's Disease
PMSF	Phenylmethylsulfonyl Fluoride
ROS	Reactive Oxygen Species
RPM	Revolutions per Minute
SDS-PAGE	Sodium Dodecyl Sulfate Polyacrylamide Gel Electrophoresis
SOD	Superoxide Dismutase
TLC	Thin Layer Chromatography
VEGF-A	Vascular Endothelial Growth Factor A

List of Figures

CHAPTER 1

INTRODUCTION

Proteins must adopt a well-defined three-dimensional structure to perform their assigned functions precisely. These specific structures of proteins are often stabilized by weak chemical interactions such as hydrogen bonding and van der Waals interactions, which are supersensitive to the exposure of cells to altered oxidative or other stressful conditions in the intra- or extracellular environments. Therefore, proteins exposed to stressful environments are sensitive to protein misfolding, leading to the formation of soluble/ insoluble toxic protein aggregates.

To keep this in check, a class of proteins known as molecular chaperones assists in the correct folding of cellular proteins involving non-covalent interactions within the polypeptide chain of a protein. Chaperones, however, are not part of the protein's final structure (Hartl et. al.2011). They prevent protein misfolding/aggregation and facilitate the clearance of misfolded or excess proteins from the intracellular environment by inducing proteasomal and autophagic pathways **(**Hartl et. al.2002). Cells are exposed to stressful conditions, both environmental and intrinsic, that disturb the homeostasis of their proteome; which necessitates an increased supply of chaperones through the induction of a stress response pathway termed heat shock response (HSR).

Heat Shock Response

Heat Shock Response (HSR), a transcriptional program, is orchestrated when a cell is exposed to stress (such as an elevated temperature). The major regulator of HSR is a ~57 kDa protein termed heat shock factor 1 (HSF1). HSF1, evolutionarily conserved from yeast to mammals, plays a major role in maintaining protein homeostasis by keeping proteotoxic stress in check. Other stress-responsive transcription factors may also participate in the HSR, however (Whitesell et. al. 2009, Mahat et. al.2016, Solis et. al.2016). HSF1 specifically keeps the cell's protein homeostasis status under surveillance, and an increase in levels of misfolded proteins in the cell causes its activation. A wide variety of stressful conditions lead to cellular protein misfolding and thus cause activation of HSF1 (Mahat et. al.2016, Solis et. al.2016, Ananthan et. al.1986) (Fig. 1.1). Upon activation, HSF1 binds with the Heat Shock Elements (HSEs) present in the promoters of its target genes (Sorger et. al.1987, Xiao et. al.1988). These target genes include (but are not limited to) general chaperones, inducible Heat Shock Protein (Hsp) -70 and -90. Elevation of the levels of cytosolic Hsp70 and Hsp90, in turn, negatively regulates HSF1 activity (Akerfelt et. al.2010). Thus, the HSF1 activation-deactivation cycle consists of a negative feedback loop. HSF1 activation increases the concentration of cellular chaperones

that take care of proteotoxic stress; these chaperones also in turn participate in the deactivation of HSF1, thereby attenuating the HSR (Satyal and Morimoto 1998).

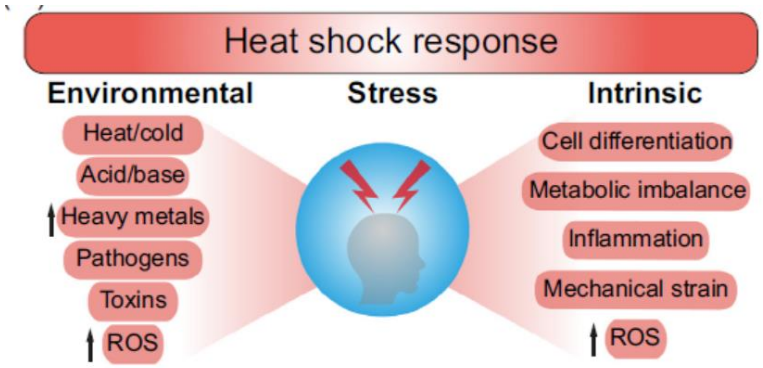

Figure 1.1: Conditions that can activate the Heat Shock Response (adapted from Kmiecik et. al. 2021)

Heat Shock Factor 1 carries distinct functional domains:

Human HSF1, a 529 amino acid long protein, consists of multiple functional domains as follows (Fig. 1.2):

1. **DNA Binding Domain (DBD):** Trimeric/ oligomeric HSF1 interacts with its cognate HSE through this domain at the N-terminus (amino acid range 1-123). It is highly conserved among heat shock factors and the only domain whose structure has been elucidated. It is a member of the winged helix-turn-helix family (Jaeger et. al.2014, Neudegger et. al.2016).
2. **Trimerization/ Oligomerization Domain:** This domain, located C-terminal to the DBD, contains three α-helical leucine zippers (LZ1-3) [amino acid range 130-203]. It is also known as Heptad Repeat (HR)-A & -B (HR-A/B). This domain is involved in trimer/ oligomer formation via hydrophobic contacts with trimerization domains from other monomers, thus giving rise to a triple-stranded coiled-coil structure (Gomez-Pastor et. al.2018, Masser et. al.2020).
3. **Regulatory Domain (RD):** Located C-terminal to the trimerization domain, RD is rich in serine and threonine residues in all eukaryotes (amino acid range 204-383). These residues undergo phosphorylation and participate in the regulation of the protein's activity (Gomez-Pastor et. al.2018, Masser et. al.2020).

4. **Leucine Zipper 4 (LZ4) domain:** Also known as HR-C, this fourth LZ domain is C-terminal to RD (amino acid range 384-409). In unstressed conditions, it interacts with LZ1-3 (intramolecular interaction) and prevents the trimerization/ oligomerization of HSF1 (Gomez-Pastor et. al.2018, Masser et. al.2020).
5. **Transactivation Domain (TAD):** The C-terminal TAD (amino acid range 410-529) consists of two subdomains: AD1 and AD2. While AD1 has an α-helical structure, AD2 carries a high percentage of helix breaker glycine and proline residues and thus remains unstructured (Gomez-Pastor et. al.2018, Masser et. al.2020).

Cells Express Different Heat Shock Factors:

The human genome encodes 6 HSFs: HSF1, HSF2, HSF4, HSF5, HSFX and HSFY. The first three members possess the amino-terminal winged helix-turn-helix DBD and the oligomerization domain. The domain organizations and functions of the other isoforms remain elusive (Gomez-Pastor et. al.2018; Akerfelt et. al.2010). HSF2 is involved in early development. It is expressed abundantly in the testis. HSF4 plays a key role in the development of the eye lens and helps to maintain it (Gomez-Pastor et. al.2018; Akerfelt et. al.2010; Anckar et. al.2011).

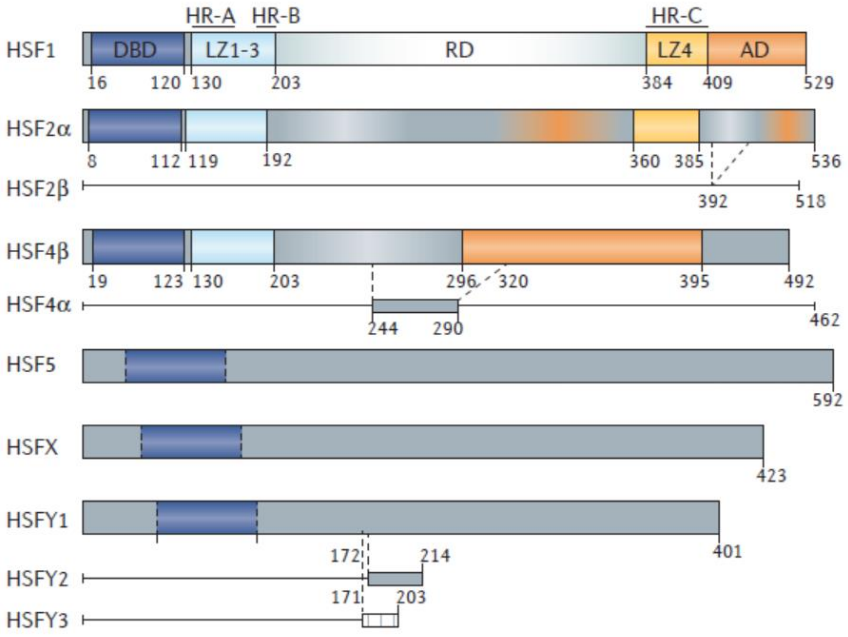

Figure 1.2: Domain organization of different HSF isoforms (adapted from Gomez-Pastor et. al.2018)

The DNA-binding domain (DBD) of HSF1:

Both the crystal structure of *K. lactis* (yeast) HSF DBD-DNA complex and the NMR structure of *Drosophila* HSF DBD showed the presence of a winged helix-turn-helix structural motif comprising of 3 α-helices and a 4-stranded β-sheet. In the *K. lactis* DBD structure, the nature of the flexible loop of the wing domain and the C-terminal helix remained unresolved.

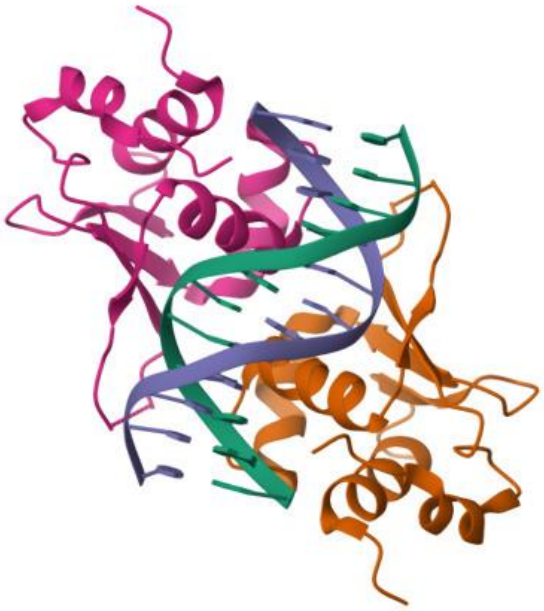

Figure 1.3: Crystal structure of human HSF1-DBD with HSE-DNA (PDB: 5D5U). The two HSF1-DBD chains are shown in red and brown. The two strands of the double-stranded DNA molecule are shown in green and purple.

Two independent teams solved the crystal structures of human HSF1- and HSF2-DBD in complex with DNA (Neudegger et. al.2016; Jaeger et. al.2016). These human proteins were also shown to be a part of the winged helix-turn-helix DNA binding domain family. The structurally unresolved portions mentioned above were also characterized in these two

studies. In both structures, it was shown that the DBD core sits atop the DNA double helix, while the C-terminal helix points downward to the opposite side of the DNA. This suggests that the trimerization domain embraces the DNA double helix and extends downwards. These structures also show the presence of a large solvent-exposed surface on HSF1-DBD, which could be a potential hub for protein-protein interactions.

The Heat Shock Element (HSE), the HSF1 recognition element on its target gene promoter consists of three inverted pentameric repeats of 5'-nGAAn-3'. It was identified to be the regulatory upstream promoter element of the fruit fly *hsp70* gene (Pelham 1982). The HSF-DBD of fruit fly binds with the 5'-nGAAn-3' motif in a stoichiometric ratio of 1:1. HSF1 in a homotrimeric form binds with the evolutionarily conserved HSE (Akerfelt et. al.2010, Jaeger et. al.2014, Kim et. al.1994). Interestingly, HSF1 and HSF2 can also hetero-oligomerize to attain DNA binding competence (Jaeger et. al.2016, Sandqvist et. al.2009). It is possible that both the type and stoichiometric ratio of the HSF isoforms within the hetero-oligomer could regulate the genomic occupancy of HSF1. As revealed by the crystal structure of the HSF1-DBD-HSE complex, DBD's Arg71 residue interacts with the guanine nucleotide of the 5'-nGAAn-3' repeat of HSE via hydrogen bonding (Gomez-Pastor et. al.2018, Neudegger et. al.2016). This amino acid residue is conserved among the HSFs (Neudegger et. al.2016, Jaeger et. al.2016, Harrison et. al.1994, Vuister et. al.1994). It is essential for the sequence-specific interaction of HSF1 with the HSE (Neudegger et. al.2016, Jaeger et. al.2016). Mutation of Arg71 to Ala severely compromises the DNA binding ability of HSF1 (Inouye et. al.2003, Ostling et. al.2007). Three lysine residues at positions 62, 80, and 118 make important interactions with the negatively charged phosphate backbone of the HSE-containing DNA (Neudegger et. al.2016). Lys80 acetylation is controlled by the histone acetyltransferase GCN5 and p300 along with the histone deacetylase SIRT1; they dictate HSF1-HSE binding and thereby regulate the biological activity of HSF1 (Westerheide et. al.2009, Zelin et. al.2015, Zelin et. al.2012, Raychaudhuri et. al.2014). Purified recombinant HSF1-DBD and HSF2-DBD can bind the same HSE sequence with comparable affinity (Jaeger et. al.2016, Jaeger et. al.2014). However, the genome-wide occupancy of these two proteins is quite different (Jaeger et. al.2016, Akerfelt et. al.2008, Vihervaara et. al.2013). This discrepancy suggests the existence of crucial regulatory mechanisms for the recruitment of HSF1 to specific loci in the genome and the differential regulation of HSF isoforms.

In contrast to the majority of winged helix-turn-helix DBDs, the wing domains of HSF1 and HSF2 DBDs do not directly contact the HSE-containing DNA (Gomez-Pastor et. al.2018).

Although the DNA binding interface of HSF1 is known to be conserved, the wing domain (which is exposed to the solvent) differs among the HSF isoforms and is thereby involved in their differential regulation. A chimeric HSF1 protein bearing the wing domain of HSF2 was expressed in Mouse Embryonic Fibroblast (MEF) cells, where this protein showed faulty binding with promoter HSE and defect in driving heat-induced gene expression only in some of the HSF1 targets. This observation that switching the wing domain of HSF1 (using recombinant DNA technology) caused a defect in the expression of only some of the HSF1 target genes shows that the wing domain is capable of locus-specific regulation of HSF isoforms.

The wing domain was shown to be involved in the differential regulation of the HSF isoforms via direct protein-protein interactions (Fujimoto et. al.2012). The protein complex known as RPA (Replication Protein A) consists of three subunits: RPA-1, -2 and -3. Only the RPA1 subunit interacts specifically with the EQG motif (residue no. 85 to 87) in the wing domain of HSF1-DBD during HSR. This helps recruit HSF1 to the *hsp70* promoter (Fujimoto et. al.2012). Mutation of the glycine residue to alanine or serine abrogates the HSF1-RPA1 interaction. Neither of these two mutations shows any fault in the *in vitro* DNA binding (Fujimoto et. al.2012). As the wing domains are not conserved among HSF isoforms, RPA1 interacts with HSF1 and not with HSF2. A HSF2 derivative bearing the EQG motif binds RPA1, which shows that this motif is both essential and adequate for this interaction (Fujimoto et. al.2012).

In summary, although the DNA binding interfaces of various HSF-DBDs are well conserved, the wing domain and the top solvent-exposed surface of DBDs are not so. This could play a key role in HSF1 regulation at specific genomic loci and in the differential regulation of various HSF isoforms (Gomez-Pastor et. al.2018, Jaeger et. al.2016, Neudegger et. al.2016, and Fujimoto et. al.2012).

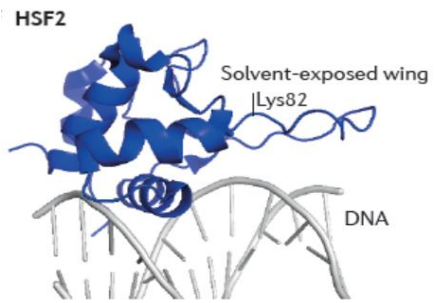

Figure 1.4: The crystal structure of HSF2-DBD (PDB: 5D8K) showing a fully resolved 'wing domain' with the Lys82 residue (which undergoes sumoylation) marked. It is evident that the wing domain does not contact the DNA backbone. Of note, the structure of the entire wing domain of HSF1 remains unresolved, although the resolved parts revealed conformational similarity with the HSF2 wing domain (adapted from Gomez-Pastor et. al.2018).

The HSF1 Activation Cycle:

Under normal stress-free conditions, mammalian HSF1 stays in an inactive monomeric form in the cytoplasm. This monomeric form is maintained in two ways: (1) by an intramolecular interaction between LZ1-3 and LZ4, and (2) by intermolecular interactions with the multi-chaperone complex comprised of Hsp40/70/90 and the molecular chaperonin TRiC (Akerfelt et. al.2010, Anckar et. al.2011, Li et. al.2017, Neef et. al.2014).

Both intrinsic and extrinsic factors can regulate the initial activation step of HSF1 (Gomez-Pastor et. al.2018, Akerfelt et. al.2010, Joutsen et. al.2019). Purified monomeric HSF1 undergoes homo-oligomerization under thermal and oxidative stress rapidly (Ahn et. al.2003). A temperature rise has been shown to disrupt the intramolecular LZ1-3-LZ4 interaction (Hentze et. al.2016). In a healthy cell, HSF1 stays in an inactive state in a complex with molecular chaperones. According to the chaperone titration model, stress cues cause the accumulation of misfolded and aggregated proteins within the cell, which titrates away the repressive multichaperone from monomeric HSF1. The monomeric HSF1 protein, thus liberated, can now oligomerize (Shi et. al. 1998, Gomez-Pastor et. al.2018, Akerfelt et. al.2010, Li et. al.2017). HSF1 oligomerizes via its oligomerization domain and attains a DNA-binding competent form; this enables it to bind HSE cooperatively with high affinity. In an *in vitro* system, the homo-oligomeric HSF1 binds HSE with a significantly higher affinity compared to its DBD, wild-type monomeric HSF1, or the constitutively monomeric derivative of HSF1 (where the oligomerization domain is deleted). This oligomerization step also exposes the bipartite nuclear localization signal lying adjacent to the oligomerization domain to facilitate its nuclear import (Gomez-Pastor et. al.2018).

RPA helps recruit HSF1 to the HSEs of its target genes in the nucleus, causing either gene induction or repression (Gomez-Pastor et. al.2018, Santagata et. al.2013, Fujimoto et. al.2012). During the larval development of *C. elegans*, however, the transcription factor E2F

helps in the recruitment of HSF1 by binding a GC-rich motif upstream of the degenerate HSEs and orchestrates a transcriptional program required for the early development of the animal (Li et. al.2016). RNA polymerase II is preloaded to the promoter-proximal region by the HSF1-RPA complex bound to the promoter. The said complex also causes the recruitment of the histone chaperone FACT (FAcilitates Chromatin Transcription), which aids in the relaxation of the local chromatin for robust induction of the HSR (Fujimoto et. al.2012). The pericentromeric protein shugoshin 2 (SGO2) helps in the recruitment of RNA polymerase II by specifically binding the free RNA polymerase II with a hypo-phosphorylated CTD. SGO2's recruitment to the promoter-bound HSF1 occurs via the phosphorylation of the Ser326 residue of HSF1 (Takii et. al.2019). RNA polymerase II needs the conserved coactivator mediator complex for activating transcription (Anandhakumar et. al.2016). The fruit fly HSF makes direct contact with the TRAP80 scaffold subunit (or Med14) and thereby recruits the mediator complex to the *hsp70* promoter (Akerfelt et. al.2010, Park et. al.2001). Similarly, yeast HSF was found to interact with the central Med 14 scaffold subunit, thus recruiting mediator complexes of multiple subspecies (Anandhakumar et. al.2016). The scaffold protein ATF1 is recruited to the promoter-bound HSF1 during the HSR by direct physical interaction with the HSF1-DBD (Takii et. al. 2015). This interaction ceases to exist when the Leu25 residue of HSF1-DBD is mutated to either Ala or Gly. But, the L25V mutation does not affect this interaction. In the crystal structure of HSF1-DBD, it is revealed that Leu25 is surrounded by other hydrophobic residues such as Leu21, Ile34, Trp36, Phe43, and Phe104. Possibly, when Leu25 is mutated to a less hydrophobic amino acid residue, the HSF1-ATF1 interaction gets perturbed because (1) either the HSF1-DBD structural integrity is adversely affected or (2) the position of the α1 helix harboring this residue is altered. The HSF1-ATF1 complex serves to create an HSF1 transcription complex on the promoter of target genes by recruiting the following factors: (1) BRG1, a chromatin remodeling factor, (2) p300, a histone acetyltransferase, and (3) the CREB binding protein CBP. BRG1 facilitates transcription by RNA polymerase II through the *hsp70* gene as necessary during acute HSR. The other two factors mentioned above (p300 and CBP) help in the attenuation phase of the HSR by acetylation of the Lys80 residue of HSF1, which adversely affects the DNA binding ability of HSF1 (Takii et. al.2015).

The activity of HSF1 is also known to be regulated by phosphorylation and proteasome-mediated degradation. Studies on Huntington's disease and melanoma have demonstrated that the two protein kinases CK2 and GSK3β phosphorylate the HSF1 Ser303/307

phosphodegron. Recognition of this phosphodegron by Fbxw7 in the Skp, Cullin, F-box containing (SCF) E3 ligase complex results in the proteasome-mediated clearance of nuclear HSF1 (Kourtis et. al.2015, Gomez-Pastor et. al.2017).

HSF1 transactivation activity was shown to be repressed by molecular chaperones like Hsp70 and -90 in a negative feedback loop as explained by the chaperone titration model (Shi et. al.1998, Gomez-Pastor et. al.2018, Akerfelt et. al.2010, Joutsen et. al.2019). The canonical model for HSF1 attenuation states the role of Hsp70, Hsp90, and the multi-chaperone complex in binding with the HSF1 homo-oligomer, removing it from the DNA and converting it back to the inactive monomeric form (Gomez-Pastor et. al.2018, Akerfelt et. al.2010, Joutsen et. al.2019, Anckar et. al.2011, Zou et. al.1998, Guo et. al.2001). The increase in the level of molecular chaperones in the cells because of the HSR prevents the further activation of any monomeric HSF1 (Akerfelt et. al.2010, Joutsen et. al.2019, Anckar et. al.2011, Kijima et. al.2018). The activity of HSF1 is repressed by the binding of Hsp70 and its co-chaperone Hsp40 with the protein's Transactivation domain (Shi et. al.1998, Krakowiak et. al.2018, Peffer et. al.2019). Hsp70 in yeast is known to make bipartite interactions with both the N-terminal and C-terminal AD of yeast HSF (Krakowiak et. al.2018, Peffer et. al.2019, Zheng et. al.2016). Survival of yeast cells under stressful conditions is very much dependent on this HSF-Hsp70 interaction, as demonstrated by a severely compromised thermotolerance of yeast at 30°C upon genetic ablation of both Hsp70 binding sites of yeast HSF (Peffer et. al.2019).

Several studies have shown that Hsp90 interacts with both the oligomerization and regulatory domains of HSF1 and represses its activity (Zou et. al.1998, Guo et. al.2001, Kijima et. al.2018, Shi et. al.1998). The molecular mechanism of Hsp70 and Hsp90 mediated attenuation and repression of HSF1 transactivation in mammalian cells is, however, still debatable. Small molecule-mediated inhibition of Hsp90 has been demonstrated to activate HSF1; it prolongs both the promoter occupancy and target gene expression of the protein. But the question remains as to the cause of the observations: is it enhancement of proteotoxic stress upon Hsp90 inhibition, the inability of Hsp90 to attenuate HSF1, or both (Zou et. al.1998, Guo et. al.2001, Kijima et. al.2018)? Some studies have emerged recently to refute this model. An *in vitro* HDX-MS study has demonstrated the inability of Hsp90 alone to disassemble HSF1 homo-oligomer and weaken its DNA binding activity (Hentze et. al.2016). The same study demonstrated HSF1 homo-trimerization to be an irreversible process; this further raised doubt on the ability of Hsp90 to disassemble homo-oligomeric HSF1 back to its

inactive monomeric form (Hentze et. al.2016). There is, however, a possibility that in an *in vitro* system, the multimer to monomer transition of HSF1 requires the complete multi-chaperone complex. Further, numerous studies have implicated nuclear HSF1 degradation mechanisms in dictating the activity of HSF1 (Kourtis et. al.2015, Gomez-Pastor et. al.2017, Kim et. al.2016).

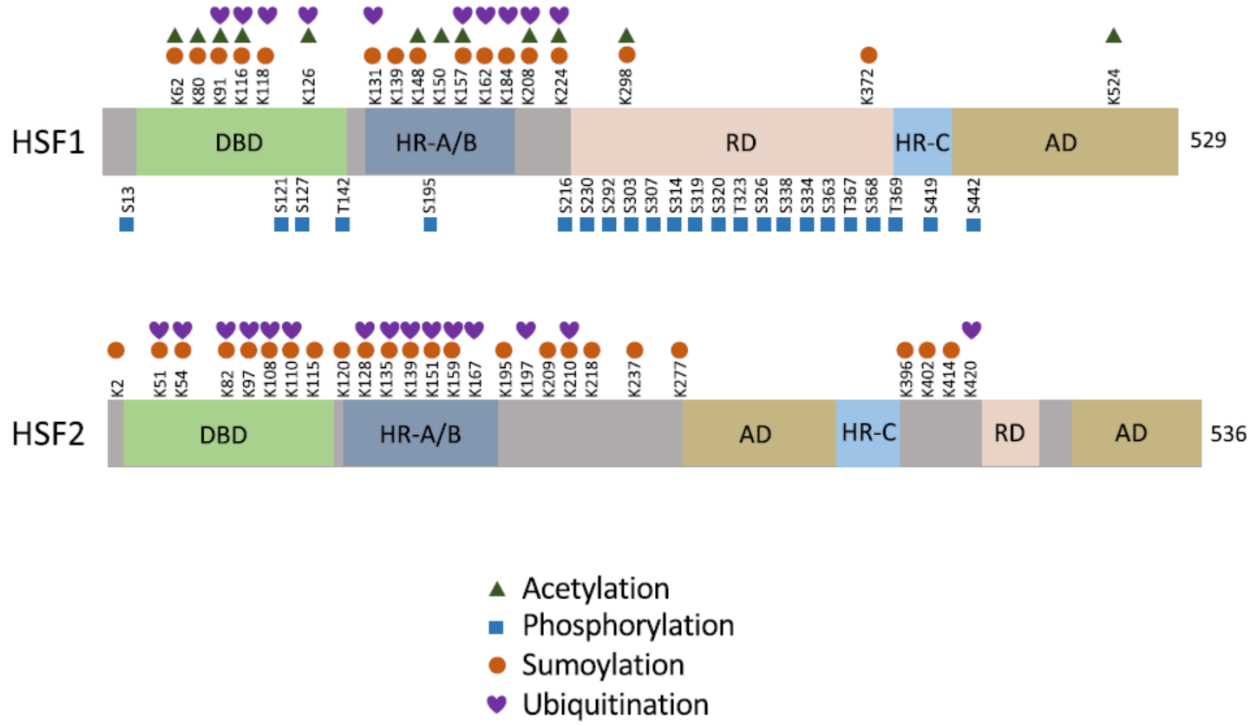

Figure 1.5: The various post-translational modifications occurring in HSF1 and HSF2. For each protein, the amino acid residues undergoing PTMs and their positions are shown, along with the nature of the modification (adapted from Roos-Mattjus and Sistonen, 2022).

Post-translational Modifications (PTMs) of HSF1:

HSF1 undergoes mainly three types of PTMs: phosphorylation, acetylation, and sumoylation, which modulate the activity and stability of the protein by various mechanisms (Gomez-Pastor et. al.2018).

HSF1 undergoes extensive phosphorylation at multiple sites: AMPK-mediated phosphorylation of the Ser121 residue in the DBD was shown to negatively regulate the protein's activity (Dai et. al.2015). Depending on cell types and pathological conditions, the Ser303/307 residues in the regulatory domain could be phosphorylated by protein kinases ERK1, CK2, and GSK3β; the phosphorylated residues play a key role in the stability of nuclear HSF1 by serving as a phosphodegron (Gomez-Pastor et. al. 2018, Joutsen et. al. 2019, Li et. al. 2017). Ser326 phosphorylation serves as a hallmark of HSF1 activation in acute stress including cancer. This residue is phosphorylated by MEK1 kinase (Tang et. al. 2015). However, the molecular mechanism of the impact of this phosphorylation on HSF1 activity is not fully understood. Although phosphorylation has a major impact on HSF1 activity, a derivative of HSF1 where all the phosphorylation sites in the regulatory domain were mutated was able to function in a mammalian cell line albeit with a lower activation threshold. Under acute thermal stress, it translocated to the nucleus and bound the *hsp70* promoter (Budzynski et. al.2015). In yeast also, a derivative of HSF where all the Ser and Thr residues were mutated to Ala performed the necessary functions of HSF, supported cell growth, and imparted modest heat tolerance even at 37°C (Zheng et. al.2016). Thus, phosphorylation may not be essential for the performance of the core HSF1 functions.

Acetylation of Lys80 residue dictates the DNA binding activity of HSF1. This acetylation masks the positive charge on the Lys residue to weaken its ionic interaction with the negatively charged DNA sugar-phosphate backbone, thereby impairing the HSF1-HSE interaction. This modification is under the control of histone acetyltransferases p300 and GCN5 and the histone deacetylases SIRT1, HDAC7, and HDAC9 (Westerheide et. al.2009, Zelin et. al.2015, Raychaudhuri et. al.2014). Similarly, p300-mediated acetylation of the Lys116 and Lys118 in the DBD compromises HSF1 DNA binding activity. The regulatory domain can also undergo acetylation and thereby regulate the protein's stability. The p300-mediated acetylation of Lys 208 and Lys298 can protect HSF1 from ubiquitination and subsequent proteasomal degradation (Raychaudhuri et. al.2014).

Phosphorylation-dependent sumoylation on Lys298 residue suppresses the activity of HSF1 (Gomez-Pastor et. al.2018): Ser303 phosphorylation of HSF1 is essential for its Lys298 sumoylation (Hietakangas et. al.2003). Differential sumoylation of the DBDs of various HSFs has been reported. In HSF2-DBD, the Lys82 residue is sumoylated, impairing its DNA binding activity, but the equivalent Lys residue in HSF1-DBD does not get sumoylated (Jaeger et. al.2016).

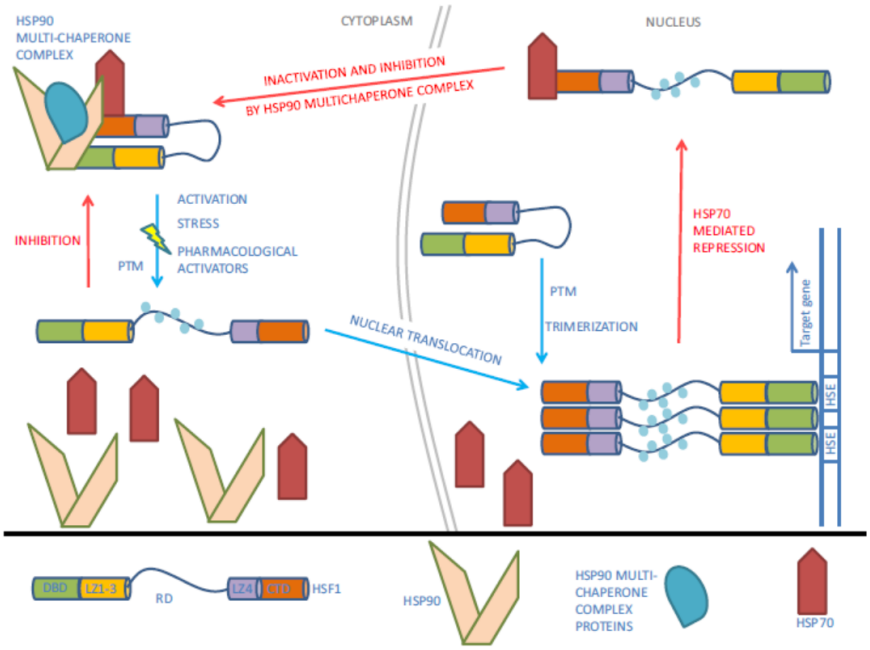

Figure 1.6: Schematic representation of the HSR (adapted from Dayalan Naidu et. al.2017). A variety of stressors cause the release of monomeric HSF1 from the multichaperone complex. Disruption of the intramolecular interaction between the LZ1-3 and LZ4 domains facilitates trimerization of HSF1. Hyperphosphorylation and nuclear translocation are followed by HSF1 binding to the heat shock elements located in the promoters of its target genes. During the attenuation phase of the heat shock response, Hsp70 binds the C-terminal transactivation domain of HSF1, thereby inhibiting its function. HSF1 also gets dephosphorylated and moves out of the nucleus to the cytosol, where it again becomes a part of the multichaperone complex.

HSF1 and neurodegenerative diseases

Apart from the stress response, Heat Shock Factors play important roles in brain development including the migration of neurons and the formation and maintenance of synapses. Moreover, neurons exposed to chronic and acute proteotoxic stress are protected by HSFs (Gomez-Pastor et. al. 2018). Loss in the activity of HSF1 is associated with multiple neurodegenerative diseases involving the accumulation of toxic protein aggregates (Anckar et. al.2011). Expansion of the polyglutamine encoding regions in the *Huntingtin* gene causes the accumulation of mutant Huntingtin protein aggregates in the central nervous system,

leading to Huntington's disease (Gomez-Pastor et. al. 2017). In this case, a decrease in HSF1 protein level caused by abnormal degradation of HSF1 has been observed. A dramatic increase in the expressions of Casein Kinase 2α' (catalytic subunit of Casein Kinase 2) and Fbxw7 was associated with enhanced degradation of HSF1 (Gomez-Pastor et. al.2017). Also, the accumulation of α-synuclein aggregates in a Parkinson's disease model induces the E3 ligase Nedd4-mediated HSF1 degradation (Kim et. al.2016). In Alzheimer's disease patients, a lowered abundance of HSF1 was found in neural-derived plasma exosomes when compared to that from control individuals with normal cognitive abilities (Goetzl et. al.2015).

Small molecules that can activate HSF1 to restore protein quality control in individuals suffering from neurodegenerative diseases are under different stages of studies.

A multitude of both exogenous and endogenous small molecules are reported to activate HSF1 (West et. al.2012). Most of these molecules indirectly boost the transcriptional activity of HSF1. The discussion elaborated below gives an account of endogenous metabolites and plant-derived compounds purified from medicinal and edible plants. Several synthetic compounds were reported to activate HSF1. Studies on the chemical properties of these molecules have offered valuable insights into the pathways of HSR activation. Sulfhydryl reactivity, a property shared among multiple HSF1 activators, modulates the functioning of HSF1 as well as some of its regulators such as Hsp90, SIRT1, and its upstream regulatory kinases (Dinkova-Kostova 2012).

Endogenous activators of HSF1:

Endogenously generated electrophilic oxidized and nitrated lipids and α, β-unsaturated aldehydes have been shown to boost the transcriptional activity of HSF1. 4-hydroxy-2-nonenal, acrolein, nitro-oleic acid and 15-deoxy-$\Delta^{12, 14}$-prostaglandin J2 fall under these categories. 4-hydroxy-2-nonenal has been implicated in the accumulation of HSF1 in the nucleus, upregulation of Hsp70 and Hsp40, and HSE-dependent expression of luciferase reporter in colon cancer cells. HSF1 silencing achieved by siRNA was shown to terminate these gene inductions (Jacobs et. al.2007). Nitro-oleic acid, known to exert cytoprotective effects, induced HSR in human endothelial cells (Kansanen et. al.2009). Acrolein, a product of lipid peroxidation, was demonstrated to boost the expression of Hsp70 and Hsp40 in the human lung cancer cell line A549 (Thompson et. al.2008). 15d-PGJ2 by facilitating the HSE binding of HSF1 led to robust induction of Hsp70 in the heart of male Wistar rats under

ischemia–reperfusion injury (Zingarelli et. al.2004). 17β-estradiol at elevated levels can activate HSF1-mediated Hsp70 expression (Hamilton et. al.2004, Hou et. al.2010). It is worthy of mention here that in contrast to all the other endogenous activators discussed above; 17β-estradiol is not an electrophilic compound. However, it is known to be metabolically converted to 2-hydroxy and 4-hydroxy estradiol, both of which are electrophilic and could be responsible for HSR induction (Zhu et. al.1998).

Hydrogen peroxide (H_2O_2) was shown to directly activate the HSF1-driven HSR. Notably, HSF1 itself senses H_2O_2. The activation of mouse HSF1 by H_2O_2 is driven by the formation of an intermolecular (between different subunits in the trimeric/ multimeric structure) disulfide bridge between the Cys residues 35 and 105 (Ahn et. al.2003). In human HSF1, the corresponding Cys residues at positions 36 and 103 also form an intermolecular disulfide bridge facilitating multimerization and subsequent DNA binding of the protein (Lu et. al.2008). Two aromatic amino acid residues, Trp37 and Phe104, have been shown to undergo intermolecular interaction and facilitate the approach of the two Cys residues (36 and 103) to form a multimeric structure (Lu et. al.2009). However, an intramolecular disulfide bridge formation involving the three Cys residues 153, 373, and 378 was shown to block multimer formation and DNA binding of HSF1 (Lu et al. 2008). Nitric oxide (NO), an important signaling molecule, has been implicated in HSF1 activation and Hsp70 upregulation in the vascular smooth muscle cells (Xu et. al. 1997). Notably, the ATPase activity of human Hsp90α was shown to be blocked upon S-nitrosylation of the protein's Cys 597 residue (Martinez-Ruiz et. al.2005). Mutation of this residue to Asn and Asp (both of which mimic S-nitrosylation) caused a loss of the protein's activity (Retzlaff et. al.2009). Probably, NO-mediated HSF1 activation is caused by inhibition of Hsp90 activity.

Electrophilic and reactive oxygen species, formed in various physiological and pathological processes, can activate HSF1. This explains the activation of HSF1 in atherosclerotic lesions. Cytokine-mediated stimulation and mechanical stretching of smooth muscle cells are implicated in hyper-phosphorylation and nuclear localization of HSF1 and consequent upregulation of Hsp70 (Metzler et al. 2003). Vascular endothelial cells in culture, upon stimulation by glycated low-density lipoproteins (LDL) and oxidized very low-density lipoproteins (VLDL) activate HSF1. This results in the generation of plasminogen activator inhibitor-1 (Zhao et. al.2007, Zhao et. al.2008). Here, induction of NADPH oxidase generates superoxide, which then ultimately activates HSF1 (Sangle et. al. 2010, Zhao et. al. 2013).

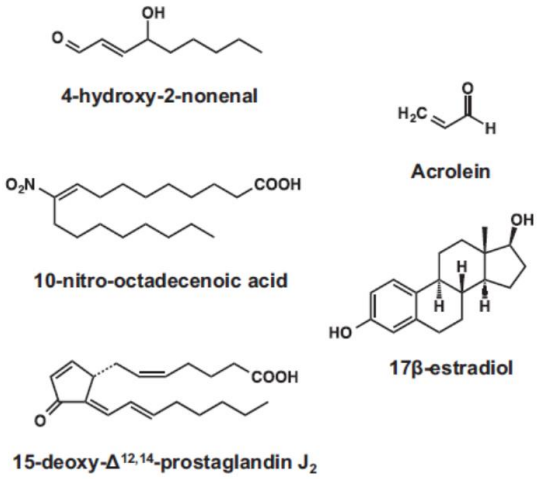

Figure 1.7: Endogenous small molecule activators of HSF1 (adapted from Dayalan Naidu et. al. 2017)

<u>Plant-derived activators of HSF1:</u>

The human cervical cancer cell line HeLa was stably transfected with a construct harboring the luciferase coding sequence under the *hsp70* promoter. This reporter cell line was employed in the screening of bioactive small molecules for the identification of HSF1 activators. The study revealed the phytochemical celastrol to be an activator of the HSR (Westerheide et. al.2004). This compound, obtained from the Chinese medicinal plant *Tripterygium wilfordii,* is a quinone methide triterpenoid. Celastrol was also shown to stimulate the *hsp70* promoter-reporter construct in MCF7 and BT474 (breast cancer), H157 (non-small cell lung carcinoma), and SH-SY5Y (neuroblastoma) cells. The similarity in the magnitude of HSR activation by heat shock exposure (42°C) and celastrol treatment was observed (Westerheide et. al.2004). It has been suggested that celastrol-mediated inhibition of Hsp90 causes the dissociation of HSF1 from the protein complex (Salminen et. al.2010, Hieronymus et. al.2006).

Gedunin, a tetranortriterpenoid purified from the Neem tree (*Azadirachta indica*), has been reported to activate HSF1 through functional inhibition of Hsp90. However, it has lower

potency compared to celastrol (Hieronymus et. al.2006, Brandt et. al.2008). Four compounds structurally similar to gedunin, namely deoxygedunin, deacetoxy-7-oxogedunin, deacetylgedunin, and sappanone A, have been shown to activate HSF1 and drive HSF1-mediated Hsp70 upregulation. They were found to rescue cells from MG-132 (proteasomal inhibitor) induced cell death. Cytoprotective effects of these compounds were lost upon knockdown of HSF1. In two mammalian cell-based models of Huntington's disease, these compounds were proven to boost cellular survival (Zhang et. al.2009). Gedunin has been demonstrated to interact directly with p23 (a co-chaperone of Hsp90), thereby causing the inactivation of the Hsp90 machinery and consequent destabilization of steroid receptors (Patwardhan et. al.2013).

Withaferin A**,** a withanolide isolated from the plant *Withania somnifera* was identified as an activator of HSF1 upon screening of more than 80,000 natural and synthetic compounds using cell-based enhanced green fluorescent protein (EGFP) reporter assay (Santagata et. al.2012). Withaferin A is also known to cause activation of HSF1 by inhibition of the functioning of Hsp90 (Yu et. al.2010, Grover et. al.2011). This same screen brought to light multiple natural compounds that are inducers of the HSR, apart from confirming the HSR-inducing activities of celastrol, gedunin, and withaferin A. Among these active compounds are the limonoids such as anthothecol, cedrelone, and 7-desacetoxy-6,7-dehydrogedunin, and the fungal compound dehydrocurvularin (Santagata et. al.2012). Notably, a common feature of these compounds is the presence of α, β-unsaturated carbonyl group, which accentuates the importance of electrophilicity for the induction of HSR.

The polyphenolic compound curcumin isolated from *Curcuma longa* is reported to upregulate Hsps in multiple cell cultures and *in vivo* models (Kanitkar et al. 2008, Calabrese et. al. 2003). This compound also mediates this function through functional inhibition of the Hsp90. Curcumin disrupts the interaction of the Hsp90-p23 complex with its client p210 BCR/ABL, which results in degradation of the kinase in CML cells; suggesting Hsp90 inhibition as a possible mechanism for curcumin-mediated HSF1 activation (Wu et. al.2006). Numerous clinical trials are registered to assess curcumin in different pathological conditions, including several forms of cancer and neurodegenerative diseases (www.clinicaltrials.gov).

The phenolic compound coniferyl aldehyde was isolated from the traditional medicinal plant *Eucommia ulmoides*. It enhances the stability of HSF1 protein as well as stimulates the

activities of MAPKs ERK1/2, JNK1, and p38. It induces HSF1 Ser326 phosphorylation correlating with the upregulation of Hsp70 and Hsp27. It offered HSF1-dependent protection against damaging ionizing radiations or taxol in cell and mouse models (Kim et. al.2015).

The aromatic chalcone derivative (±)-4, 2', 4'-trihydroxy-3'-[(6E)-2-hydroxy-7-methyl-3-methylene-6-octenyl] chalcone was purified from the areal parts of the edible plant *Angelica keiskei* Koidzumi (Umbelliferae). It can stimulate HSF1-mediated transcription in the human lung cancer cell line NCI-H460 (Kil et. al.2015).

Sulforaphane, an isothiocyanate abundant in cruciferous vegetables such as broccoli was shown to cause accumulation of HSF1 in the nucleus and subsequent increase in the expression of Hsps in many cell lines and animal model following a single oral dose (Hu et. al.2006, Gan et. al.2010, Sharma et. al.2010).

Phenethyl isothiocyanate, isolated from the plant *Nasturtium officinale,* also upregulates the expression of Hsps in both cell culture and animal model (Dayalan Naidu et al. 2016, Hu et al. 2006). It was shown to inhibit Hsp90, stimulate the activity of p38 MAPK, and phosphorylate HSF1 Ser326 residue to enhance the HSF1 target gene expression (Dayalan Naidu et. al.2016).

Mounting experimental evidence suggests that to activate HSF1, the isothiocyanates target Hsp90. These evidences are as follows:

- When sulforaphane and the known Hsp90 inhibitor 17AAG (17-allylamino 17-demethoxygeldanamycin) were treated together, the latter's anticancer potential was found to be increased in pancreatic cancer (Li et. al.2011).
- The interaction of Hsp90 and its co-chaperone Cdc37 was found to be abrogated upon sulforaphane treatment (Li et. al.2011).
- Mutant p53, Raf1 and Cdk4, the 'client' proteins of Hsp90, were synergistically downregulated by 17AAG and sulforaphane treatment (Li et. al.2011).
- Covalent modification of Hsp90 was observed both in cells and in a purified system by a sulfoxythiocarbamate derivative of sulforaphane (Ahn et. al.2010, Zhang et. al.2011, Zhang et. al.2014).

- Treatment with phenethyl isothiocyanate diminished the content of Hsp90-bound HSF1 in cells (Dayalan Naidu et. al.2016).
- Compromised activity of HDAC caused by sulforaphane has been implicated in the altered acetylation and consequent diminution of Hsp90 activity (Myzak et. al.2004, Myzak et. al.2006, Myzak et. al.2006, Pledgie-Tracy et. al.2007, and Gibbs et. al.2009). It has been observed that the de-activation of HDAC6 causes acetylation and consequent abrogation of Hsp90's chaperone function (Bali et. al.2005). Also, hyperacetylation of Hsp90 was caused by the sulforaphane-mediated decrease in HDAC6 activity (Gibbs et. al.2009).

Resveratrol, a stilbene, was reported to activate HSF1 by stabilizing its binding with the HSE and delaying the attenuation phase of HSR (Westerheide et. al.2009). It stimulates the SIRT1 deacetylase to facilitate the maintenance of HSF1 in a deacetylated state, and enhance its DNA binding capability (Sinclair et. al.2014). However, the effect of other plant-derived SIRT1 activators such as fisetin and butein on the activation of HSF1 remains unknown (Wood et. al.2004).

Azadiradione, a limonoid purified from *Azadirachta indica* was demonstrated to ameliorate protein aggregation-associated diseases in fruit fly and mouse models (Nelson et. al. 2016, Singh et. al. 2018). A series of results indicate that AZD functions through a unique mechanism.

Interestingly, treatment of cell lines and living organisms with the above-discussed phytochemicals often exhibits non-linear dose responses. Indeed, the enhancement of a biological activity at low concentrations of a compound and inhibition of the same activity at high concentrations is well-known, which generates a J-shaped or an inverted U-shaped dose-response curve. This phenomenon is known as hormesis (Calabrese et. al.2015, Calabrese et. al.2010). Oral administration of phytochemicals like curcumin has been shown to cause mild cellular stress characterized by the generation of free radicals, ion fluxes, and an increase in energy demand (Calabrese et. al.2008, Mancuso et. al.2007). Subsequently, adaptive stress response pathways, such as the HSR, are activated, which boost cellular survival. This hormetic response, once activated, can offer protection against more severe stresses, thereby dampening their lethality.

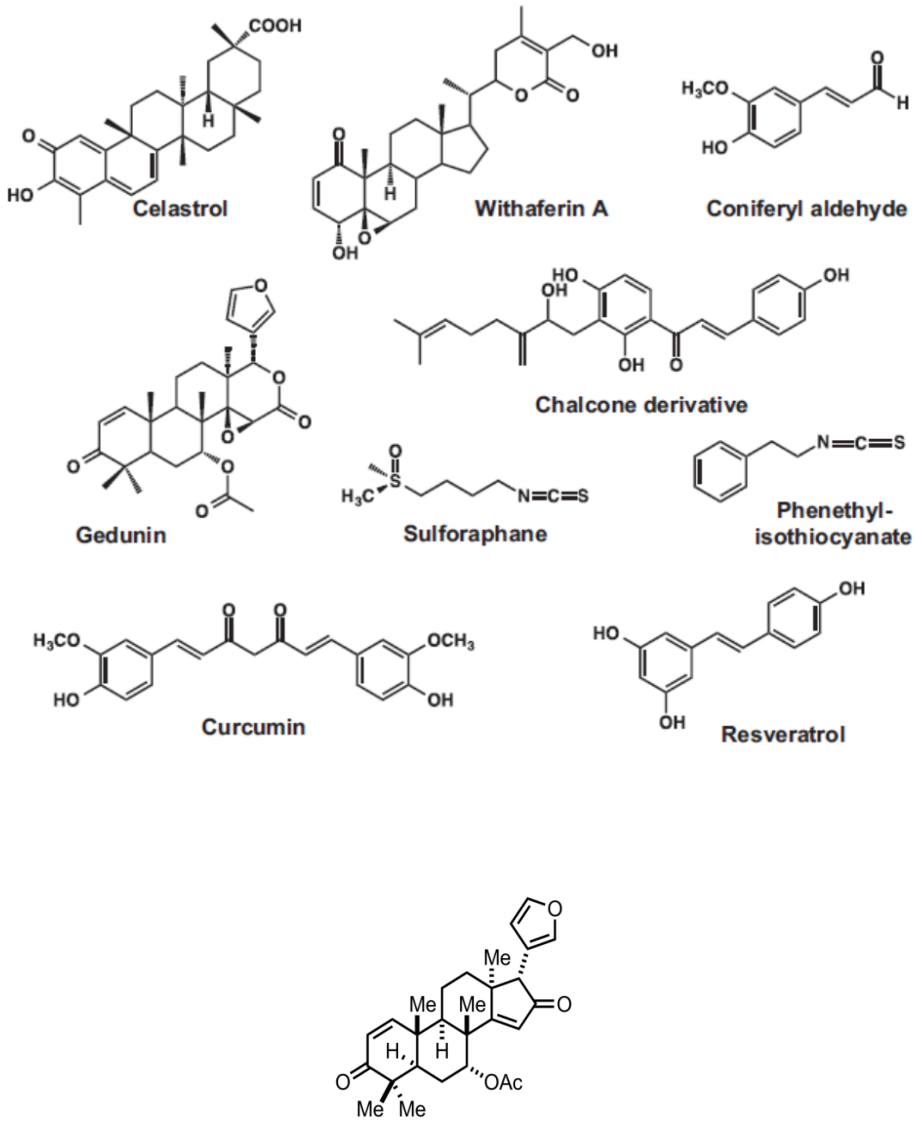

Figure1.8: Plant-derived small molecule activators of HSF1 (adapted from Dayalan Naidu et. al.2017)

Synthetic molecules that activate HSF1:

Neef and colleagues developed a humanized yeast-based high throughput screen; lacking sensitivity to proteotoxic stress and inhibition of Hsp90 (which are known activators of HSF1) (Neef et. al.2010). This screen identified two potent HSF1 activators from a library of more than 10,000 compounds. These molecules, named HSF1A and HSF1C, are benzyl pyrazole derivatives, the former being more potent than the latter. Treatment of HSF1A in HeLa and wild-type MEF cell lines was shown to boost the expression of *hsp70* via activation of HSF1. This effect was, however, not observed in the *hsf1-/-* MEF cell line, strongly indicative of HSF1-dependency of the effect. The HSR-inducing activity of this compound was shown to be unaffected by DTT pre-incubation, unlike the electrophilic molecules that activate HSF1. A later study evidenced that HSF1A exhibited this function by directly inhibiting TRiC/CCT, a chaperonin complex that negatively regulates HSF1 (Neef et. al.2014).

Screening of ~900,000 compounds by a cell-based reporter assay yielded ~200 HSR-inducing small molecules (Calamini et. al.2012). Many of the active compounds were electrophilic. Compound A1 (a cyclohexanone derivative) harbors the α, β-unsaturated carbonyl group, which is electrophilic. It is structurally similar to bis (benzylidene) acetone and its derivative bis (2-hydroxy benzylidene) acetone, the HSR-inducing potency of the latter far exceeding that of the former (Zhang et. al.2011). As there is a strong correlation between HSR-inducing potential and sulfhydryl reactivity, bis (benzylidene) acetone exhibits slow reactivity towards the thiol groups of glutathione and DTT (Dinkova-Kostova et. al.2001) and is thus a very poor inducer of HSR (Zhang et. al.2011). Its hydroxylated derivative, however, strongly activates HSF1 (Zhang et. al.2011). TBE-31, another electrophilic compound, has been shown to react strongly as well as reversibly with thiol groups (Dinkova-Kostova et. al.2010). It upregulates Hsp70 at high nanomolar concentrations in wild-type MEF cells, not in *hsf1-/-* MEF cells (Zhang et. al.2011).

The electrophilic synthetic compound STCA (sulfoxythiocarbamate alkyne) can form adducts with the thiol groups of the following Cys residues of recombinant Hsp90 at positions 412, 564, and 589/ 590. It has been shown to boost the HSF1-dependent upregulation of a luciferase reporter gene, as also of the endogenous *hsp70* gene in various cell lines like HeLa, MCF7, and MEF (Ahn et. al.2010, Zhang et. al.2014). Two thiol-reactive compounds, namely pyrrolidinedithiocarbamate and 1,2-dithiole-3-thione, boost the HSF1-dependent upregulation of the *hsp70* gene (Kim et. al.2001, Andringa et. al.2007). Pro-electrophilic diphenols, upon oxidation, yield electrophilic metabolites that induce the HSR via HSF1 activation (Satoh et. al.2011).

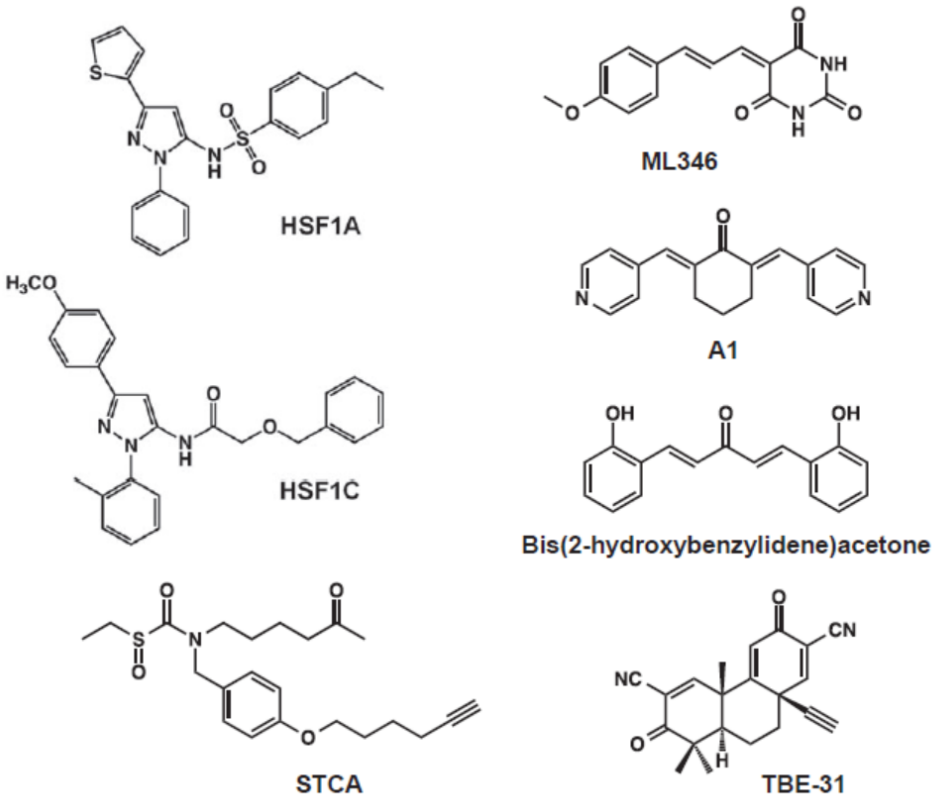

Figure 1.9: Synthetic small molecule activators of HSF1 (adapted from Dayalan Naidu et. al.2017)

HSF1 and Cancer

HSF1 has been shown to play multiple roles in the cellular processes associated with tumorigenesis, e.g., changes in the tumor microenvironment, genome repair, etc (Wang et. al.2020). HSF1 is also involved in the cell death pathways, such as apoptosis, autophagy, and ferroptosis (Toma-Jonik et. al.2019, Dokladny et. al.2015, and Sun et. al.2015). In contrast to non-transformed cells, cancer cells have higher levels of HSF1 in general (Wang et. al.2020, Chen et. al.2021). Activation of HSF1 in the tumor stroma indicates a poor prognosis (Scherz-Shouval et. al.2014).

Along with the Hsp-dependent pathway, other oncogenic pathways such as RAS-MAPK and PI3K-Akt-mTOR are also linked with HSF1 (Home et. al.2015). Moreover, Hsp90 is known to bind and stabilize many proteins crucial to tumor cell survival (Whitesell et. al.2005). In addition, loss of HSF1 activity has been implicated in the repression of aneuploidy and the diminution of cellular proliferation in several types of cancer (Carpenter et. al.2019). Thus, pharmacological inhibition of HSF1 is a promising approach for anticancer therapy (Dong et. al.2019).

Inhibitors of HSF1:

Although HSF1 has been successfully inhibited *in vitro* and animal models, limitations in the clinical use of each inhibitor exist. HSF1 is essential for cancer cells. It is also necessary for normal cells when they are exposed to stressful conditions. So, care should be taken to ensure that inhibition of HSF1 in cancer cells does not cause toxicity to normal cells. This could be achieved by making derivatives of the existing compounds via alteration of their functional groups, as well as by the purification of novel compounds from natural sources. Novel compounds could also be synthesized in the laboratory (Velayutham et. al.2018).

It is a daunting task to develop HSF1 inhibitors, given the dearth of potential “druggable” sites on its tertiary structure (Velayutham et. al.2018, Cheeseman et. al.2017). Moreover, the pathway of activation of this protein is quite a complex one, involving multichaperone complexes and PTMs. Nevertheless, some synthetic and natural source-derived inhibitors of HSF1 have been developed. The molecular basis of action of some of these compounds is not yet fully understood (McConnell et. al.2015, Zhang et. al.2016).

KRIBB11: The compound KRIBB11 has been demonstrated to inhibit the activity of HSF1 by blocking the binding of pTEFb (positive transcription elongation factor b) with the *hsp70* promoter region, thereby weakening the ability of HSF1 to induce the transcription of stress response genes (Dong et. al.2019, Yoon et. al.2011). When model animals were administered with this compound, HSF1 inhibition was achieved, demonstrated by a diminution in Hsp70 levels and a reduction in tumor mass and volume (Yoon et. al.2011). KRIBB11 blocked the lymphatic metastasis of bladder cancer cells considerably and was shown to have little toxicity (Huang et. al.2022). A combinatorial treatment of KRIBB11 and danusertib, an Aurora Kinase inhibitor, exerted a significant anti-cancer effect on liver cancer both *in vitro* and *in vivo*. The combination treatment with these two drugs triggered apoptotic death of cancer cells, activated the UPR, and thereby inhibited tumor growth (Shen et. al.2021). Another study however showed that this compound alone did not significantly affect the expression, phosphorylation, or nuclear translocation of HSF1 suggesting that it is not a direct inhibitor of HSF1 (Brown et. al.2021).

Schizandrin-A: A natural product known as deoxyschizandrin or schizandrin A (Sch-A) purified from the plant *Schisandra chinensis* exhibited HSF1 inhibitory activity. This compound interacts directly with HSF1 and induces conformational changes at the site of binding. This leads to cell cycle arrest and apoptosis in human colorectal cancer cell lines. Sch-A was shown to repress the HSR which is induced by heat shock. Sch-A treatment achieved downregulation of the expression of HSF1 target genes like Hsp70, Hsp90, and Hsp27 under both normal and heat shock conditions (Chen et. al.2020, Szopa et. al.2017).

Quercetin: The flavonoid quercetin is a dietary antioxidant present in onion, tea, apple, berry, and many other foods. It has numerous health benefits. It has been reported to inhibit the interaction of HSF1 with HSE on the promoters of HSF1 target genes (Sarkar et. al.2022). Following combination therapy, quercetin reduced the accumulation of Hsp70 in tumors and caused the induction of cellular apoptosis by the HSF1 pathway. In an *in vivo* study, quercetin in combination with radiofrequency ablation was shown to activate caspase 3, leading to apoptosis and a diminution in the expression of Hsp70 (Yang et. al.2016).

Triptolide: Isolated from *Tripterygium wilfordii*, triptolide is also an inhibitor of HSF1. Treatment with this compound has been shown to induce apoptosis in cultured and primary chronic lymphocytic leukemia (CLL) cells. Treatment with triptolide causes inhibition of

HSF1 which results in the decrease of Hsp90 levels. The cytosolic complex consisting of HSF1, p97 (a segregase having ATPase activity), Hsp90, and HDAC6 (Histone deacetylase 6- which deacetylates Hsp90) falls apart. As a result, inhibition of HSF1 leads to acetylation of Hsp90, compromising its function as a molecular chaperone, which manifests as the anti-cancer activity of triptolide (Ganguly et. al.2015).

Triazole nucleoside: This compound causes downregulation of HSF1 as well as various chaperones including Hsp27, Hsp70, and Hsp90 in prostate cancer. It also decreases the expression of androgen receptor (AR) and causes cell cycle arrest (Xia et. al.2015).

PGPIPN: This is a hexapeptide that is derived from the amino acid residues 63-68 of bovine β-casein (Meisel 2005). It was shown to sensitize ovarian cancer cells to cisplatin by targeting the HSF1/Hsp70 signaling pathway. The expression levels of HSF1, Hsp70, and MDR1 (Multi Drug Resistance 1) were found to be reduced by this peptide. PGPIPN and cisplatin possibly act in synergy against ovarian cancer (Guo et. al.2021).

DTHIB: The synthetic compound, Direct Targeted HSF1 Inhibitor (DTHIB a.k.a. SISU-102), was shown to interact directly with the HSF1-DBD. The compound selectively bound HSF1 and facilitated the degradation of multimeric, active HSF1 in the nucleus, thereby causing inhibition of the protein's functions and decreasing the abundance of the multichaperone complex. When compared with enzalutamide, the ability of DTHIB to reduce cell viability and cause inhibition of AR signaling and PSA (prostate-specific antigen) expression was found to be considerably higher in prostate cancer. Moreover, DTHIB has been demonstrated to inhibit tumor growth by causing a diminution of cell proliferation. Side effects like behavioral changes and body weight loss were not recorded in mouse models (Dong et. al. 2020). In an *in vivo* model of acute myeloid leukemia (AML), DTHIB has been shown to repress the self-renewal of leukemia stem cells without affecting normal hematopoietic stem or progenitor cells (Dong et. al. 2022). DTHIB was found in this study to block the expression of HSF1 target genes like Hsp90 and compromise the mitochondrial oxidative phosphorylation by downregulating succinate dehydrogenase C (SDHC) (Dong et. al. 2022).

CCT251236 and CCT361814: The synthetic compound CCT251236 exhibited significant HSF1 inhibition and anticancer activity in a preclinical model of ovarian cancer (Cheeseman et. al.2017). A derivative of this compound, CCT361814, was demonstrated to block the heat shock pathway in multiple myeloma cells, as evidenced by a dose-dependent decrease in Hsp72 and Hsp27, and exhibit significant anti-myeloma activity (Menezes et. al.2017).

CCT361814 has shown promise and entered a phase I clinical trial for advanced solid tumors (Diane Marsolini 2022, Workman et. al.2022).

Table: HSF1 inhibitors

Name of the HSF1 inhibitor	Source	Biological activities	Type of cancer	References
Quercetin	Citrus fruits, apple, onion, tea, red wine, etc.	Induction of apoptosis	Liver and breast	Yang et. al.2016
Triptolide	*Tripterygium wilfordii*	a. Induction of apoptosis in a dose-dependent manner b. Downregulation of proliferative pathway c. Induction of cell death	a. Chronic Lymphocytic Leukemia b. Pancreatic c. Liver and multiple myeloma	a. Ganguly et. al.2015 b. Banerjee et. al.2013 c. Sangwan et. al.2015, Heimberger et. al.2013
2,4-Bis (4-hydroxybenzyl) phenol	*Gastrodiaelata*	Arrests cell growth & induces apoptosis	Lung	Yoon et. al.2014
Cantharidin	*Meloidae sp.*	Achieves HSF1-dependent inhibition of Hsp70 and BAG3, causes downregulation of	Colon, lung, prostate, breast	Kim et. al.2013

		anti-apoptotic Bcl-2 family		
Rohinitib	Plants of genus *Aglaia (Meliaceae)*	Causes downregulation of genes upregulated by HSF1 & de-repression of genes suppressed by HSF1; lowers cellular glucose uptake and lactate generation	Leukemia	Iwasaki et. al.2016, Santagata et. al.2013
SNS-032	Sulphur compounds	Cyclin Dependent Kinase (CDK) inhibitor; causes repression of Hsp70 expression	Leukemia	Chen et. al.2009, Wu et. al.2012, Rye et. al.2016
4,6-disubstituted pyrimidines	Aromatic heterocyclic compound	Inhibits HSF1 indirectly	Osteosarcoma	Rye et. al.2016
KNK-437	Benzylidene lactam compound	Causes inhibition of the pro-survival Akt/HSF1 pathway in breast cancer; suppresses HSF1-driven transcription and causes apoptosis; causes inhibition of acquired thermotolerance	Colon, breast, squamous cell carcinoma	Whitesell et. al.2009, Oommen et. al.2012, Sharma et. al.2018

CCT361814	Bisamide	Directly inhibits HSF1 and induces apoptosis	Multiple myeloma, solid tumor (under phase I clinical trial)	Menezes et. al.2017, Diane Marsolini 2022, Workman et. al.2022
DTHIB		Causes degradation of nuclear HSF1 selectively	Prostate, leukemia	Dong et. al.2020, Dong et. al.2022
KRIBB11	Pyridinediamine	Causes growth arrest and apoptosis	Lung, multiple myeloma	Lee et. al.2021, Yoon et. al.2011, Sharma et. al.2018, Kang et. al.2017, Fok et. al.2018
I_{HSF} 115	Thiazole acrylamide	Binds HSF1-DBD; intervenes in the assembly of ATF1 containing complex and thereby blocks HSF1 transcriptional activity	Breast, multiple myeloma	Sharma et. al.2018, Vilaboa et. al.2017
Dorsomorphin		Blocks accumulation of HSF1 in the nucleus	Colon, prostate	Li et. al.2019
PW3405	Anthraquinone	Blocks phosphorylation of HSF1	HeLa cell line (cervical cancer)	Zhang et. al.2016, Sharma et. al.2018
CCT251236	Bisamide	Blocks HSF1 transcription	Ovarian	Cheeseman et. al.2017
NZ28	Emetine	Blocks translation of Hsp mRNA;	Prostate, lung, breast, myeloma	Zaarur et. al.2006,

		blocks HSF1 activation resulting in compromised cell migration and invasion		Schilling et. al.2015

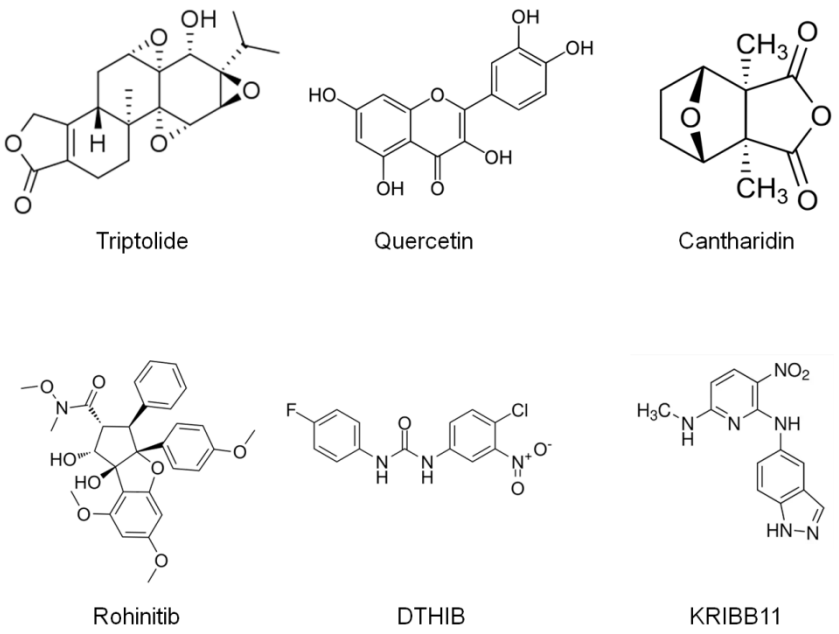

Figure 1.10: Structures of some HSF1 inhibitors [1]

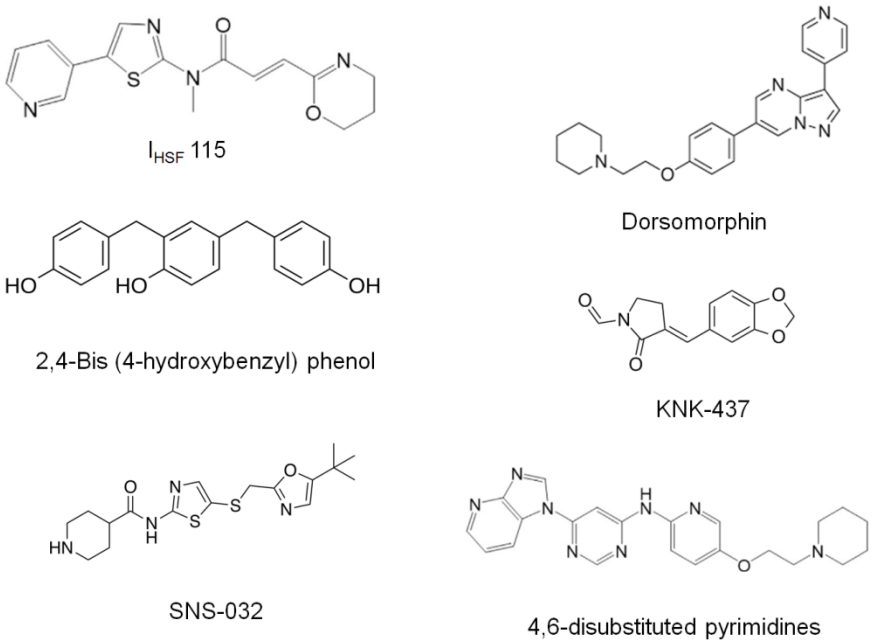

Figure 1.11: Structures of some HSF1 inhibitors [2]

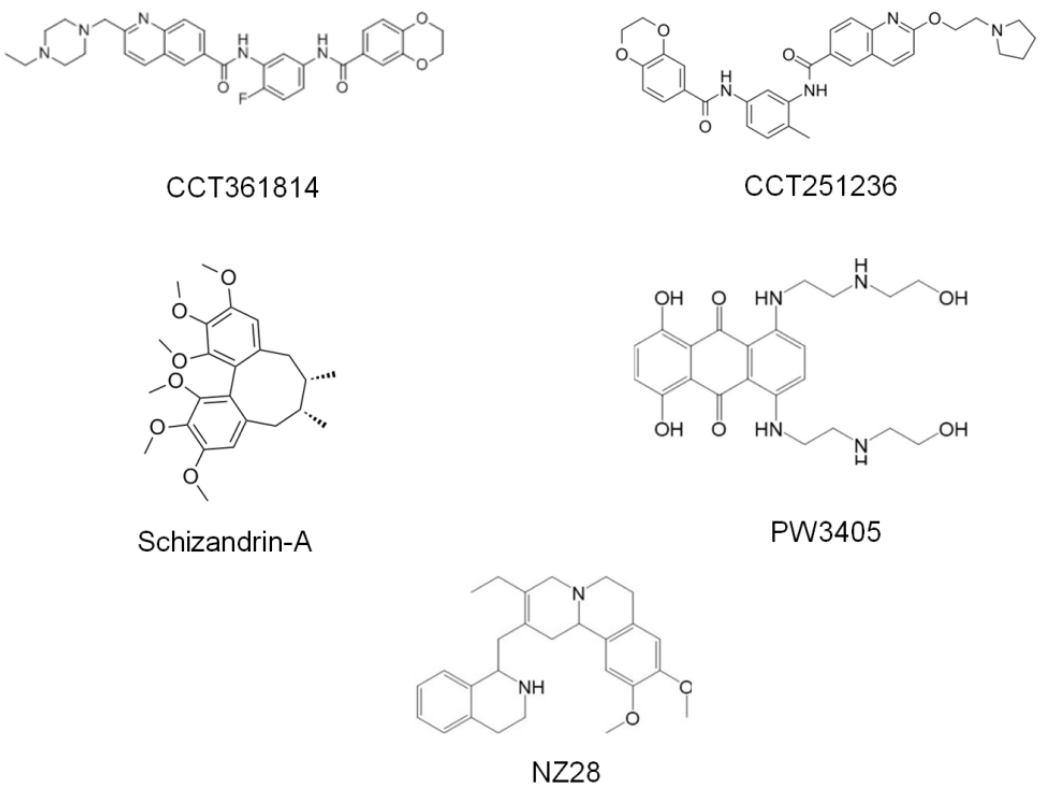

Figure 1.12: Structures of some HSF1 inhibitors [3]

Background of the present study

As discussed earlier, individuals suffering from neurodegenerative diseases such as Parkinson's disease and Alzheimer's disease carry an impaired HSR, resulting in the accumulation of toxic protein aggregates in distinct regions of their brains. These aggregates ultimately cause the death of the neurons (neurodegeneration). Small molecule-mediated forcible activation of HSF1/ HSR to activate the cellular protein quality control system is a promising approach to treating such diseases. The small molecule activators of HSF1 described previously were shown to boost the protein's activity indirectly. Our laboratory, however, reported a phytochemical named Azadiradione (AZD), which was found to activate HSF1 uniquely (Nelson et. al. 2016).

AZD, purified from the seeds of *Azadirachta indica* (Neem), activates HSF1 by direct interaction to facilitate the protein's DNA binding. Notably, it is the only compound reported so far to have this unique mode of action. In addition to not affecting the cellular oxidative status, AZD showed little effect on the activities of cellular Hsp90 and 26S proteasome unlike various small molecule HSF1 activators reported thus far, which are believed to be toxic for cells. AZD has already been shown to clear toxic polyglutamine protein aggregates in cellular and fruit fly models (Nelson et. al. 2016). AZD could effectively restore protein quality control in a mouse model of Huntington's disease and improve disease pathology (Singh et. al. 2018).

Intriguingly, AZD has been shown to activate HSF1 in the absence of proteotoxic stress, at a concentration non-toxic for cells (Nelson et. al. 2016). Therefore, an in-depth study on how AZD accomplishes this task is critical to advance the understanding of HSF1 biology as well as for designing efficient small molecule activators of HSF1 in the future.

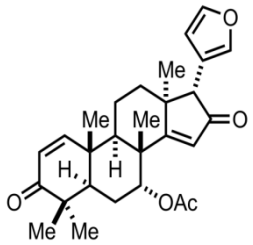

Figure 1.13: Structure of AZD

The present study has the following objectives:

1. To obtain AZD from Neem seeds in pure form.
2. To purify human HSF1 protein and its mutant derivatives.
3. To study the underlying molecular basis of the interaction of AZD with human HSF1 by various biochemical and biophysical approaches.

CHAPTER 2

MATERIALS AND METHODS

Materials:

Bacterial strain used for protein expression: *E. coli* BL21 (DE3). This strain harbours the λ prophage DE3. This prophage carries the T7 RNA polymerase gene which is under transcriptional control of the lacUV5 promoter and lacIq. IPTG (Isopropyl β-D-1-thiogalactopyranoside) induces the expression of T7 RNA polymerase. The pET15b plasmid transformed in this strain harbours an expression system directed by the T7 promoter. Thus, expression of the heterologous protein occurs only after IPTG-induced expression of T7 RNA polymerase. This strain lacks the lon protease and OmpT (outer membrane protease), which minimizes the degradation of the overexpressed heterologous protein (Studier et.al. 1986).

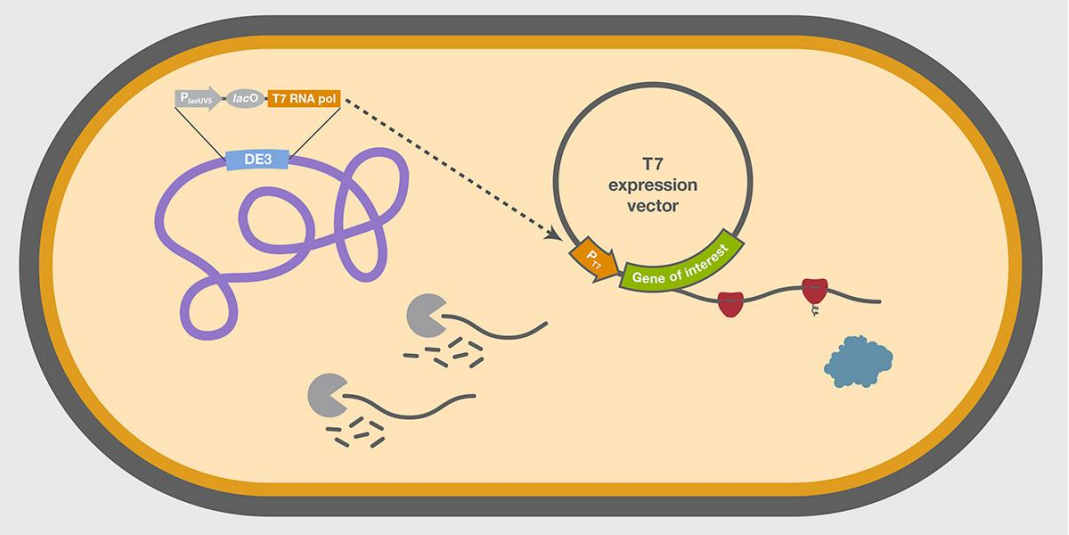

Figure 2.1: The *E. coli* BL21 (DE3) strain for overexpressing heterologous proteins

(Source: https://www.thermofisher.com/in/en/home/life-science/cloning/cloning-learning-center/invitrogen-school-of-molecular-biology/molecular-cloning/transformation/competent-cell-selection-applications.html)

Bacterial strain used for cloning: *E. coli* DH5α

Plasmid used for protein expression: pET15b

Reagents used:

1. *Organic solvents*: Hexane, dichloromethane, ethyl acetate, methanol, glacial acetic acid, absolute ethanol (molecular biology grade), dimethyl sulfoxide (cell culture grade), acetonitrile (HPLC grade)
2. Silica gel (230-400 mesh), silica-coated TLC plates

3. *Salts:* Sodium chloride, calcium chloride, Sodium Dodecyl Sulfate, Ammonium Persulfate
4. *Buffers*: HEPES [4-(2-hydroxyethyl)-1-piperazineethanesulfonic acid], Tris [2-Amino-2-(hydroxymethyl)-1,3-propanediol] base, Tricine
5. Luria-Bertani medium
6. Agar
7. Ampicillin
8. IPTG (Isopropyl β-D-1-thiogalactopyranoside)
9. Imidazole
10. Lysozyme (3× crystallized)
11. PMSF (Phenylmethanesulfonyl fluoride)
12. Ni-NTA (Nickel-Nitrilotriacetic acid) agarose beads
13. Dialysis membrane (MW cutoff: 10-12 kDa)
14. Glycerol
15. TEMED (N,N,N′,N′-Tetramethyl ethylenediamine)
16. Acrylamide and bisacrylamide
17. Glycine
18. Coomassie Brilliant Blue G250 and R250
19. Bromophenol Blue
20. Prestained protein ladder
21. 6-aminohexanoic acid
22. Protein molecular weight standards (for Size Exclusion Chromatography)
23. Bradford reagent
24. Synthetic DNA oligonucleotides (FAM labelled and unlabelled)
25. ANS (8-Anilinonaphthalene-1-sulfonic acid)
26. ThT (Thioflavin T)
27. Restriction Enzymes (*NdeI* and *XhoI*)
28. T4 DNA ligase
29. Q5 DNA polymerase
30. Deoxynucleoside triphosphates (dNTPs)
31. Plasmid purification kit (miniprep) and gel extraction kit
32. Agarose
33. Ethidium bromide
34. Sodium hydroxide pellets

35. Hydrochloric acid (37%)
36. EDTA (Ethylenediaminetetraacetic acid)
37. Ultrapure water

Primers used for cloning: The DNA sequences encoding HSF1-DBD (aa residues 1-123), HSF1-ΔRD-LZ4-TAD (aa residues 1-203), HSF1-ΔLZ4-TAD (aa residues 1-383) and HSF1-ΔTAD (aa residues 1-409) were PCR amplified from the coding sequence of full-length human HSF1. For this, the following primers were used:

Common forward primer:

5'-AGACATATGATGGATCTGCCGGTGGGTC-3'

HSF1-DBD reverse primer:

5'-AGACTCGAGTTAACTCACAGAGGTGACTTTGCGTTTG-3'

HSF1-ΔRD-LZ4-TAD reverse primer:

5'-AGACTCGAGTTACAGAATACGATTGCTCTGCACCAGC-3'

HSF1-ΔLZ4-TAD reverse primer:

5'-AGACTCGAGTTATTCATTTTTATCCAGACACGCAACAGACAGGC-3'

HSF1-ΔTAD reverse primer:

5'-AGACTCGAGTTACACACTAAAGCCGTGGCTCGACAG-3'

Methods:

Purification of Azadiradione

Azadiradione (AZD) was purified using the procedure described elsewhere with some modifications (Nelson et. al. 2016). Briefly, powdered seeds of *Azadirachta indica* (Neem), purchased from the local market, were soaked in methanol for about 7 days at room temperature with agitation at regular intervals to ensure proper solubilization of the compounds present in the seed. The methanolic extract of Neem seed, obtained after filtration through a Whatman

filter paper, was concentrated using a vacuum rotary evaporator set at 55°C. The concentrated extract thus obtained was mixed with silica gel (230-400 mesh) and exposed overnight to solvents of increasing polarity sequentially: hexane, dichloromethane (DCM), and ethyl acetate, for elution of the compounds present in the methanolic extract. The respective eluents were filtered off and dried to obtain hexane, DCM, and ethyl acetate fractions. Thin-layer chromatography (TLC) was carried out to identify the fraction with major AZD content by comparing it with previously purified AZD in our laboratory (control). TLC was done using a solvent system consisting of hexane and ethyl acetate mixed in the volume ratio 4:1. The DCM fraction, thus identified as the fraction with major AZD content, was mixed with silica gel (230-400 mesh) to prepare a slurry, which was then packed onto a glass column (length: 25 cm, diameter: 4 cm) having silica gel of the same mesh size. After an initial hexane wash, the contents of the DCM fraction were eluted with a solvent system having hexane and ethyl acetate in the volume ratio of 4:1 under gravity flow. About 100 ml fractions were collected. The TLC profile of each fraction was checked to pool the fractions containing the major amount of relatively pure AZD. The pooled fractions were dried as described above. The column purification was repeated with the pooled fractions to obtain AZD with maximum purity. To confirm the purity, analytical HPLC was performed with the AZD preparations using a C-18 column (dimension: 4.6 mm × 250 mm) and a mobile phase having 60% acetonitrile and 40% water. 20 µl of the sample was injected into the column. The flow rate of the mobile phase was maintained at 1ml/min. The identity of the purified compound was confirmed by performing NMR spectroscopy (^{1}H, ^{13}C, and DEPT-135) of the preparations and comparing the NMR spectra with that of pure AZD from published literature.

Workflow of AZD purification

Powdered seeds of *Azadirachta indica* (5 kg)

↓

Soaked in methanol and filtered to obtain methanolic extract

↓

Methanolic extract fractionated using Hexane, Dichloromethane, and Ethyl Acetate

AZD obtained mostly in DCM fraction (as per TLC analysis)

DCM fraction concentrated and packed in silica gel column (230-400 mesh). Mobile phase Hexane: EtOAc :: 4:1 passed through column and fractions collected

Fractions containing relatively pure AZD (tested by TLC profile) pooled together, concentrated, and dried. Column purification was repeated with the pooled fractions to obtain AZD of high purity.

HPLC profile and NMR spectra of AZD preparations were checked and compared with published literature.

Protein expression and purification

The codon-optimized DNA fragments encoding human HSF1 wild type and its mutants HSF1-ΔLZ1-3 and HSF1-LZ4m cloned in pET15b expression vector at *NdeI/XhoI* restriction sites were kind gifts from Prof. Dennis J. Thiele (Sisu Pharma). The C-terminal truncation

derivatives, HSF1-DBD (amino acid residues 1-123), HSF1-ΔLZ4-TAD (amino acid residues 1-383), and HSF1-ΔTAD (amino acid residues 1-409) were constructed similarly in pET15b vector, amplified from the codon-optimized *hsf1* sequence.

The above-mentioned constructs were transformed into *E. coli* strain BL21 (DE3) to overexpress the proteins in secondary cultures (OD_{600}~0.5) using 0.5 mM IPTG for 2-3 h at 28°C.

The cell pellets obtained by centrifugation of the cultures were resuspended in an ice-cold Lysis Buffer [50 mM HEPES-NaOH (pH 7.4), 300 mM NaCl, 25 mM imidazole (pH 8), 10% (v/v) glycerol,1 mM PMSF and 0.4 mg/ml lysozyme] for 30 min followed by sonication for 5 min in an ice-bath sonicator (30-sec bursts with 60-sec gaps). The crude lysate thus obtained was immediately centrifuged at 12000 rpm for 30 min at 4°C to collect the supernatant in a fresh tube. HSF1 protein is highly sensitive to proteases, so the following steps were performed in a cold room using ice-cold buffers. The cleared lysate was mixed with 2 ml of Ni-NTA agarose beads per liter of culture (pre-equilibrated in Lysis Buffer) and incubated in a rotary shaker for 2 h. This suspension was transferred to a column to collect the flowthrough under gravity. The settled beads in the column after washing once with 5× bead volume of Wash Buffer [50 mM HEPES-NaOH (pH 7.4), 300 mM NaCl, 30 mM imidazole (pH 8), 10% (v/v) glycerol] were eluted with an Elution Buffer [50 mM HEPES-NaOH (pH 7.4), 300 mM NaCl, 250 mM imidazole (pH 8), 10% (v/v) glycerol] in small fractions. The protein-containing fractions collected were analyzed by SDS-PAGE followed by Coomassie Brilliant Blue R250 gel staining. The fractions containing higher concentrations of desired protein (monitored by analyzing a small aliquot of each fraction) with minimal degradation products were pooled together and dialyzed overnight against Dialysis Buffer [25 mM HEPES-NaOH (pH 7.4), 150 mM NaCl, and 10% (v/v) glycerol].

Size Exclusion Chromatography of Affinity Purified Proteins

The oligomeric status of the affinity-purified proteins was determined by Size Exclusion Chromatography (SEC) using a Superdex200 Increase 10/300 GL column (GE Healthcare), pre-calibrated with standard molecular weight markers for SEC (purchased from Sigma

Aldrich) run in AKTA system. A standard curve was obtained by plotting these markers' log [Molecular weight] versus Elution Volumes. The column was run at a flow rate of 0.5 ml/min with Dialysis Buffer [25 mM HEPES-NaOH (pH 7.4), 150 mM NaCl, and 10% (v/v) glycerol] as the mobile phase. The elution profile of each protein preparation was monitored by associated absorbance at 280 nm. The protein concentrations of each (200 µl) fraction were estimated by Bradford assay for subsequent analysis of an aliquot by Blue Native PAGE. The fractions were finally flash-frozen in liquid nitrogen and stored at -80°C for further studies (Hentze et.al. 2016).

Blue Native PAGE

Blue Native PAGE was performed with various molecular species separated by SEC following the protocol described by Wittig et al. (2006) with some modifications. Briefly, protein samples were mixed with 10X Sample Buffer [Glycerol 50% (v/v), Coomassie Brilliant Blue G250 solution 0.2%, and Cathode Buffer-B 10% (v/v) *] and resolved in a 7% polyacrylamide native gel using Cathode Buffer-B [50 mM Tricine; 7.5 mM Imidazole (pH 7)] in the upper tank and Anode Buffer [25 mM Imidazole (pH 7)] in the lower tank at 4°C for 2-4 h. The gel was run at a constant current (15 mA) except at 100 V in the beginning for allowing the samples to enter the gel. It was monitored that the voltage did not exceed 500V for a gel dimension of 0.16 × 14 × 14 cm that was used. Protein bands were readily visible in the gel due to the Coomassie G250 dye in the sample buffer.

*Cathode Buffer-B 10% (v/v) is composed of 1ml Cathode Buffer-B in a total volume of 10ml Sample Buffer (10X)

Fluorescence Polarization Assay (FP Assay)

To study the interaction of human HSF1 and its derivatives with the cognate heat shock element (HSE), the DNA sequence 5'-CCTGGAATATTCCCGAACTGGC-3' containing three inverted 5'-nGAAn-3' repeats (three-site HSE or 3X-HSE; also referred to as the canonical HSE or cHSE) was tagged with fluorescein amide (FAM) at its 5' end (Jaeger et. al.2014). For obtaining a double-stranded DNA probe, the tagged sequence and its untagged complementary sequence

were annealed by heating them together at equimolar concentrations in an annealing buffer (5× annealing buffer composition: 50 mM Tris pH 8, 0.5 mM EDTA, 0.75 M NaCl) at 95°C in a heat block for 5 min followed by slow cooling to room temperature.

1 nM of the probe was titrated with increasing concentrations of HSF1 and its various derivatives in the absence and presence of AZD (10 μM). Fluorescence polarization was measured at 25°C in a quartz cuvette using an excitation wavelength of 495 nm and an emission wavelength of 517 nm. For this, the fluorescence intensities at 517 nm were measured for each sample in the following four orientations of the excitation and emission polarizers: HH, HV, VH, VV (in each case, the first and second letters indicate the relative positions of the excitation and emission polarizer, respectively; H: Horizontal, V: Vertical). Fluorescence Polarization (P) was calculated for each sample using the following equation (Lakowicz 2006):

$$\mathbf{P} = \frac{\mathbf{IVV} - \mathbf{G}.\mathbf{IVH}}{\mathbf{IVV} + \mathbf{G}.\mathbf{IVH}}$$

Here, G (Grating correction factor) $= \frac{\mathbf{IHV}}{\mathbf{IHH}}$

Binding curves for all HSF1 derivatives were obtained by plotting milli-polarization (mP) values obtained with increasing protein concentrations and dissociation constant (K_d) values determined for all protein-DNA interactions using one site-specific binding fit in GraphPad Prism 5.

The interaction of monomeric HSF1 with mutant HSE (mHSE) in the presence and absence of AZD was studied similarly. The sequence for mHSE is:

5’-CCTG**G**<u>**CG**</u>TA<u>**G**</u>**T**CCC<u>**CGC**</u>CTGGC-3’.

(The underlined bases shown have been mutated in the mHSE sequence.)

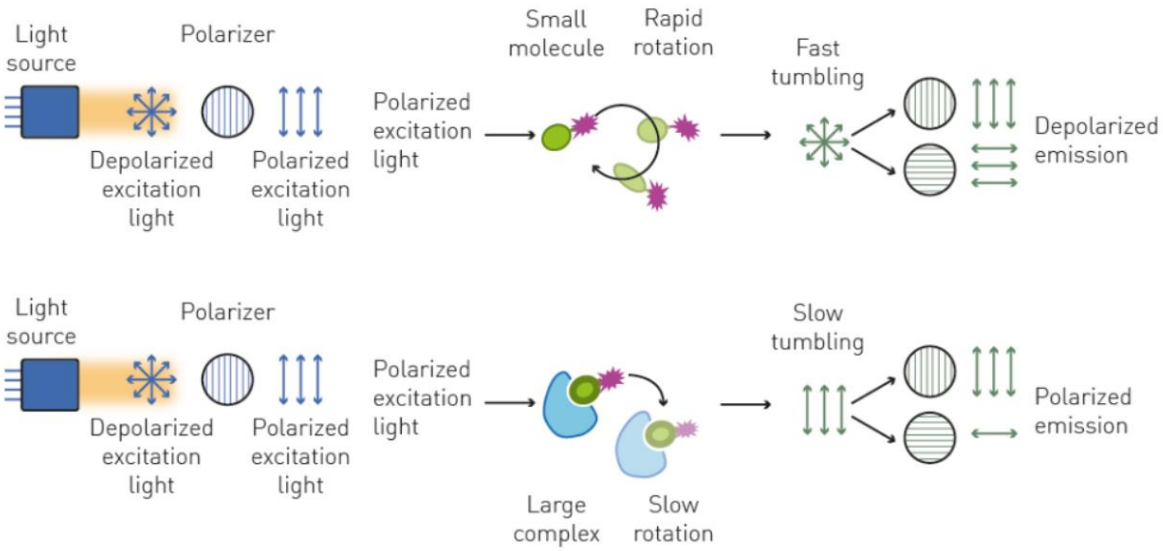

Figure 2.2: Principle of fluorescence polarization assay

(adapted from https://www.bmglabtech.com/en/fluorescence-polarization/)

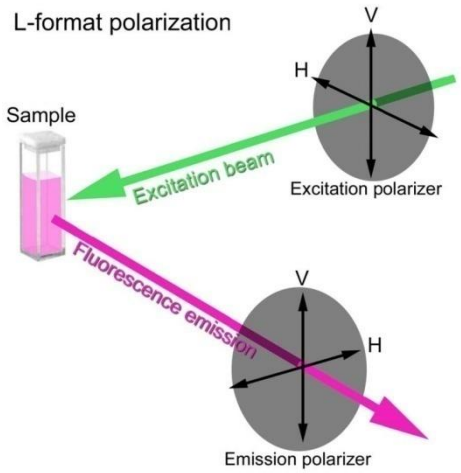

Figure 2.3: Schematic representation of the sample compartment and polarizers in a spectrofluorometer measuring fluorescence polarization (the 'L' format).

Source: https://www.horiba.com/int/scientific/applications/biotechnology-biomedical/pages/fluorescence-anisotropy-studies/

Dynamic Light Scattering (DLS) Assay

To compare the oligomeric status of human HSF1 and its derivatives in the presence and absence of AZD, dynamic light scattering assays were performed using Zetasizer Nano S (Malvern Instruments, Malvern, UK). The protein samples in the dialysis buffer [25 mM HEPES-NaOH (pH 7.4), 150 mM NaCl, and 10% (v/v) glycerol] were passed through a 0.22 µm syringe filter to remove any particulate matter before performing the assays. Samples (protein: ligand molar ratio set as 1:5) were incubated for 10 min at 25°C and scanned for DLS. Each data was taken as an average of 10 scan results. The hydrodynamic radius (R_H) was calculated by the instrument's software using the Stokes-Einstein equation:

$$R_H = \frac{kT}{6\pi\eta D}$$

where k is Boltzmann's constant, T is absolute temperature, η is the medium's viscosity, and D is the translational diffusion coefficient of the particle (Roy et. al. 2022).

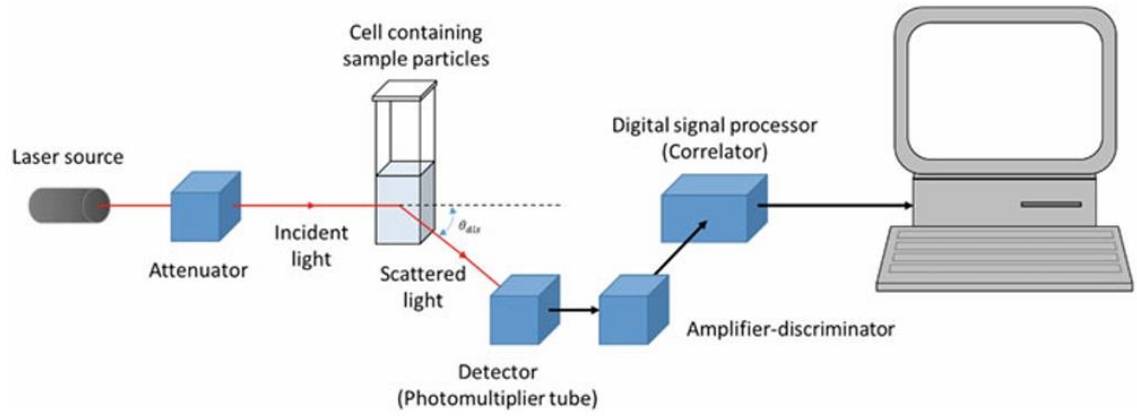

Figure 2.4: Diagram representing the experimental setup of DLS

(adapted from Leong et. al. 2018)

Protein Intrinsic Fluorescence Spectroscopy

The interaction of AZD with HSF1-WT monomer, HSF1-CM, and HSF1-DBD was studied in the absence of HSE using the intrinsic fluorescence of these proteins. The studies were conducted in the previously mentioned dialysis buffer [25 mM HEPES-NaOH (pH 7.4), 150

mM NaCl, and 10% (v/v) glycerol]. 2 μM of each protein was incubated with increasing concentrations (0-10 μM) of AZD in separate microfuge tubes at 4°C. DMSO was kept at 2% (v/v) for each reaction mixture. Next, the protein-AZD mixtures were excited at 280 nm, and the emission spectra were recorded from 300 to 400 nm at 25°C keeping the excitation and emission slit widths at 5 nm. The fluorescence spectrum of AZD in the buffer was subtracted from the protein spectra. The fluorescence intensity values at the maximum emission wavelength (λ_{max}) for each concentration of AZD were noted for each of these proteins. These values were then plotted against AZD concentrations to obtain binding isotherms. Data were analyzed in GraphPad Prism 5 using nonlinear regression with a 'one site-specific binding' model to obtain the K_d values (Seal et.al. 2023).

Analysis of HSE-AZD interactions by fluorescence spectroscopy

The interaction of AZD with canonical three-site HSE and mutant HSE was studied in the dialysis buffer [25 mM HEPES-NaOH (pH 7.4), 150 mM NaCl, and 10% (v/v) glycerol]. 10 nM 5'-FAM labeled double-stranded HSE (oligonucleotides) mentioned previously was incubated with varying concentrations (0-10 μM) of AZD in separate microfuge tubes at 4°C, maintaining DMSO concentration at 2% (v/v). Fluorescence emission spectra of the HSE-AZD mixtures were recorded at 25°C from 505-560 nm upon excitation at 495 nm setting the excitation and emission slit widths at 5 nm. The fluorescence intensity values at 520 nm (λ_{max}) at each concentration of AZD were noted for each of the oligonucleotides. These values were then plotted against increasing AZD concentrations to obtain binding isotherms. The equilibrium dissociation constant (K_d) values were obtained by analyzing the data in GraphPad Prism 5 using nonlinear regression with a 'one site-specific binding' model (Jaeger et. al. 2014, Seal et. al. 2023).

Cold competition assay for analyzing the interaction of canonical three-site HSE (double-stranded) with AZD

Four reactions were set up at 4°C in dialysis buffer as follows:

a. 10 nM FAM-labelled 3X-HSE + DMSO (vehicle)

b. 10 nM FAM-labelled 3X-HSE + 10 μM AZD

c. 10 nM FAM-labelled 3X-HSE + 10 nM cold 3X-HSE + 10 μM AZD

d. 10 nM FAM-labelled 3X-HSE + 100 nM cold 3X-HSE + 10 μM AZD

DMSO concentration was maintained at 2% (v/v) in all the reaction mixtures. Following incubation, the fluorescence intensities of these reaction mixtures were recorded at 25°C with emission in the range of 505-560 nm following excitation at 495 nm. The fluorescence intensities recorded at 520 nm for all the samples were plotted in a bar graph using GraphPad Prism 5 and compared.

The fluorescence polarization (FP) of FAM-labeled 3X-HSE was analyzed under identical conditions as elaborated above. Here, FP values of the samples at 520 nm were recorded after excitation at 495 nm, and these were plotted and compared in a bar graph.

8-Anilinonaphthalene-1-sulfonic acid (ANS) Binding Assay

For ANS binding experiments, proteins (2 μM) were incubated with varying concentrations of AZD (0-10 μM) for 30 minutes at 4°C in the dark with DMSO maintained at 2% (v/v) in each reaction mixture. The assay was conducted in the previously mentioned Dialysis Buffer [25 mM HEPES-NaOH (pH 7.4), 150 mM NaCl, and 10% (v/v) glycerol]. Next, 8-Anilinonaphthalene-1-sulfonic acid (ANS) solution prepared in dialysis buffer was added at a final concentration of 40 μM (20-fold molar excess of proteins) to the reaction mixtures, followed by a further incubation of 30 minutes in the dark at 4°C. After this, the emission spectra of the reactions were recorded in the range from 420 to 600 nm at 25°C following excitation at 390 nm (Sonawane et. al. 2021). Both the excitation and emission slit widths were set at 5 nm. The fluorescence intensity values at the maximum emission wavelength (λ_{max}) for each protein were plotted against the AZD concentrations.

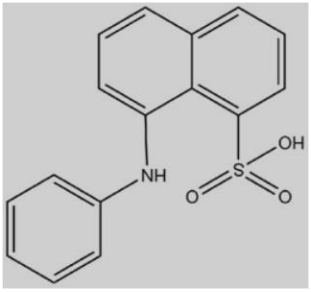

Figure 2.5: The structure of ANS

Thioflavin T (ThT) Binding Assay

Proteins (2 μM) were incubated with increasing concentrations of AZD (0-10 μM) in dialysis buffer for 30 minutes in the dark at 4°C. DMSO was maintained in all the reaction mixtures at 2% (v/v). ThT stock solution was prepared in dialysis buffer [25 mM HEPES-NaOH (pH 7.4), 150 mM NaCl, and 10% (v/v) glycerol] and was added at a final concentration of 4 μM to the reaction mixtures (molar ratio of Protein: ThT was 1:2) followed by a further incubation of 30 minutes in the dark at 4°C. After this, the emission spectra of the reactions were recorded in the range from 450 to 600 nm at 25°C following excitation at 440 nm (Zaman et. al. 2016). Appropriate blanks were also prepared by incubating AZD at varying concentrations with 4 μM ThT in dialysis buffer, and their emission spectra were subtracted from the sample spectra. The fluorescence intensity values at λ_{max}were plotted against AZD concentrations.

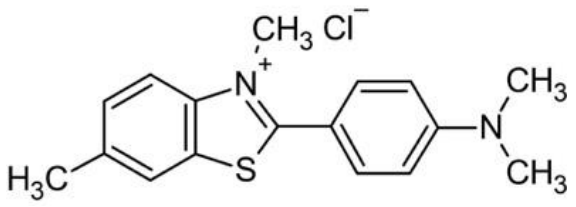

Figure 2.6: The Structure of Thioflavin T

Isothermal Titration Calorimetry

Isothermal Titration Calorimetry (ITC) was attempted to determine the thermodynamic parameters pertaining to the human HSF1-AZD interaction. A VP-ITC microcalorimeter (Microcal, Northampton, MA) was used for this purpose. The protein (10 μM) in Dialysis

Buffer [25 mM HEPES-NaOH (pH 7.4), 150 mM NaCl, and 10% (v/v) glycerol] was put in the reaction cell. AZD in Dialysis Buffer (at 100 µM concentration) was placed in the syringe. 2% DMSO (v/v) was maintained in both the solutions (in the reaction cell and syringe). The titration was done at 25°C. 10 µl of the AZD solution was injected into the reaction cell 25 times at 2 min intervals with constant stirring of the reaction mixture at 310 rpm. The heat of dilution of AZD in the buffer was subtracted from the titration data. Microcal Origin 7.0 (OriginLab Corporation, Northampton, MA) software was used for analyzing the data by the one-site binding model (Sinha et.al. 2021).

Statistical analyses

The results are presented as mean ± SD. Data analyses were done using one-way ANOVA (while comparing more than two groups) and two-tailed unpaired t-test (while comparing two groups) in GraphPad Prism 5 software. Results were statistically significant at $P < 0.05$.

CHAPTER 3

RESULTS

Purification of Azadiradione (AZD)

Azadiradione (approx. 800 mg) was purified from (5 kg) Neem seed powder as described in 'Materials and Methods'. The purity of the compound was verified by analysing the sample employing TLC followed by analytical HPLC. The preparation was close to 95% pure. The identity of the compound/ preparation was further confirmed by Nuclear Magnetic Resonance (NMR) spectroscopy (1H-NMR, 13C-NMR, and DEPT135-NMR) [Figs 3.1-3.5].

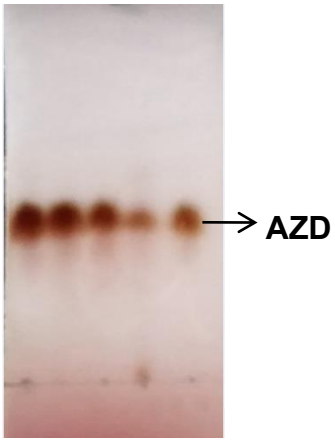

Figure 3.1: Thin Layer Chromatography (TLC) profile of an AZD preparation. TLC was performed using silica gel coated TLC plates (Merck) with mobile phase Hexane: Ethyl acetate :: 4:1

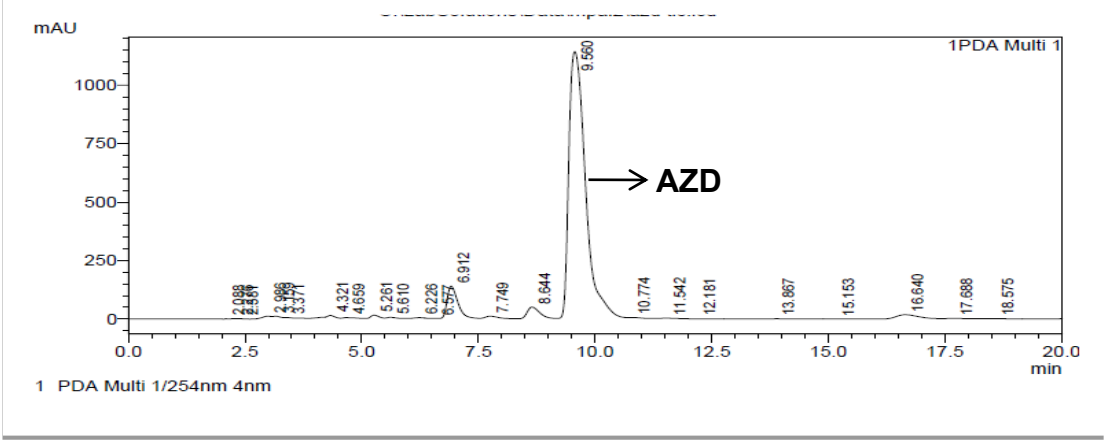

Figure 3.2: Analytical High-Performance Liquid Chromatography (HPLC) profile of an AZD preparation. The analysis involved a C-18 column with a mixture of acetonitrile (60%) and water (40%) as the mobile phase. The AZD retention time of 9.56 min is indicated by an arrow.

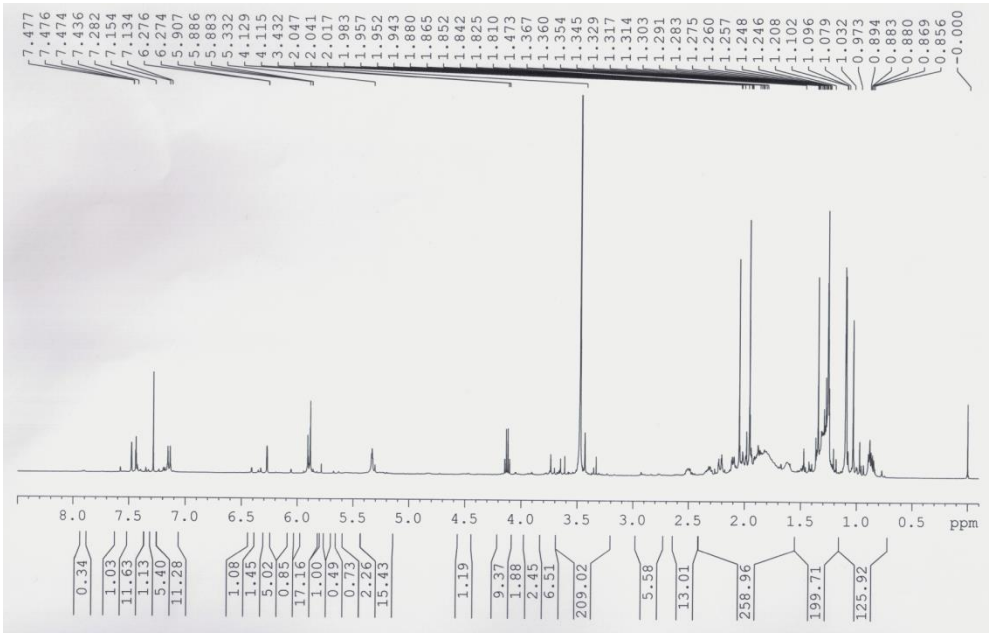

Figure 3.3: 1H-NMR spectrum of AZD.

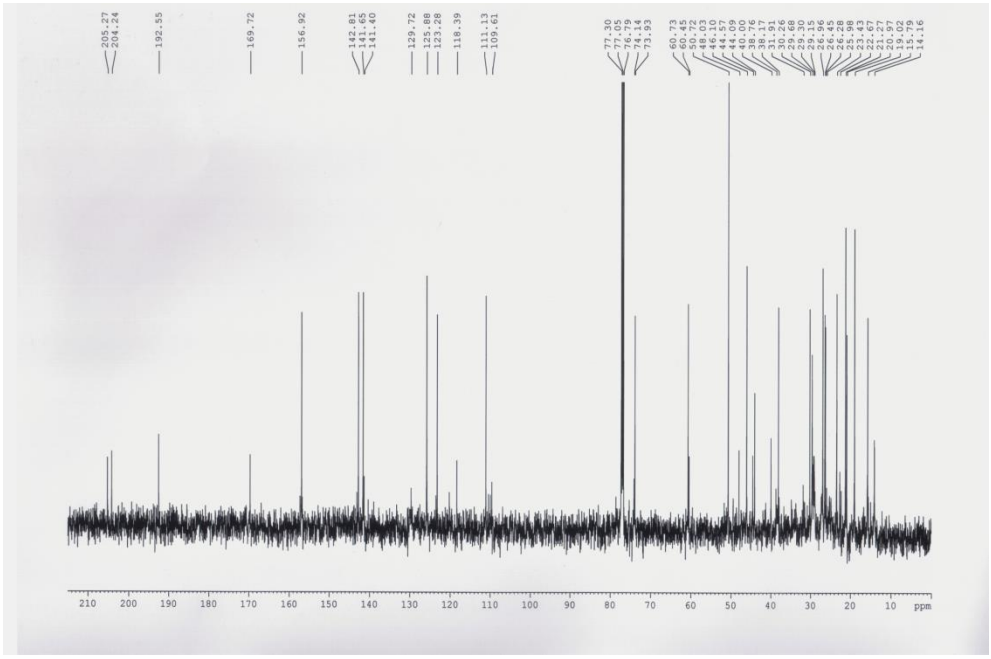

Figure 3.4: 13C-NMR spectrum of AZD.

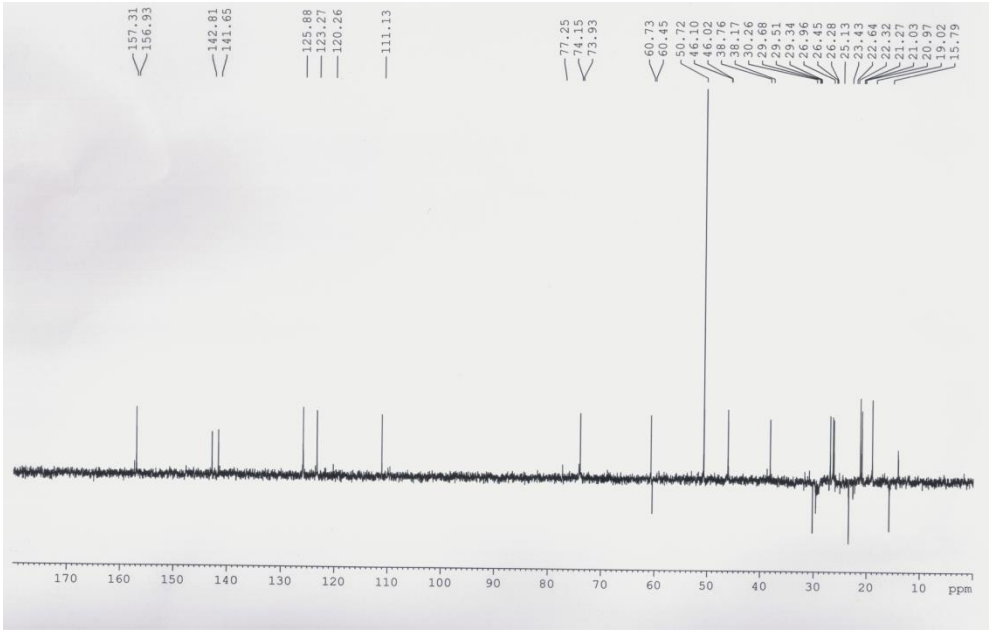

Figure 3.5: DEPT-135 NMR spectrum of AZD.

Purification of human HSF1 protein and its mutant derivatives from overexpressing *E. coli* strain using Ni-NTA agarose beads

To perform in vitro binding assays of AZD with different derivatives of human HSF1 protein, the following HSF1 mutants were generated (Fig.3.6):

1. HSF1-ΔLZ1-3, in which the oligomerization domain of HSF1 has been deleted. This protein stays in a constitutively monomeric form (Jaeger et.al. 2014).
2. HSF1-LZ4mutant (LZ4m), in which three residues (L391M, L395P, and L398P) in the C-terminal leucine zipper domain (LZ4) of HSF1 have been mutated to disrupt the interaction of the first Leucine Zipper domain LZ1-3 (a.k.a. the oligomerization domain) with LZ4. This protein stays in a constitutively trimeric/ oligomeric form (Jaeger et. al. 2014).
3. HSF1-DNA Binding Domain or HSF1-DBD consists of residues 1-123 of HSF1.

4. HSF1-ΔLZ4-TAD consists of the DBD, oligomerization, and the regulatory domain of HSF1.
5. HSF1-ΔTAD consists of the DBD, oligomerization, regulatory, and the LZ4 domain of HSF1.

We have also made several attempts to purify a truncation derivative of HSF1 consisting of the DBD and oligomerization domain (amino acid residues 1-203), but this derivative precipitated out of solution due to aggregation during dialysis, presumably due to its high level of hydrophobicity in the solution exposed regions. Hence, it could not be used in the present study.

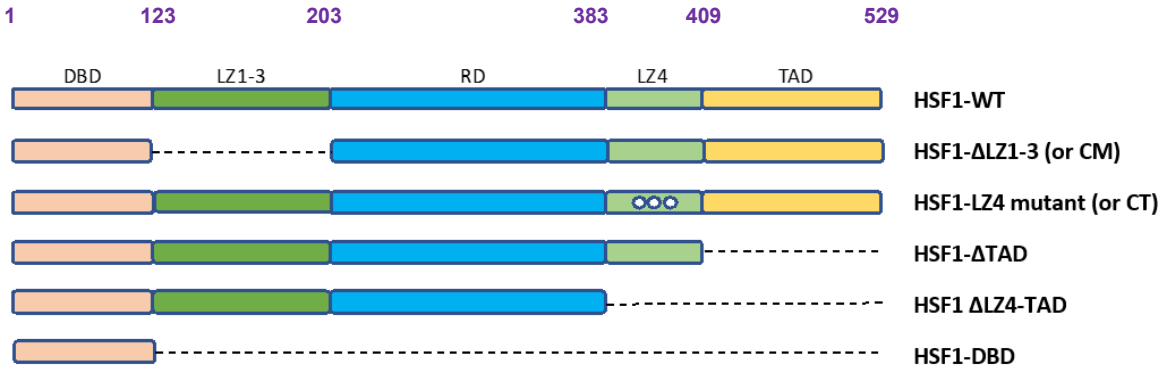

Figure 3.6: Human HSF1 protein (full length, 529 aa) and its derivatives used in the present study. Amino acid residue numbers marking the domain boundaries are indicated. [CM: Constitutive Monomer; CT: Constitutive Trimer; TAD: Transactivation Domain; DBD: DNA-Binding Domain; LZ: Leucine Zipper]

The above-mentioned derivatives along with the wild-type HSF1 were purified as described in the 'Materials and Methods' section. SDS-PAGE profiles of all the derivatives showed a single major band with minimal degradation.

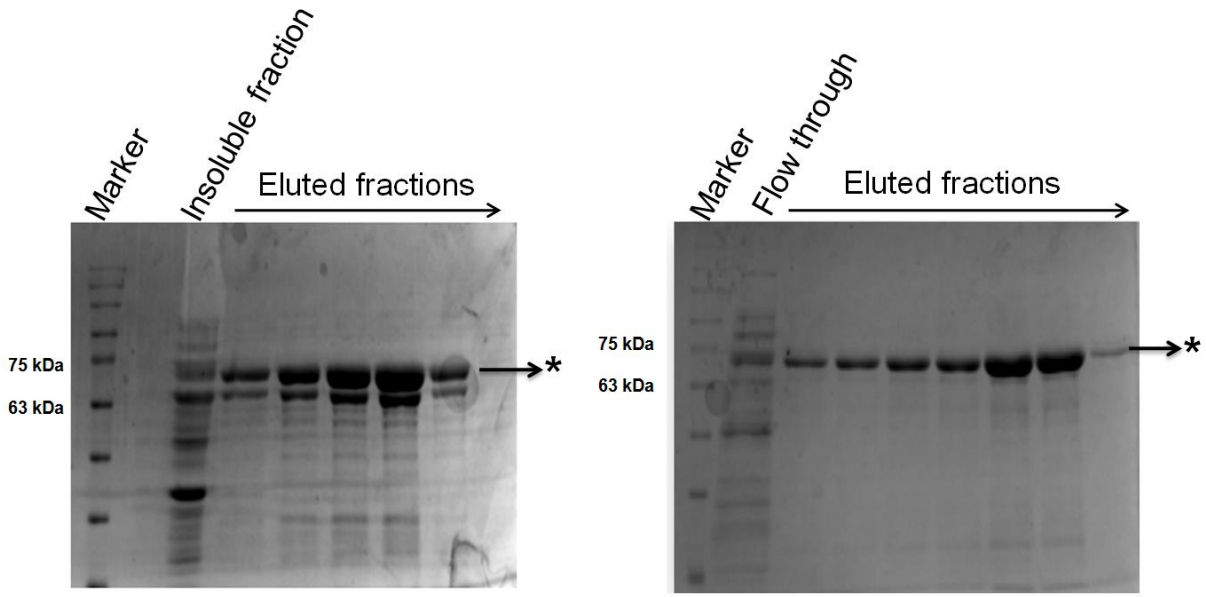

Figure 3.7: Coomassie-stained 10% SDS-polyacrylamide gels representing the purified HSF1-WT protein. HSF1-WT protein (calculated MW ~57 kDa) with significant cleavage (left) and minimal cleavage after proper standardization of the purification protocol (right). 20 µl aliquot from each fraction (~200 µl) was loaded into the gel. Arrows on the top indicate the order of fraction collection. (* The arrow indicates the intact HSF1-WT band.)

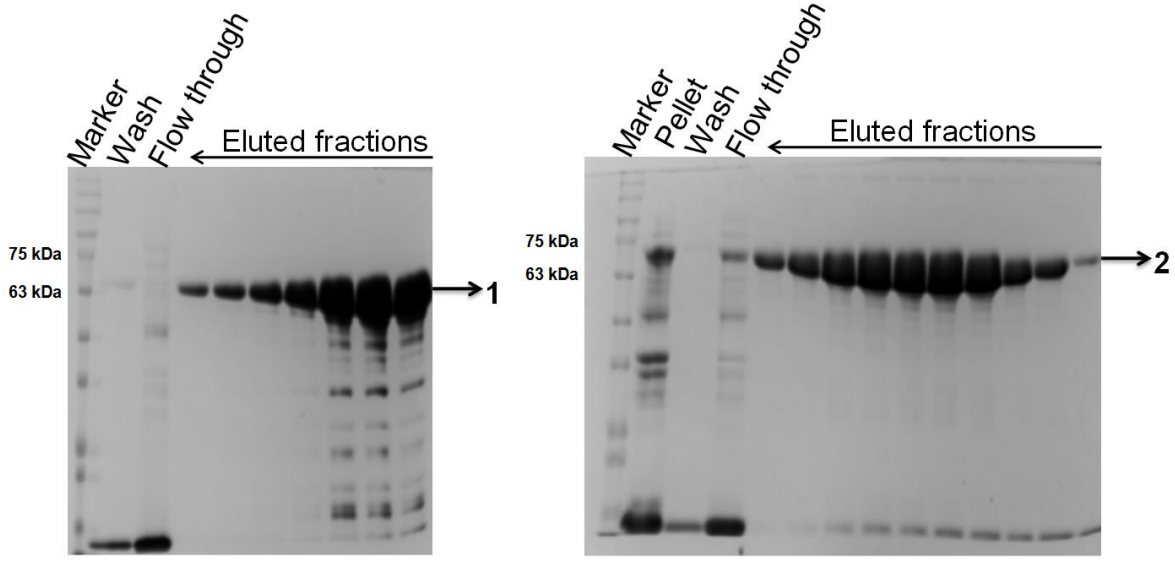

Figure 3.8: Coomassie-stained 10% SDS polyacrylamide gels representing the purified HSF1-ΔLZ1-3 (marked 1) and HSF1-LZ4m (marked 2). The calculated molecular weights (MWs) of HSF1-ΔLZ1-3 and HSF1-LZ4m are ~50 kDa and ~57 kDa, respectively. 20 µl

aliquot from each fraction (~200 µl) was loaded into the gel. Arrows on the top indicate the order of fraction collection.

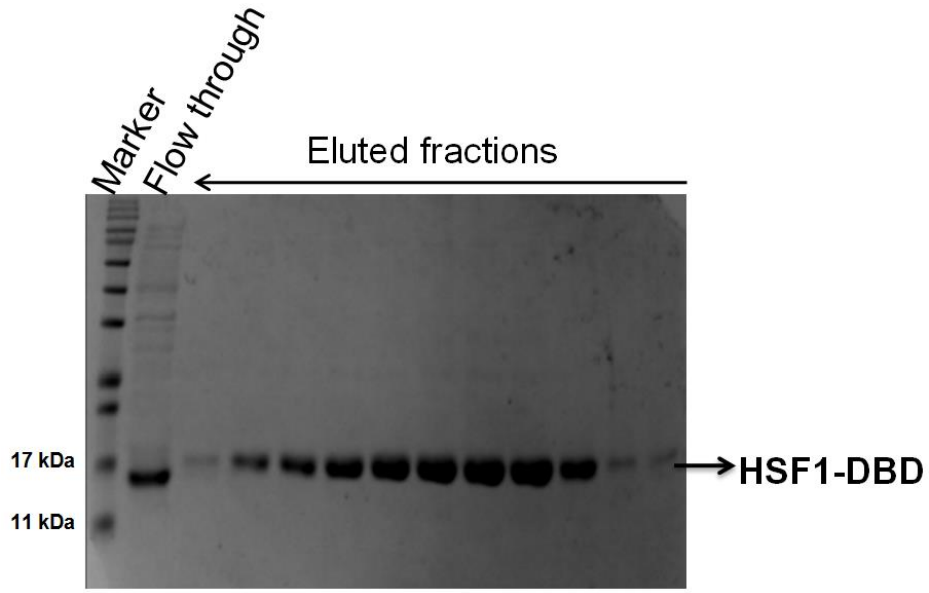

Figure 3.9: Coomassie-stained SDS-polyacrylamide gel (15%) representing the purified HSF1-DBD. Calculated MW is ~14 kDa. 20 µl aliquot from each fraction (~200 µl) was loaded into the gel. The arrow on the top indicates the order of fraction collection.

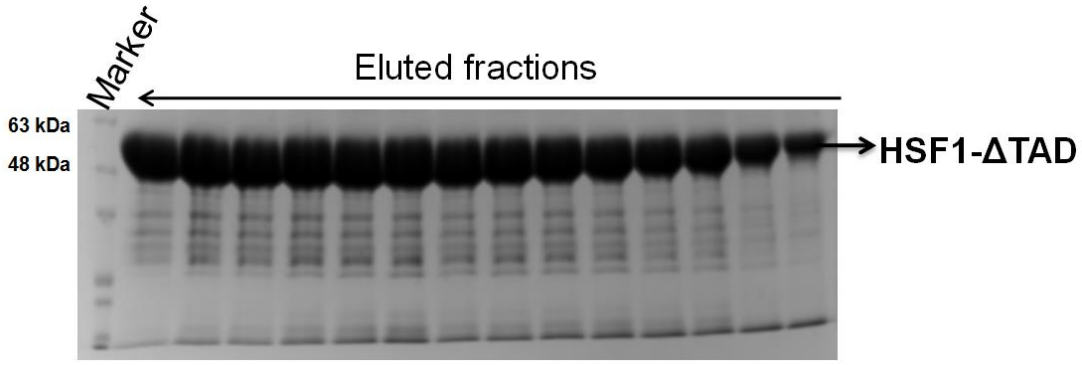

Figure 3.10: Coomassie-stained 10% SDS-polyacrylamide gel representing the purified HSF1-ΔTAD. The calculated MW is ~44.6 kDa. 20 µl aliquot from each fraction (~200 µl) was loaded into the gel. The arrow on the top indicates the order of fraction collection.

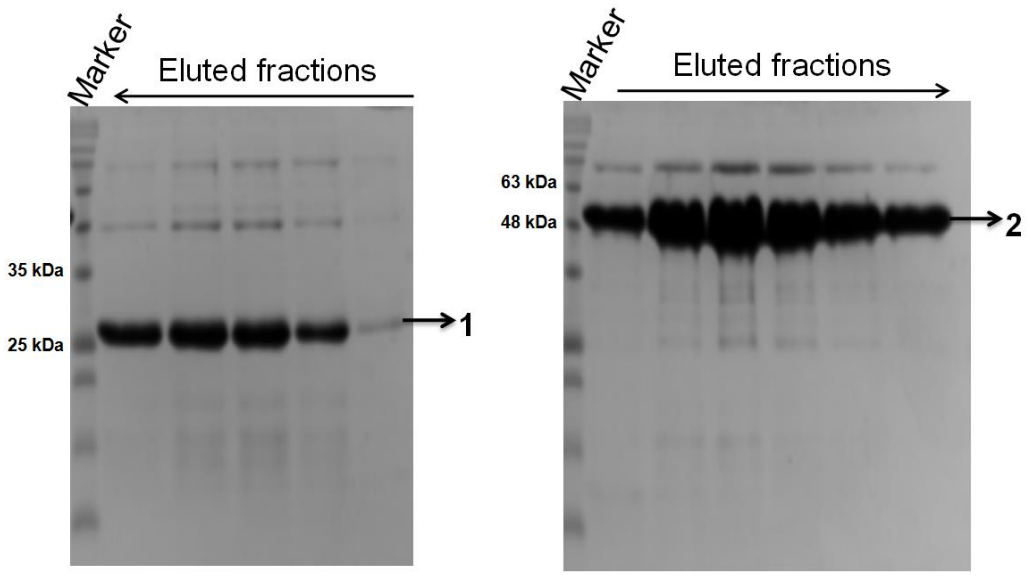

Figure 3.11: Coomassie-stained SDS-polyacrylamide gels (15%) representing the purified HSF1-ΔRD-LZ4-TAD (marked 1) and HSF1-ΔLZ4-TAD (marked 2). The calculated molecular weights of HSF1-ΔRD-LZ4-TAD and HSF1-ΔLZ4-TAD are ~23.14 kDa and ~41.81 kDa; respectively. HSF1-ΔRD-LZ4-TAD precipitated out of solution during dialysis, and hence could not be included in the present study. 20 µl aliquot from each fraction (~200 µl) was loaded into the gel. Arrows on the top indicate the order of fraction collection.

Isolation of monomer and oligomer of HSF1 by Size Exclusion Chromatography of the Affinity Purified Proteins

HSF1-WT purified from overexpressing *E. coli* strain has been reported to be a mixture of multiple molecular species (Jaeger et. al. 2014; Hentze et. al. 2016). Therefore, the proteins after Ni-NTA column purification were subjected to size exclusion chromatography (SEC) for further purification of different possible oligomeric species for each of these preparations as described in 'Materials & Methods.' The SEC profile of HSF1-WT revealed two prominent peaks: a taller peak (Peak 1) eluting at 8.77 ml and a smaller one at 12.44 ml (Peak 3). In addition, a small hump eluting at 10.59 ml was denoted as Peak 2. To determine the identity of these two peaks, we compared the SEC profiles of HSF1-ΔLZ1-3 and HSF1-LZ4m with that of the wild-type protein. HSF1-ΔLZ1-3, which remains in a constitutively monomeric (CM)

state, shows a major peak eluting at 11.86 ml, which is close to the elution volume (EV) of Peak 3 of HSF1-WT. On the other hand, HSF1-LZ4m (constitutive trimer, CT) shows a major peak at 8.52 ml, close to the EV of Peak 1 in HSF1-WT. When fractions containing all these peaks were analysed by blue native PAGE, Peak 3 of HSF1-WT (12.44 ml) and the major peak of HSF1-ΔLZ1-3 (11.86 ml) were found to have similar electrophoretic mobilities, the band position of the latter being slightly lower (as it is a deletion mutant, having residues 138-198 deleted). Peak 1 of HSF1-WT (8.77 ml) and the major peak of HSF1-LZ4m (8.52 ml) also showed very similar electrophoretic mobilities (Figs.3.12-3.15).

When heat shock was applied to fractions containing Peak 3 of HSF1-WT and run on a native gel, its band almost disappeared and a new band appeared higher up in the gel corresponding to the band position of Peak1 of HSF1-WT. Upon treating the heat-shocked sample with 10 mM DTT, the original band position was restored to some extent, corresponding to the non-heat-shocked sample. Heat shock treatment of the major peak of HSF1-ΔLZ1-3 caused no shift in its band position (Fig. 3.16). Taken together, it may be concluded that Peak 3 of HSF1-WT corresponds to the monomeric species, which upon heat shock treatment oligomerizes, and a shift in the band position is observed. DTT treatment post heat shock has been reported to cause monomerization of oligomeric HSF1 by disruption of an inter-subunit disulfide bond (Lu et al. 2008). This agrees with our observation. HSF1-ΔLZ1-3, the oligomerization domain-deficient mutant failed to oligomerize upon heat shock, thus no change in its band position was found. The Peak 1 of HSF1-WT corresponds to the trimeric/ higher oligomeric species which accounts for its similarity with the major peak of HSF1-LZ4m.

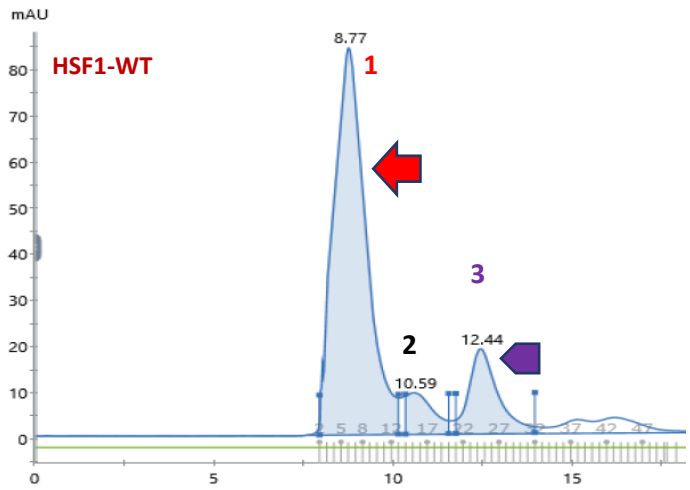

Figure 3.12: SEC profile of HSF1-WT preparation. The red and purple arrows indicate the trimeric/ oligomeric and monomeric species, respectively.

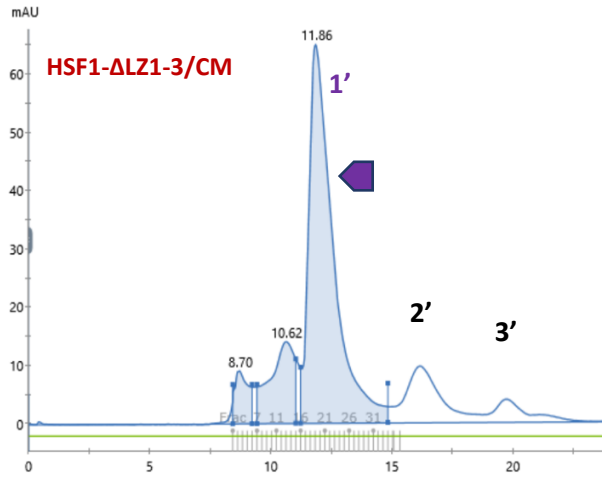

Figure 3.13: SEC profile of HSF1-Constitutive Monomer (CM) preparation. The purple arrow indicates the peak corresponding to HSF1-CM.

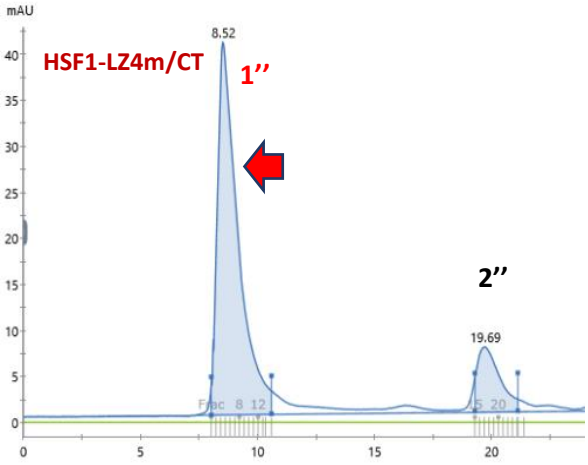

Figure 3.14: SEC profile of HSF1-Constitutive Trimer (CT) preparation. The red arrow indicates the peak corresponding to HSF1-CT.

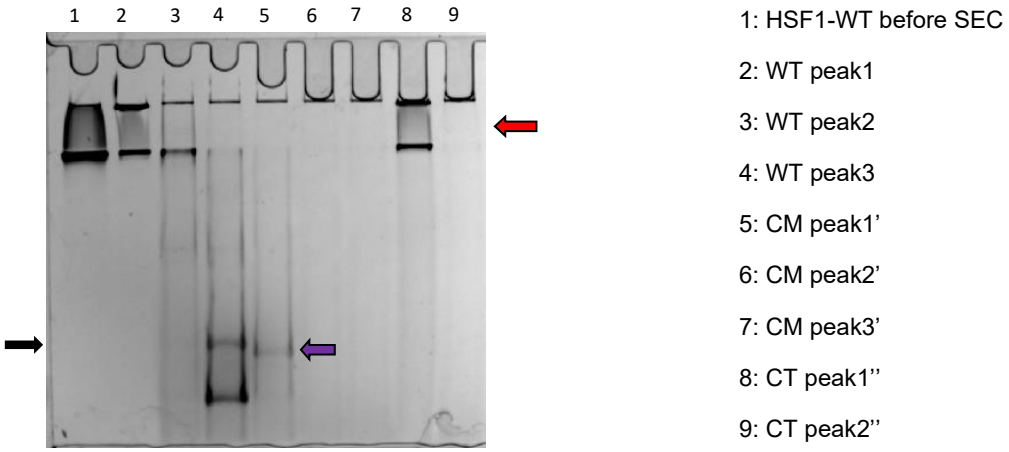

Figure 3.15: Resolution of molecular species of HSF1 derivatives obtained by SEC (shown in figures 3.12-3.14) using Blue Native PAGE (7%). The black arrow indicates the band position of the HSF1-WT monomer, the purple arrow indicates the band position of HSF1-CM, and the red arrow indicates the position of the trimeric/ oligomeric species of both HSF1-WT and -CT.

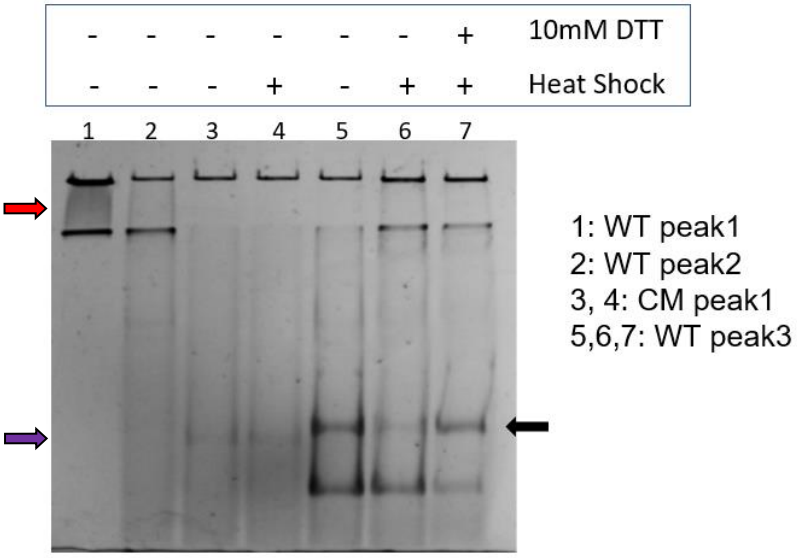

Figure 3.16: Analysis of SEC purified HSF1-WT monomer by Blue Native PAGE to confirm the purification of the HSF1-WT monomer as indicated by the black arrow. HSF1-CM is indicated by the purple arrow and HSF1-WT trimer/ oligomer by the red arrow.

The SEC profile of HSF1-DBD revealed the existence of a major peak (EV: 17.03 ml) along with a shorter peak at a lower EV **(**Fig. 3.17). We calculated the molecular weight of the major peak by putting its EV in the SEC MW standard curve as described in 'Materials and Methods' to be 17.78 kDa. This agrees well with the actual molecular weight of His_6-tagged DBD (~16 kDa). Thus, the major peak was identified as HSF1-DBD, and the shorter peak probably consisted of protein aggregates/ impurities. The Molecular weights of the other proteins used in this study could not be calculated similarly owing to the presence of intrinsically disordered regions (IDRs) in them (Iakoucheva et.al. 2001).

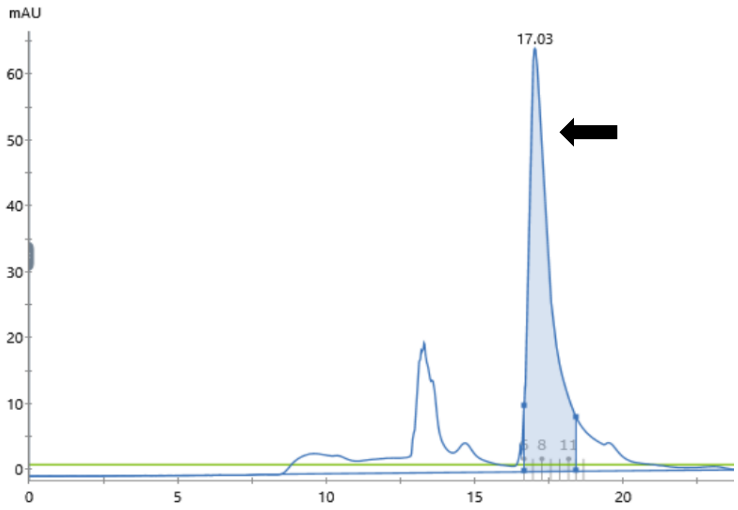

Figure 3.17: SEC profile of HSF1-DBD preparation. The arrow indicates the peak corresponding to HSF1-DBD.

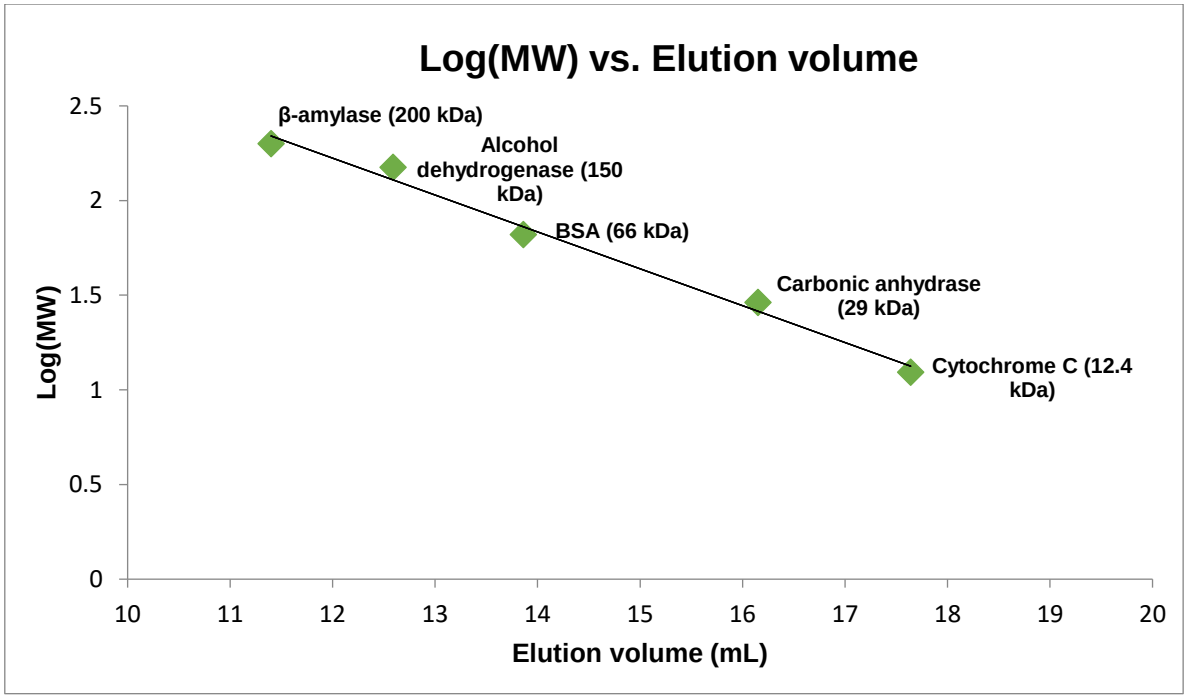

Figure 3.18: SEC standard curve obtained by resolving the indicated purified MW standards in the Superdex200 Increase 10/300 GL column. Log (MW) versus elution volumes were plotted. The molecular weight of His_6-tagged HSF1-DBD was calculated from this curve.

The SEC profile of HSF1-ΔLZ4-TAD eluted as a major peak at EV of 8.59 ml. This derivative is expected to remain in a multimeric form constitutively due to the absence of the LZ4 domain, which inhibits multimer formation. The observed EV, in this case, is in good agreement with the EVs of the trimeric/ oligomeric form of HSF1-WT and HSF1-LZ4m (Fig. 3.19).

For HSF1-ΔTAD, the SEC profile revealed a predominance of multimeric species (EV: 8.03 ml) followed by a very small quantity of monomeric species eluted at 13.57 ml. Attempts to concentrate this monomeric species resulted in its aggregation. For this reason, we used this derivative directly after the affinity purification for further studies without subjecting it to SEC (Fig. 3.20).

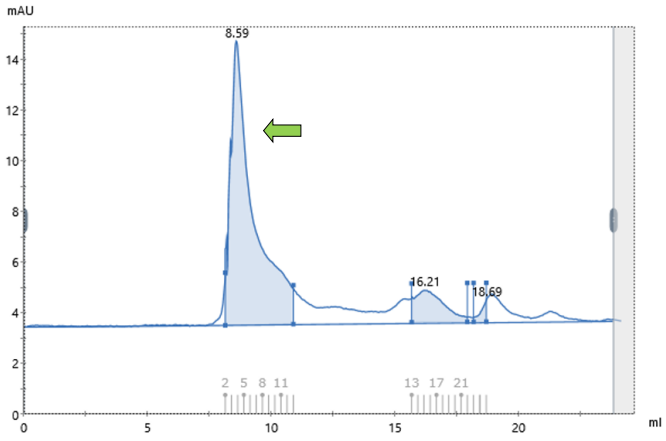

Figure 3.19: SEC profile of HSF1-ΔLZ4-TAD preparation. The major peak indicated by the green arrow corresponds to the protein.

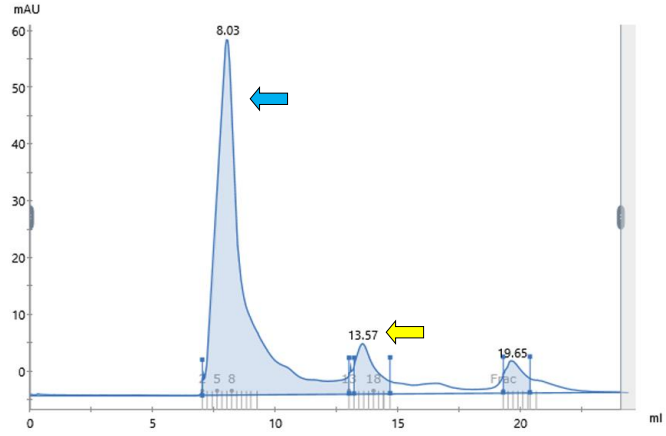

Figure 3.20: SEC profile of HSF1-ΔTAD preparation. The major peak indicated by the blue arrow corresponds to the multimeric species of the protein. The peak indicated by the yellow arrow possibly corresponds to the monomeric species.

Monomeric HSF1 forms homomultimer upon incubation with AZD and binds the heat shock element with high affinity

To understand the effect of AZD on the interaction of monomeric wild-type HSF1 with canonical heat shock element (HSE), we used Fluorescence Polarization Assay (FP Assay) to determine the affinity of their interaction both in the presence and absence of the compound.

When a fluorophore is excited with polarized light, it emits light having the same plane of polarization. If there is rotation of the fluorophore between excitation and emission, the plane of polarization of the emitted light will also rotate with it, resulting in depolarization of the emitted light. The rotational diffusion of a fluorophore can, therefore, be studied using fluorescence polarization. In our case, the fluorophore is a Fluorescein Amide (FAM) moiety covalently attached to the 5' end of one of the annealed complementary oligonucleotide strands of canonical HSE (23 bp) (Fig. 3.21). When no protein is bound to the HSE, the fluorophore enjoys a high rate of rotational diffusion, and as a result polarization of emitted light is low for unbound DNA. As more and more protein binds with HSE in the solution, it restricts the rate of rotational diffusion of the fluorophore, increasing the polarization of emitted light. By measuring the increase in polarization upon titration of protein to a fixed concentration of fluorophore-tagged DNA, a binding curve is obtained and the dissociation constant (K_d) value of the interaction can be determined from the curve.

The interaction of monomeric HSF1 with canonical HSE in the absence of AZD yielded a mean K_d value of 56.74 nM. When 10 μM AZD was present in the reaction mixture, the mean K_d value dramatically reduced to 7.8 nM (Fig. 3.21). A decrease in the K_d value indicates an increase in the binding affinity. Thus, AZD was found to increase the binding affinity of monomeric HSF1 with HSE by ~7.1-fold. To understand if this increase in binding affinity was due to the formation of a trimeric/ higher HSF1 oligomeric structure, we performed a Dynamic Light Scattering (DLS) assay. The addition of AZD to monomeric HSF1 in the absence of HSE was found to increase the hydrodynamic radius of the protein appreciably. Thus, AZD causes multimerization of HSF1-WT monomer here in the absence of proteotoxic stress, increasing its binding affinity for HSE considerably.

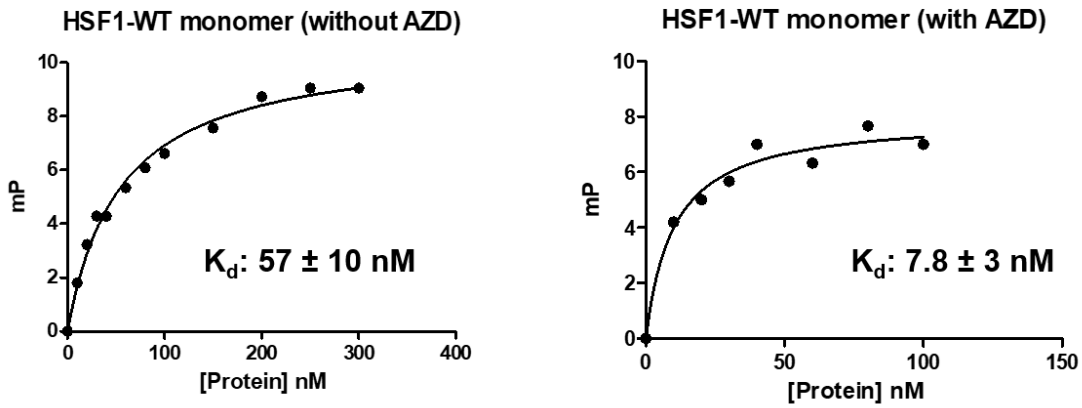

FAM-5'-CCTGGAATATTCCCGAACTGGC-3'

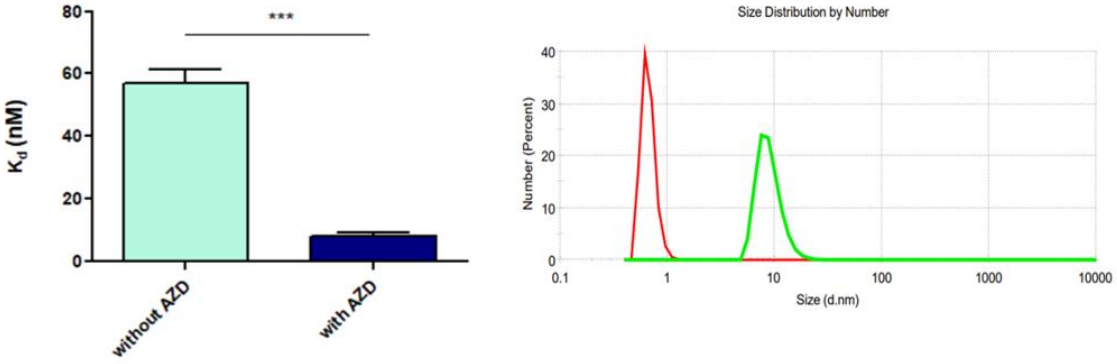

Figure 3.21: AZD increases the binding affinity of HSF1-WT monomer to FAM-labelled canonical HSE as determined by Fluorescence Polarization Assay.

Upper panel: Binding curve obtained by plotting the millipolarization values corresponding to protein concentrations (in nM) in the absence and presence of AZD. K_d values were obtained using GraphPad Prism 5 software.

FAM (fluorescein amide) labelled canonical HSE nucleotide sequence is shown with 5'--GAA--3' units underlined.

Lower panel (left): Bar graph representing the K_d values in the presence and absence of AZD.

Lower panel (right): The effect of AZD on the oligomeric status of HSF1-WT monomer (in the absence of HSE) studied by Dynamic Light Scattering (DLS) Assay. The peak drawn in red

indicates the size distribution of the protein without AZD. The peak drawn in green (with a greater hydrodynamic radius) indicates the protein's size distribution in the presence of the compound.

AZD increases the binding affinity of constitutively monomeric HSF1 for heat shock element

The oligomerization domain of HSF1 (LZ1-3) is essential for the heat shock-induced trimerization/ multimerization of the protein by forming a triple-stranded coiled-coil structure. An internal deletion construct lacking this domain (HSF1-ΔLZ1-3) has been shown not to oligomerize upon heat shock treatment (Fig. 3.16). We wished to study the effect of AZD on this construct and compare it with that on wild-type monomeric HSF1. As expected, HSF1-ΔLZ1-3 bound canonical HSE sequence with very low affinity having a mean K_d value of 490.92 nM (Fig. 3.22). However, to our astonishment, in the presence of 10 μM AZD, the binding affinity was dramatically increased, yielding a mean K_d value of 6.35 nM (Fig. 3.22). Thus, as previously reported, HSF1-ΔLZ1-3 binds the canonical HSE with a much lower affinity compared to the HSF1-WT monomer in the absence of AZD (Jaeger et.al. 2014). Intriguingly, the affinity of HSF1-ΔLZ1-3 and HSE interaction becomes comparable to that of HSF1-WT monomer-HSE interaction in the presence of AZD (Figs. 3.21 and 3.22).

Consistently, in the DLS study, the hydrodynamic radius of HSF1-ΔLZ1-3 increased considerably upon incubation with AZD in the absence of HSE, like the HSF1-WT monomer (Fig. 3.21). These results point to the idea that the absence of the oligomerization domain does not affect AZD-induced multimerization and DNA binding of HSF1, which is in stark contrast to heat shock-induced activation. Additional studies will clarify the molecular basis of this finding.

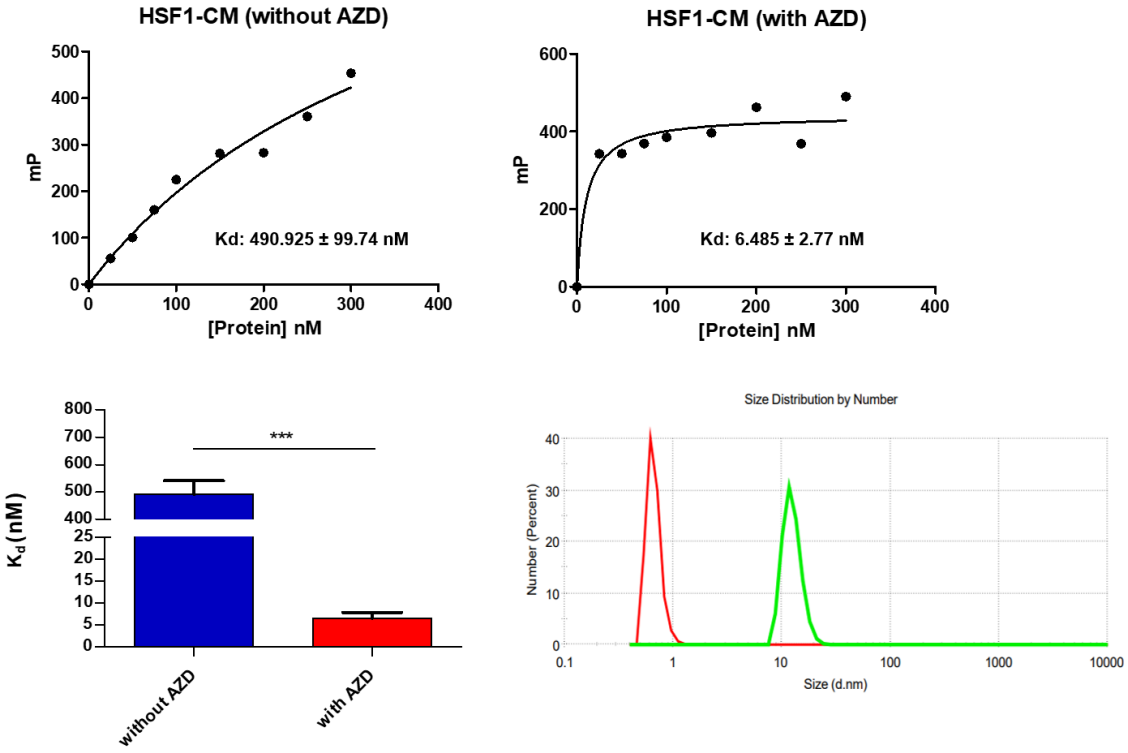

Figure 3.22: AZD facilitates the binding of HSF1-CM to the FAM-labelled canonical HSE as determined by Fluorescence Polarization Assay.

Upper panel: Binding curve derived by plotting the millipolarization values corresponding to protein concentrations (in nM) in the absence and presence of AZD. The K_d values were obtained using GraphPad Prism 5 software.

Lower panel (left): Bar graph representing the K_d values in the presence and absence of AZD.

Lower panel (right): The effect of AZD on the oligomeric status of HSF1-CM (in the absence of HSE) studied by DLS Assay. The peak drawn in red indicates the size distribution of the protein without AZD. The peak drawn in green (with a greater hydrodynamic radius) indicates the protein's size distribution in the presence of the compound.

Azadiradione interrupts the binding of trimeric/multimeric HSF1 with heat shock element

One of the key steps in the activation of HSF1 is its trimerization/ multimerization upon exposure to stressful conditions, which increases the affinity of HSF1 protein for the HSE sequences present in the promoters of its target genes (Dayalan Naidu et. al. 2017). We wished to study the effect of AZD on the interaction of the trimeric/ multimeric form of HSF1-WT protein (obtained by SEC) with canonical HSE. FP assay determined the mean K_d of this interaction in the absence of AZD to be 17.45 nM. In the presence of 10 μM AZD, the mean K_d value of this interaction increased to 112.59 nM. Thus, AZD causes a decrease in the binding affinity of HSF1-WT trimer/ oligomer for the HSE sequence by ~6.4-fold (Fig. 3.23). Notably, AZD increased the affinity of HSF1-WT monomer from 56.74 nM to 7.8 nM (7.1 -fold) (Fig. 3.21).

Next, we studied the effect of AZD on the interaction of HSF1-LZ4mutant with canonical HSE sequence. As mentioned earlier, this mutant remains in a constitutively trimeric/ oligomeric form and shares the same SEC elution profile with the HSF1-WT trimer/ oligomer (Figs. 3.12 and 3.14). Without AZD, this interaction yielded a mean K_d value of 25.06 nM. However, in the presence of 10 μM AZD, the mean K_d value increased to 114.12 nM. Thus, like HSF1-WT trimer/ oligomer, AZD was found to compromise the binding of HSF1-LZ4mutant with canonical HSE, decreasing the binding affinity by ~4.5-fold (Fig. 3.24).

To check whether this decrease in HSE binding affinity is caused by a disruption of the oligomeric structures by AZD, we performed a DLS assay. Interestingly, DLS studies have revealed a small increase in the hydrodynamic radii of these two forms of HSF1 upon incubation with AZD. This could indicate a destabilization of the proteins upon AZD binding (Ishtikhar et. al. 2016), which accounts for their decrease in binding affinity with canonical HSE.

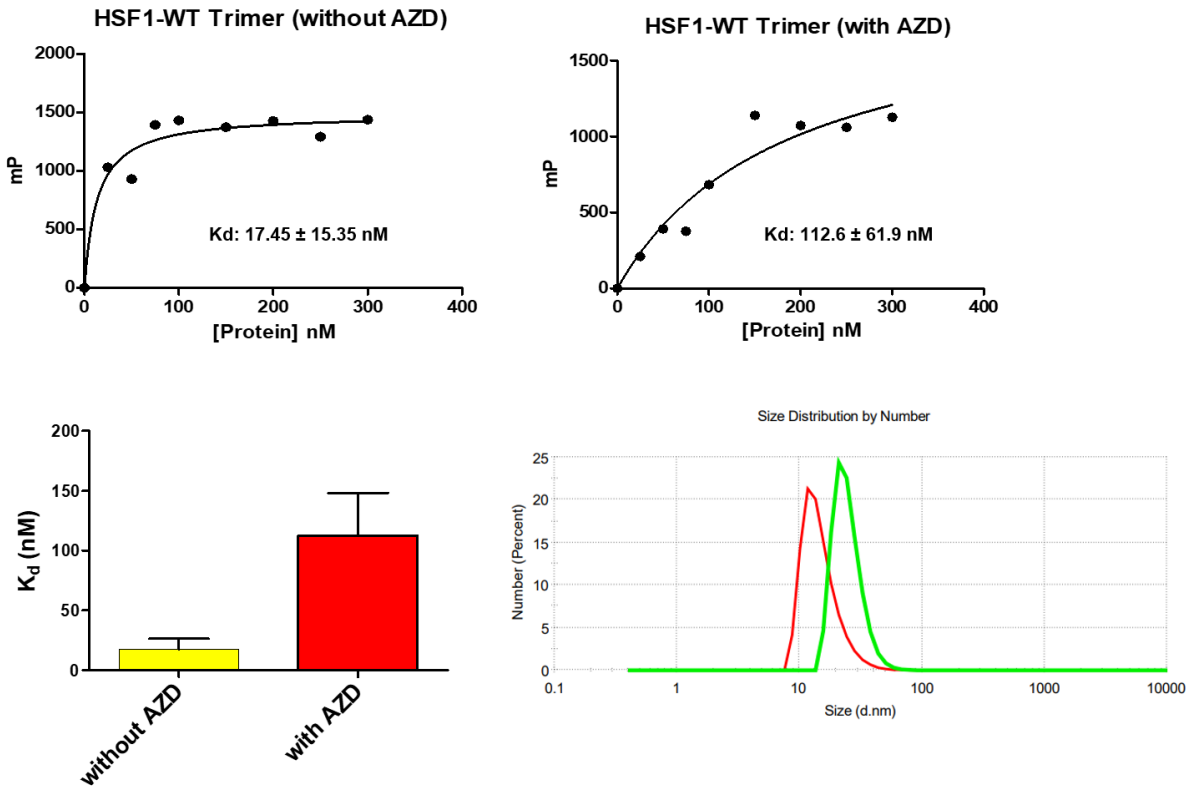

Figure 3.23: AZD disrupts the binding of HSF1-WT trimer and FAM labelled canonical HSE as revealed by Fluorescence Polarization Assay.

Upper panel: Binding curve derived by plotting the millipolarization values corresponding to protein concentrations (in nM) in the absence and presence of AZD. The K_d values were obtained using GraphPad Prism 5 software.

Lower panel (left): Bar graph representing the K_d values in the presence and absence of AZD.

Lower panel (right): Effect of AZD on the oligomeric status of HSF1-WT Trimer/ oligomer (in the absence of HSE) studied by DLS Assay. The peak drawn in red indicates the size distribution of the protein without AZD. The peak drawn in green (with a greater hydrodynamic radius) indicates the protein's size distribution in the presence of the compound.

.

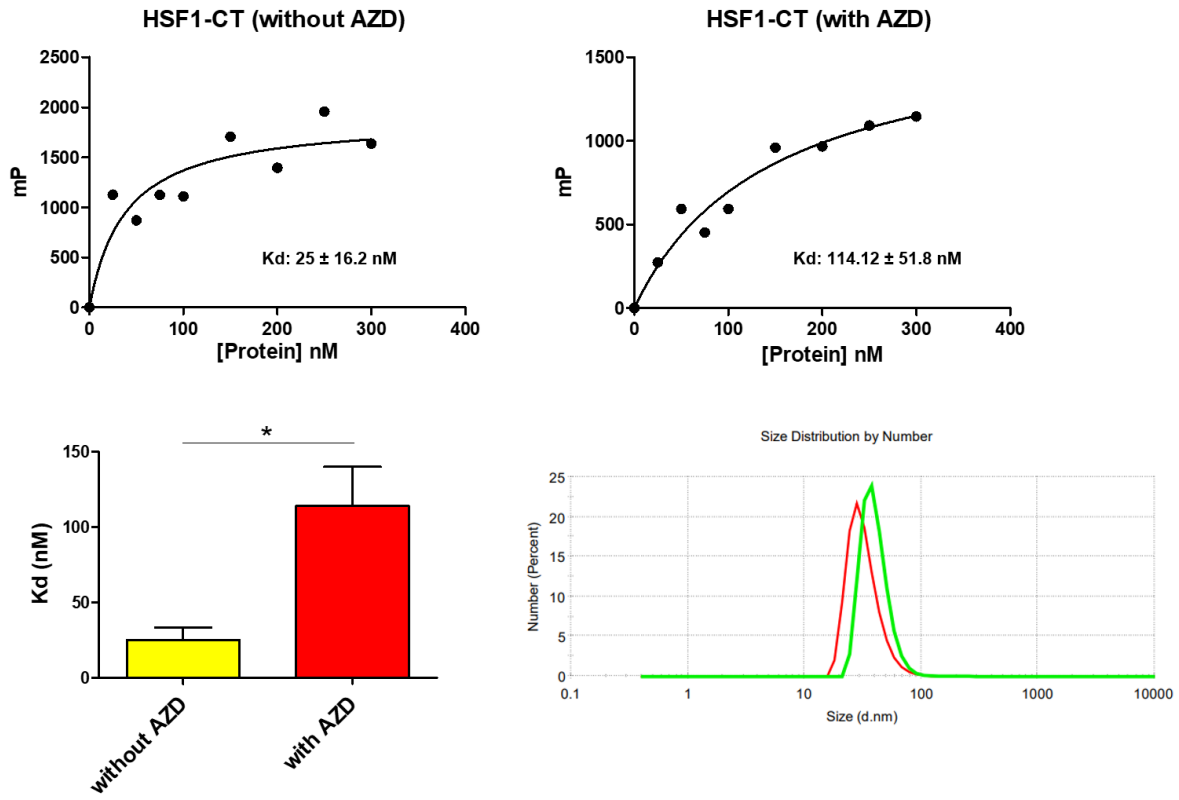

Figure 3.24: AZD disrupts the binding of HSF1-CT and FAM labelled canonical HSE as revealed by Fluorescence Polarization Assay.

Upper panel: Binding curve derived by plotting the millipolarization values corresponding to protein concentrations (in nM) in the absence and presence of AZD. The K_d values were obtained using GraphPad Prism 5 software.

Lower panel (left): Bar graph representing the K_d values in the presence and absence of AZD.

Lower panel (right): Effect of AZD on the oligomeric status of HSF1-CT (in the absence of HSE) obtained by DLS Assay. The peak drawn in red indicates the size distribution of the protein without AZD. The peak drawn in green (with a greater hydrodynamic radius) indicates the protein's size distribution in the presence of the compound.

The DNA Binding Domain of HSF1 plays a significant role in the AZD-induced binding of HSF1 to heat shock element

We have prepared C-terminal truncation derivatives of HSF1 to gain insight into the domain(s) involved in AZD-induced binding of HSF1 to HSE. HSF1-ΔTAD was shown to bind canonical HSE sequence with a mean K_d value of 58.68 nM, which was increased to 202 nM in the presence of 10 μM AZD. DLS study showed a small increase in the hydrodynamic radius of HSF1-ΔTAD upon incubation with AZD in the absence of HSE (Fig. 3.25). This result suggests destabilization of the protein structure upon AZD binding, contributing to the reduction in HSE binding affinity.

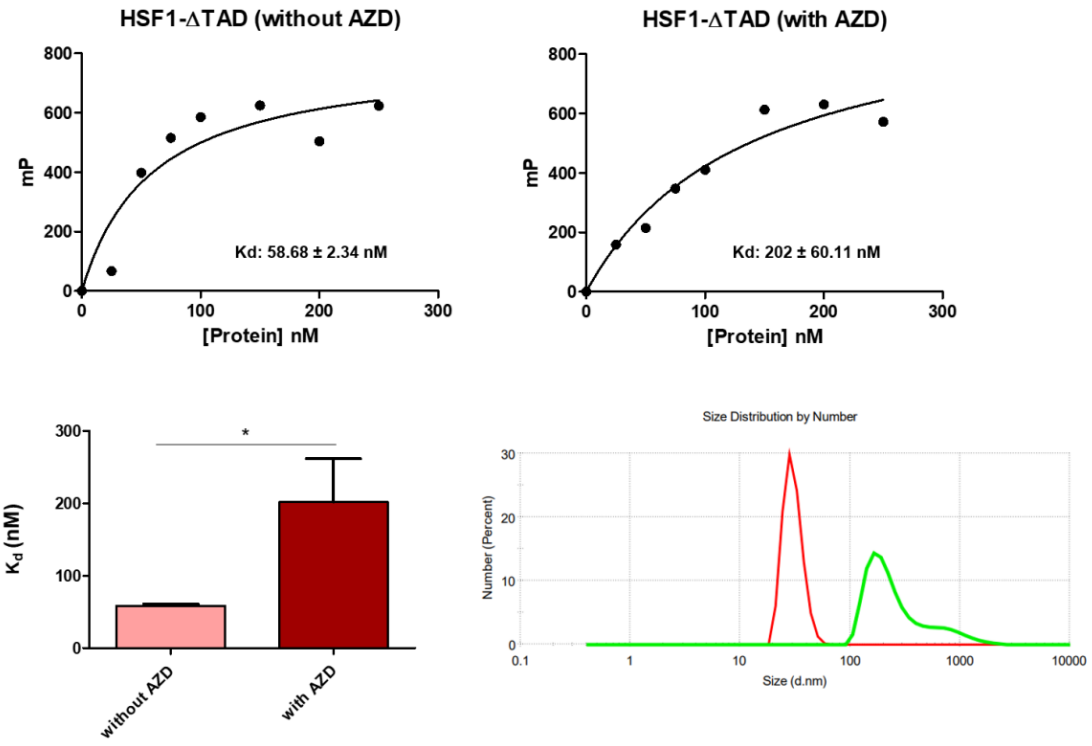

Figure 3.25: AZD disrupts the binding of HSF1-ΔTAD and FAM labelled canonical HSE as revealed by Fluorescence Polarization Assay.

Upper panel: Binding curve derived by plotting the millipolarization values corresponding to protein concentrations (in nM) in the absence and presence of AZD as indicated. The K_d values were obtained using GraphPad Prism 5 software.

Lower panel (left): Bar graph representing the K_d values in the presence and absence of AZD.

Lower panel (right): Effect of AZD on the oligomeric status of HSF1-ΔTAD (in the absence of HSE) studied by DLS Assay. The peak drawn in red indicates the size distribution of the protein without AZD. The peak drawn in green (with a greater hydrodynamic radius) indicates the protein's size distribution in the presence of the compound.

HSF1-ΔLZ4-TAD, consisting of DBD, LZ1-3, and RD, is expected to remain in a multimeric state, as it lacks the autoinhibitory LZ4 domain (which can bind with LZ1-3 and prevent multimer formation). We found this protein to bind canonical HSE with a mean K_d value of 22.56 nM in the absence of AZD. The binding affinity increased by a small margin (mean K_d value of 12.92 nM) in the presence of 10 µM AZD. DLS study indicated a slight increase in the protein's hydrodynamic radius upon AZD exposure. As this protein's affinity for canonical HSE underwent only a small change upon exposure to AZD (when compared to the other proteins used in this study), it was not studied further (Fig. 3.26).

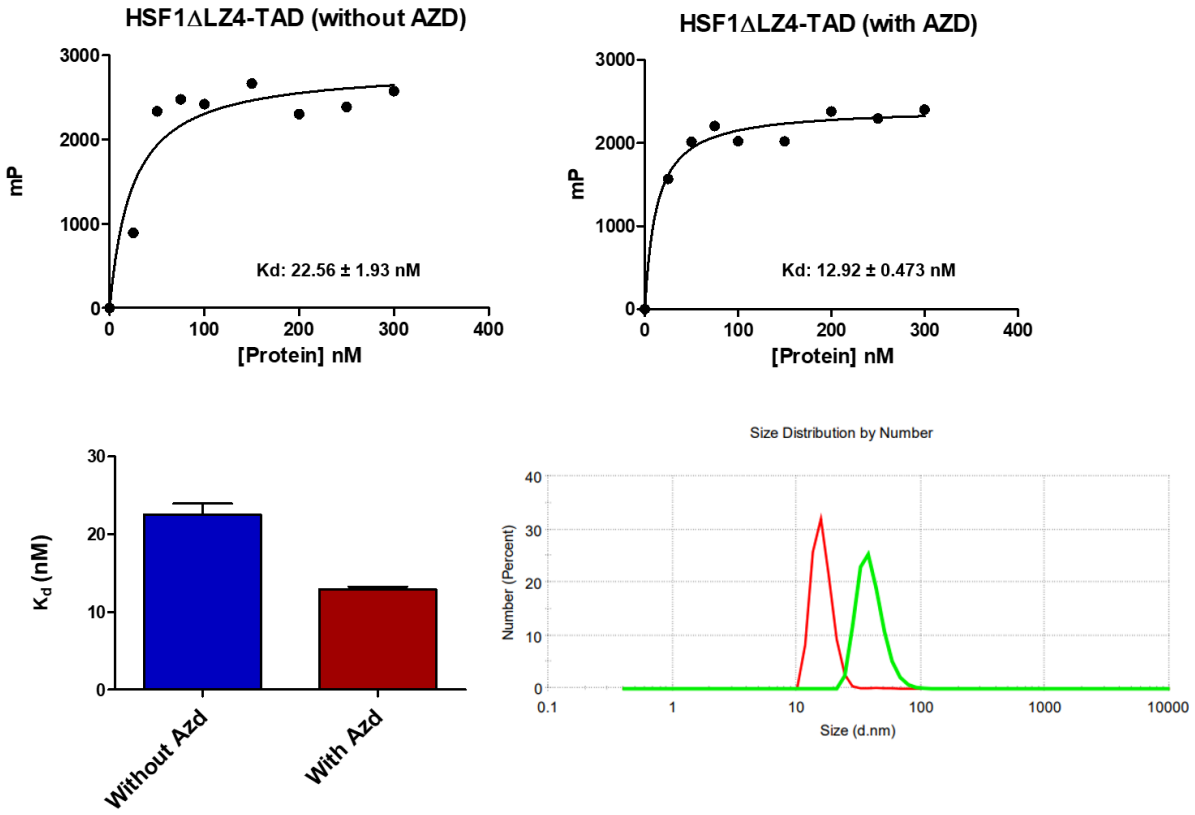

Figure 3.26: AZD stimulates the binding of HSF1-ΔLZ4-TAD and FAM-labelled canonical HSE as revealed by Fluorescence Polarization Assay.

Upper panel: Binding curve derived by plotting the millipolarization values corresponding to protein concentrations (in nM) in the absence and presence of AZD as indicated. K_d values were obtained using GraphPad Prism 5 software.

Lower panel (left): Bar graph representing the K_d values in the presence and absence of AZD.

Lower panel (right): Effect of AZD on the oligomeric status of HSF1-ΔLZ4-TAD (in the absence of HSE) studied by DLS Assay. The peak drawn in red indicates the size distribution of the protein without AZD. The peak drawn in green (with a greater hydrodynamic radius) indicates the protein's size distribution in the presence of the compound.

The DNA Binding Domain of HSF1, situated at Its N-terminus, helps the protein bind with its cognate HSE. The binding strength of purified DBD with HSE is expected to be low owing to the absence of the oligomerization domain. Although certain residues have been shown to mediate DBD-DBD contacts in the crystal structure of the DBD-HSE complex (Neudegger et. al. 2016), these are thought to be insufficient for maintaining a stable trimeric/ multimeric structure. Indeed, HSF1-DBD was found to bind canonical HSE with a very low affinity (mean K_d: 314.56 nM) in the absence of AZD. The presence of 10 μM AZD however increased the binding affinity by ~4-fold (mean K_d: 86.51 nM). This suggested the formation of a multimeric structure comprising HSF1-DBD subunits stabilized by AZD, which bound HSE with high affinity. Indeed, our DLS study demonstrated the formation of a multimeric structure upon incubation of HSF1-DBD with AZD in the absence of HSE (Fig. 3.27). Understanding how AZD achieved this feat and its implications in the activation of full-length HSF1 protein requires further studies.

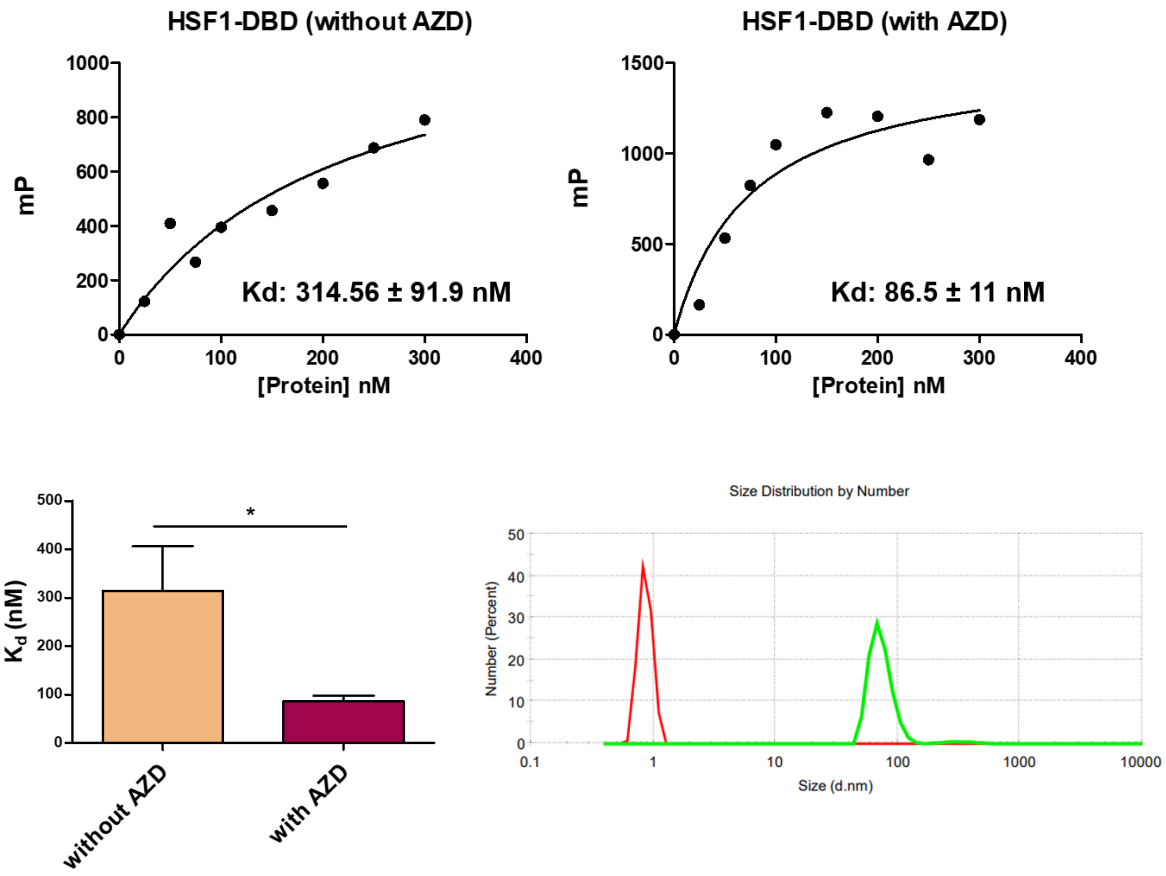

Figure 3.27: AZD enhances the binding of HSF1-DBD and FAM-labelled canonical HSE as revealed by Fluorescence Polarization Assay.

Upper panel: Binding curve derived by plotting the millipolarization values corresponding to protein concentrations (in nM) in the absence and presence of AZD as indicated. K_d values were obtained using GraphPad Prism 5 software.

Lower panel (left): Bar graph representing the K_d values in the presence and absence of AZD.

Lower panel (right): Effect of AZD on the oligomeric status of HSF1-DBD (in the absence of HSE) studied by DLS assay. The peak drawn in red indicates the size distribution of the protein without AZD. The peak drawn in green (with a greater hydrodynamic radius) indicates the protein's size distribution in the presence of the compound.

AZD interacts with HSE-DNA in the absence of protein

Nelson et. al. (2016) analysed the possible interactions of HSE and HSF1-DBD by docking AZD in the crystal structure published by Neudegger et. al. (2016), which has indicated the binding of AZD at the protein-DNA interface, contacting both HSE and HSF1-DBD. In the crystal structure, however, a two-site HSE was used (Neudegger et. al. 2016). Here, we were interested in studying the interaction of canonical three-site HSE with AZD *in vitro* in the absence of protein by fluorescence spectroscopy. Upon titration of FAM-labelled HSE (10 nM) with increasing concentrations of AZD, the fluorescence intensity at 520 nm was found to increase in a concentration-dependent manner, ultimately reaching saturation (λ_{ex} 495 nm). Fluorescence of AZD in the buffer was negligible in this range. The mean K_d value of this interaction was 1.35 µM. This suggested that AZD interacts with the DNA molecule occupying specific binding site(s), and gradually increasing the concentration of AZD saturates these site(s) (Fig. 3.28).

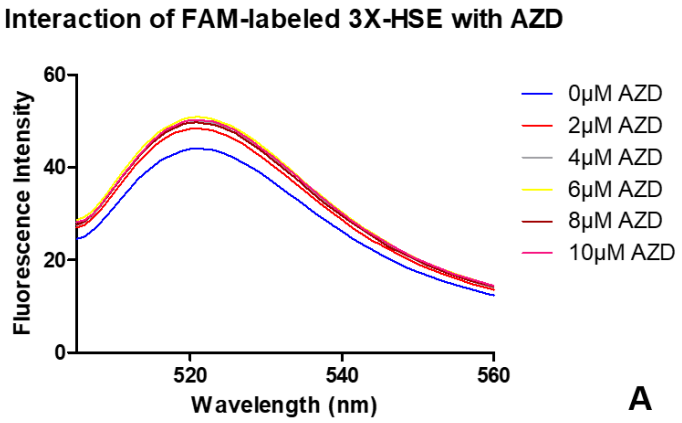

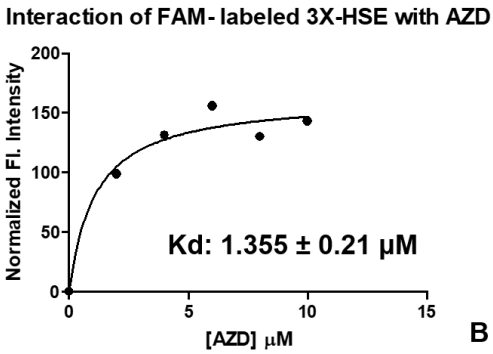

Figure 3.28: AZD alters the fluorescence spectra of FAM-labelled heat shock element containing DNA (HSE-DNA).

A. Fluorescence spectra of FAM-labelled 3X-HSE (10 nM) recorded at various concentrations of AZD (0-10 μM) upon excitation at 495 nm.

B: Binding curve derived by plotting normalized fluorescence emission intensity (at 520 nm) obtained at corresponding AZD concentrations.

To further investigate this interaction, we performed a competition assay using unlabelled (cold) canonical three-site HSE having a sequence identical to that of the labelled probe. Incubation of labelled HSE (10 nM) with 10 μM AZD caused a significant increase in its fluorescence intensity at 520 nm, compared to that of the vehicle (DMSO)-exposed labelled HSE, as expected. However, when the labelled probe-AZD mixture was incubated with cold probe (10 nM), the fluorescence intensity diminished. A further decrease in fluorescence intensity was observed when 100 nM cold probe was present in the reaction mixture (Fig. 3.29). Thus, a dose-dependent decrease in fluorescence intensity of the labelled HSE-AZD mixture was observed when equimolar and a ten-fold molar excess of the cold probe were added to the reaction mixture. This suggested that AZD present in the reaction mixture gets distributed between the binding site(s) on the labelled and cold probes.

The same cold competition assay was also performed by measuring the fluorescence polarization (FP) of FAM-labelled HSE at 520 nm. FP increased considerably upon incubation of labelled HSE with AZD compared to the DMSO-incubated condition. However, increasing concentrations of the cold probe in the reaction mixture caused a significant decrease in FP in a dose-dependent manner (Fig. 3.30). Thus, the result obtained was in good agreement with that of the fluorescence intensity study.

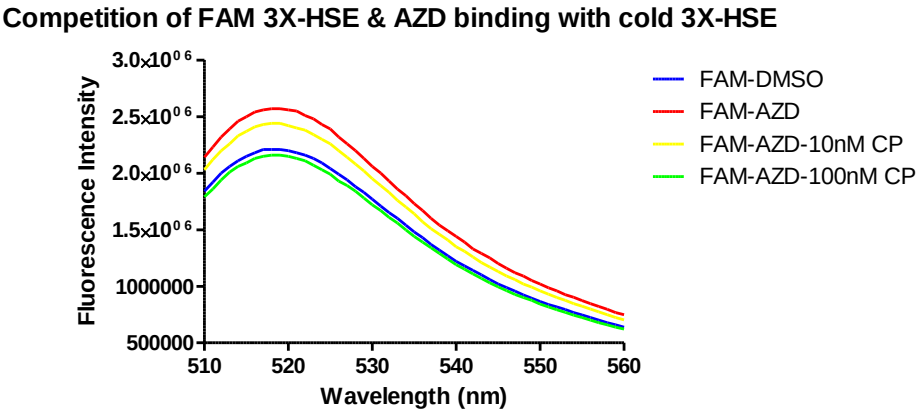

A **3X-HSE sequence:** 5'-CCTGGAATATTCCCGAACTGGC-3'

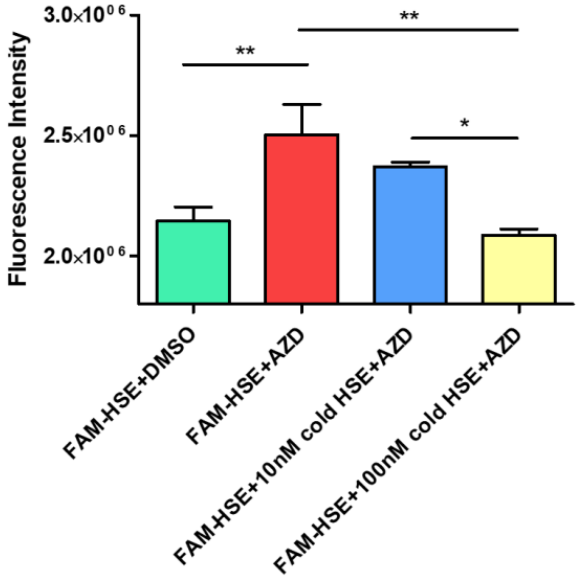

B

Figure 3.29: AZD alters the fluorescence spectra of FAM-labelled heat shock element containing DNA (HSE-DNA).

A: Alteration in the fluorescence emission spectrum of labelled HSE-AZD mixture upon incubation with unlabelled HSE (Cold Probe, CP). Two different concentrations of CP were used in this experiment.

B: Bar graph representing the change in fluorescence emission intensity at 520 nm upon the interaction of FAM labelled 3X-HSE with AZD in the absence and presence of CP.

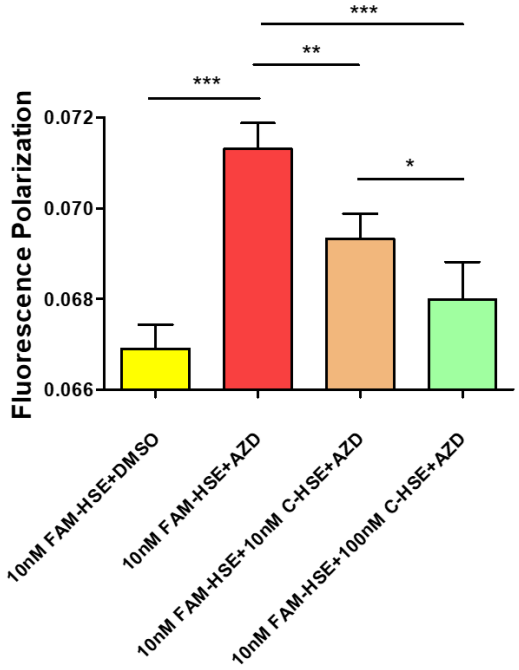

Figure 3.30: Bar graph depicting the change in fluorescence polarization of FAM labelled 3X-HSE upon its interaction with AZD in the presence and absence of CP. Two different concentrations of CP were used in this experiment as indicated.

We were curious to study the binding affinity of mutant HSE (mHSE) with AZD in the absence of protein and compare it with the affinity of canonical HSE-AZD binding (mHSE has the same length as that of canonical HSE with key bases mutated, which weakens its interaction with HSF1). The sequences of canonical and mutant HSEs are given below for comparison (the underlined bases in mHSE have been mutated):

Canonical HSE: 5'-CCTG**GAA**TA**TTC**CCC**GAA**CTGGC-3'

Mutant HSE: 5'-CCTG**GCG**TA**GTC**CCC**CGC**CTGGC-3'

Interestingly, AZD bound mHSE with an affinity comparable to the canonical HSE-AZD interaction, having a mean K_d value of 1.18 µM (Fig. 3. 31). The mean K_d value of canonical HSE-AZD interaction is 1.35 µM. This indicated a similar mode of binding of AZD with the two DNA molecules, which is independent of their nucleotide sequences.

If AZD has a similar mode of binding with the canonical and mutant HSE sequences, does it cause an increase in the binding affinity of mHSE with monomeric HSF1? We have shown AZD to induce multimerization of monomeric HSF1, but even trimeric/ multimeric HSF1 is reported to bind mHSE with an extremely low affinity (Jaeger et.al. 2014). Thus, stimulation of the monomeric HSF1-mHSE binding by AZD would indicate an AZD-induced structural alteration of the DNA molecule. To address this question, we performed an FP assay to monitor the binding of monomeric HSF1 with FAM-labelled mHSE in the presence and absence of AZD. In the absence of AZD, the protein-DNA interaction was extremely weak, as expected (mean K_d value: 1170 nM). But in the presence of 10 µM AZD, the binding affinity dramatically increased with a mean K_d value of 84.77 nM (Fig. 3.33). Thus, AZD indeed increases the binding affinity of monomeric HSF1 with mHSE considerably, although this affinity remains lower than that of the AZD-induced interaction of monomeric HSF1 with canonical HSE (for which, the mean K_d value is 7.8 nM) (Fig. 3.32).

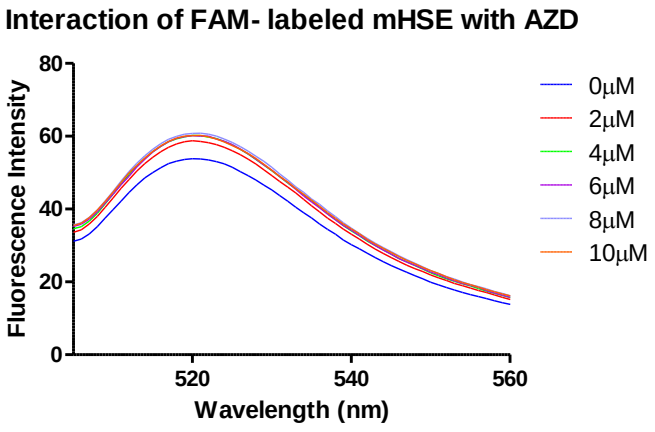

A

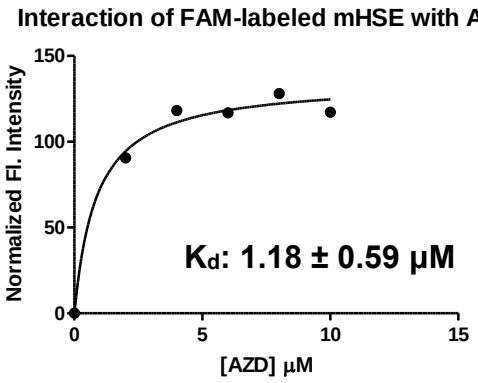

B

mHSE sequence: 5'-CCTG**GCG**TA**GTC**CC**CGC**CTGGC-3'

Figure 3.31: AZD alters the fluorescence spectra of FAM-labelled mutant heat shock element (mHSE)-containing DNA.

A: Fluorescence spectra of FAM-labelled mutant HSE (10 nM) recorded at various concentrations of AZD upon excitation at 495 nm.

B: Binding curve obtained by plotting normalized fluorescence emission intensity at 520 nm at various AZD concentrations.

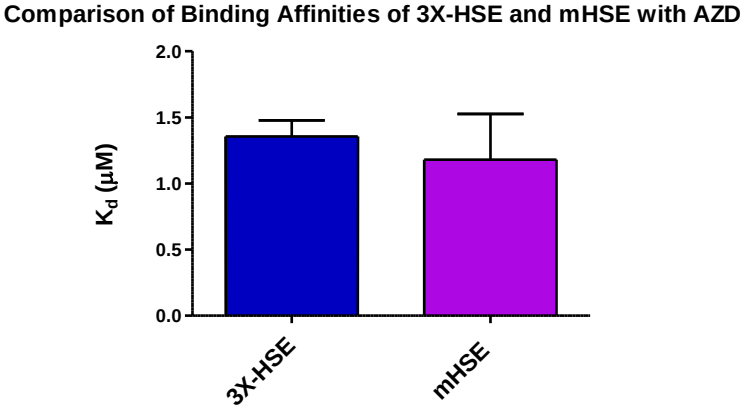

Figure 3.32: Bar graph comparing the binding affinities (K_d values) of 3X (canonical)-HSE and mHSE with AZD. No significant difference was observed.

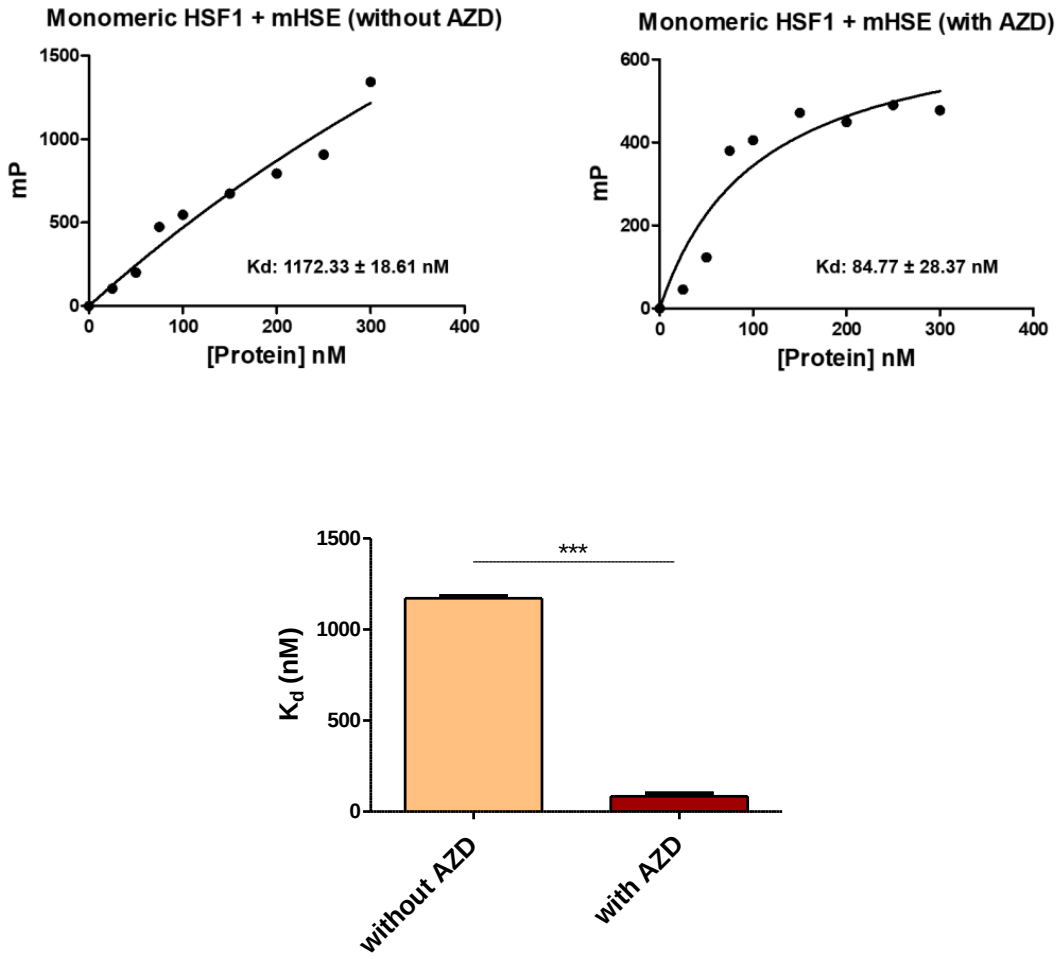

Figure 3.33: Effect of AZD on the binding of monomeric HSF1 to mHSE monitored by FP assay.

Upper panel: Binding curves were obtained by plotting the millipolarization values at different concentrations of the protein (in nM) in the presence and absence of AZD. K_d values were obtained using GraphPad Prism 5 software.

Lower panel: Bar graph representing the K_d values as indicated in the presence and absence of AZD.

Azadiradione alters the surface hydrophobicity of HSF1 and its derivatives as revealed by 1-Anilinonaphthalene-8-sulfonic acid (ANS) fluorescence analysis

1-Anilinonaphthalene-8-sulfonic acid (ANS) is routinely used as an extrinsic fluorescent probe for detecting the presence of exposed hydrophobic patches and cavities on proteins (Sonawane et.al. 2021). The formation of protein aggregates is known to be caused by increased exposure of hydrophobic patches on their surfaces. Therefore, an increase in the ANS fluorescence quantum yield under certain treatment conditions in solution suggests a greater number of ANS incorporation on the surface of proteins.

As our DLS results suggested an AZD-induced structural perturbation of the trimeric/ oligomeric forms of HSF1 and the HSF1-ΔTAD, we were interested in testing the presence of protein aggregates in these proteins upon their incubation with increasing concentrations of AZD using ANS as the probe. Indeed, the ANS fluorescence intensity increased considerably when HSF1-CT was exposed to increasing concentrations of AZD, with a concomitant blue shift of the spectral emission maxima (Fig. 3.34).

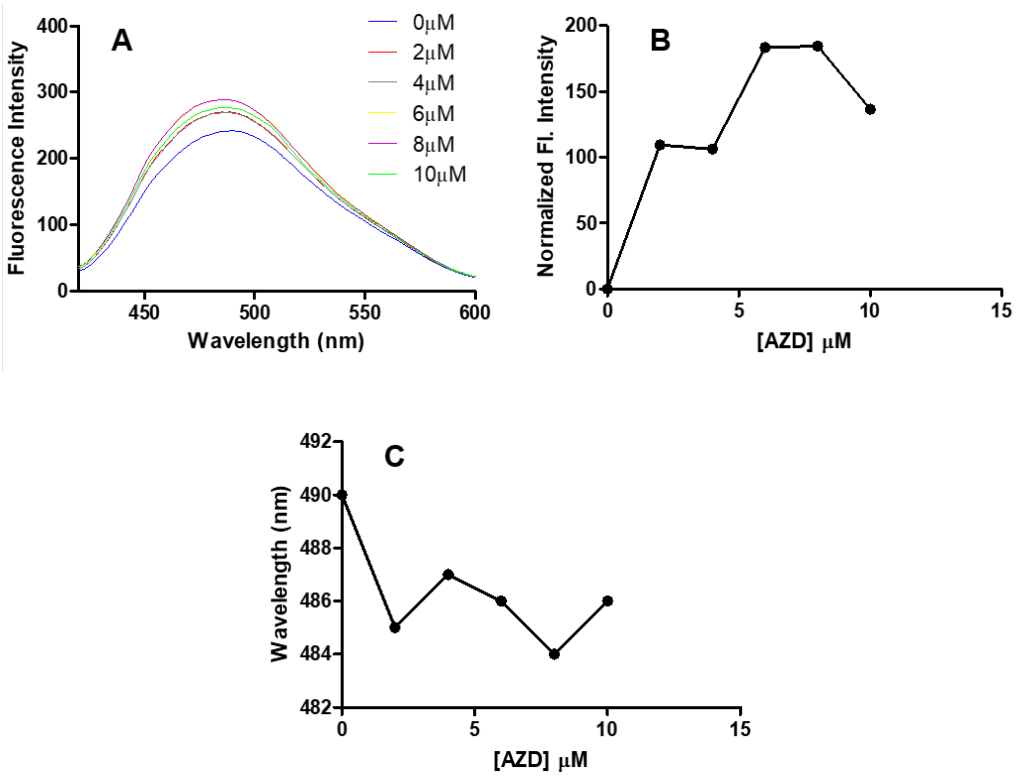

Figure 3.34: AZD increases the fluorescence quantum yield of ANS upon incubation with oligomeric HSF1-CT.

A: ANS fluorescence emission spectra of HSF1-CT exposed to various concentrations of AZD (0-10 μM) obtained at 25°C.

B: ANS fluorescence intensities of HSF1-CT at 490 nm with increasing concentrations of AZD.

C: Changes in ANS fluorescence emission maxima (λ_{max}) of HSF1-CT at varying AZD concentrations.

Similarly, HSF1-ΔTAD, upon incubation with increasing concentrations of AZD, exhibited a significant increase in the ANS fluorescence quantum yield along with a shift of the emission maxima to a lower wavelength (Fig.3.35). These results indicated the AZD-induced formation of aggregates by these two proteins.

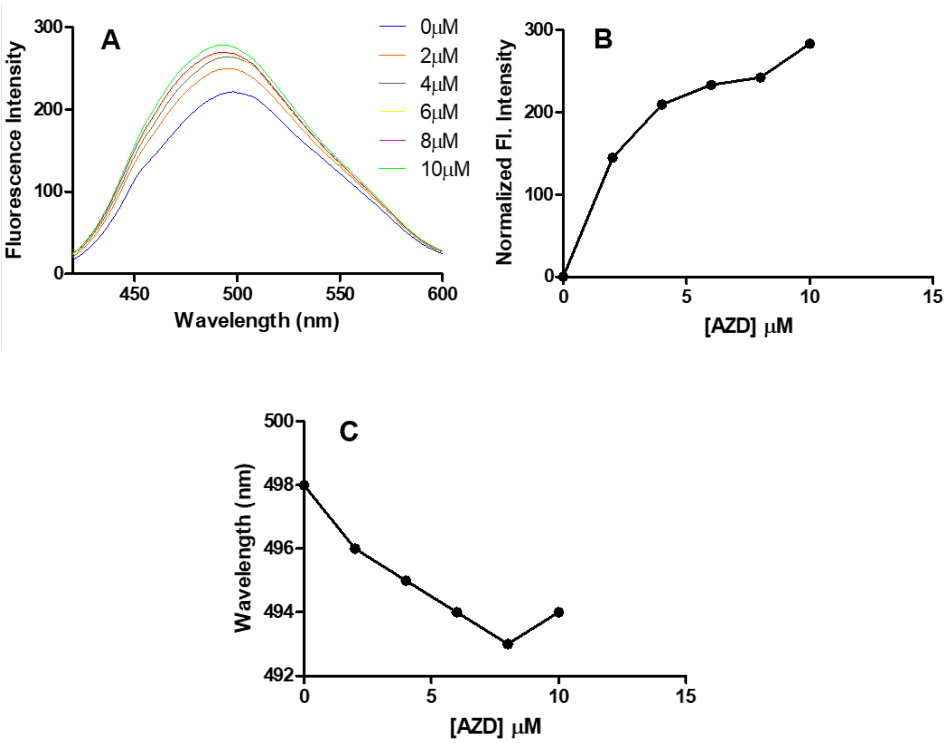

Figure 3.35: AZD increases the fluorescence quantum yield of ANS upon incubation with HSF1-ΔTAD

A: ANS fluorescence emission spectra of HSF1-ΔTAD exposed to various concentrations of AZD as indicated obtained at 25°C.

B: Changes in ANS fluorescence intensity of HSF1-ΔTAD at 490 nm with increasing concentrations of AZD as indicated.

C: Changes in ANS fluorescence emission maxima (λ_{max}) of HSF1-ΔTAD as a function of varying AZD concentrations.

The HSF1-WT trimer (isolated by SEC), however, showed an opposite effect. Exposure of this protein to increasing concentrations of AZD caused a diminution in the ANS fluorescence quantum yield with a simultaneous shift of the emission maxima to a higher wavelength (red shift). This indicates that the AZD-induced structural destabilization of the HSF1-WT trimer as found in our DLS studies is not caused by the formation of protein aggregates (Fig. 3.36).

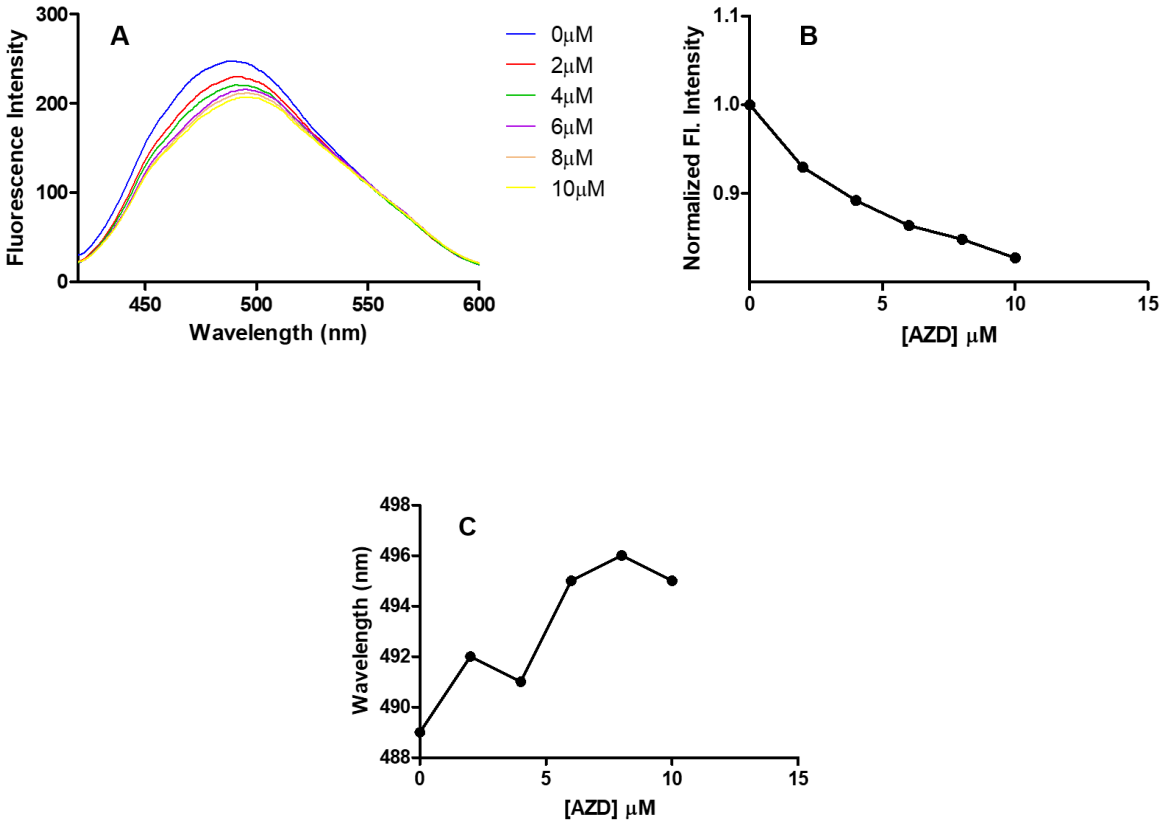

Figure 3.36: AZD reduced the fluorescence quantum yield of ANS upon incubation with HSF1-WT trimer

A: ANS fluorescence emission spectra of HSF1-WT trimer at various concentrations of AZD as indicated obtained at 25°C.

B: ANS fluorescence intensity of HSF1-WT trimer at 490 nm with increasing concentrations of AZD as indicated.

C: ANS fluorescence emission maxima (λ_{max}) of HSF1-WT trimer as a function of varying AZD concentrations as indicated.

Further, we were interested in studying the effect of AZD on the surface hydrophobicity of the monomeric forms of HSF1 (AZD increases HSE binding affinities in these cases). Interestingly, incubation of the monomeric form of HSF1-WT protein with increasing concentrations of AZD revealed an initial increase of the ANS fluorescence quantum yield at lower AZD concentrations, followed by its decrease at higher concentrations (Fig. 3.37). At the highest AZD concentration tested (10 μM), the ANS fluorescence intensity was close to that of the vehicle (DMSO) exposed protein. The ANS spectral emission maxima exhibited an initial blue shift at lower AZD concentrations, followed by a slight red shift at higher concentrations (Fig. 3.37). In the case of HSF1-CM, a similar pattern was observed: an initial increase in the ANS fluorescence intensity at lower AZD concentrations was followed by its reduction at higher AZD concentrations. The ANS fluorescence intensity recorded for the 10 μM AZD-exposed protein was close to that of the vehicle-exposed protein. The ANS spectral emission maxima, in this case, exhibited a blue shift at low AZD concentrations, followed by a return to its initial value at higher AZD concentrations (Fig. 3.38). Exposure of HSF1-DBD to increasing concentrations of AZD caused an initial rise in the ANS fluorescence intensity, which was followed by its decline at higher AZD concentrations. Incidentally, the ANS quantum yield at the highest AZD concentrations was lower than that of the control. However, changes in the ANS spectral emission maxima with the increase in AZD concentrations, in this case, were found to be erratic, the reason for which is presently not clear (Fig. 3.39).

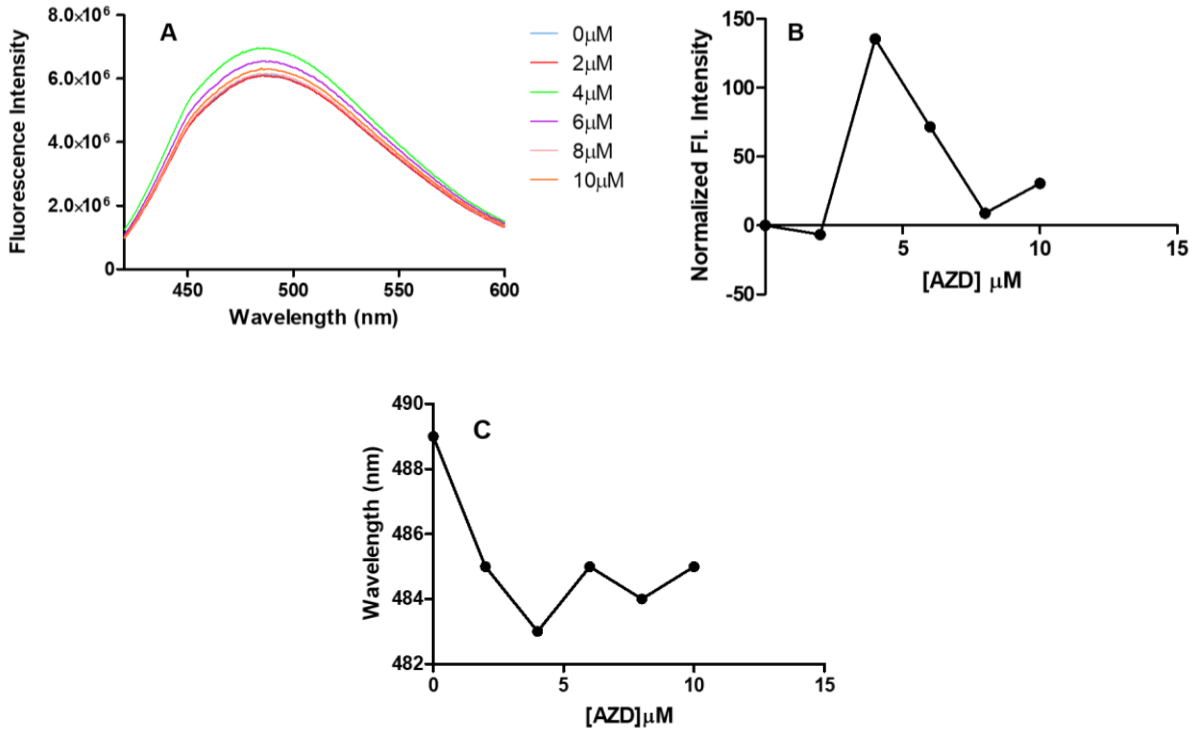

Figure 3.37: AZD exhibited a distinct effect on the fluorescence quantum yield of ANS upon incubation with HSF1-WT monomer.

A: ANS fluorescence emission spectra of HSF1-WT monomer at various concentrations of AZD as indicated, obtained at 25°C.

B: ANS fluorescence intensity of HSF1-WT monomer at 490 nm with increasing concentrations of AZD as indicated.

C: ANS fluorescence emission maxima (λ_{max}) of HSF1-WT monomer as a function of varying AZD concentrations as indicated.

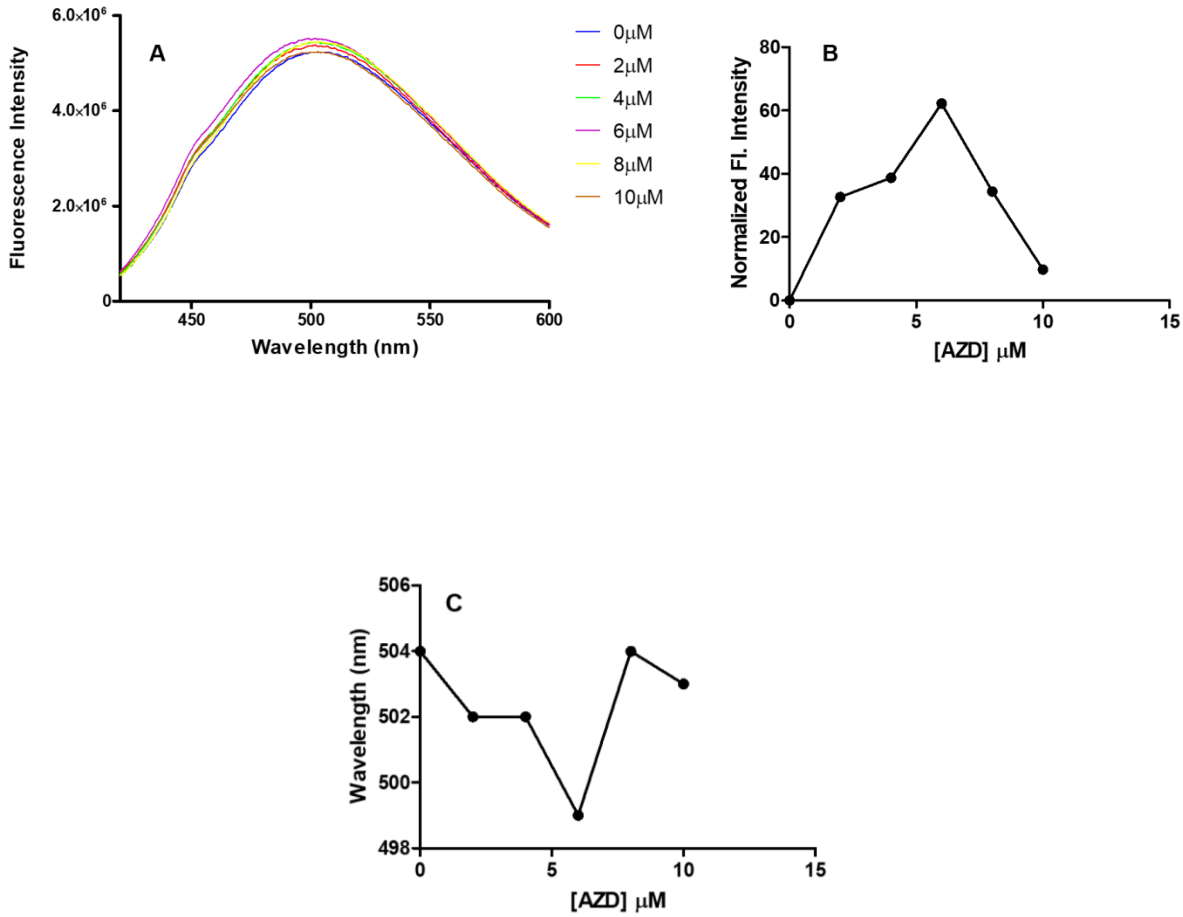

Figure 3.38: AZD alters the fluorescence quantum yield of ANS upon incubation with HSF1-CM

A: ANS fluorescence emission spectra of HSF1-CM at various concentrations of AZD as indicated obtained at 25°C.

B: ANS fluorescence intensity of HSF1-CM at 490 nm with increasing concentrations of AZD as indicated.

C: ANS fluorescence emission maxima (λ_{max}) of HSF1-CM as a function of varying AZD concentrations as indicated.

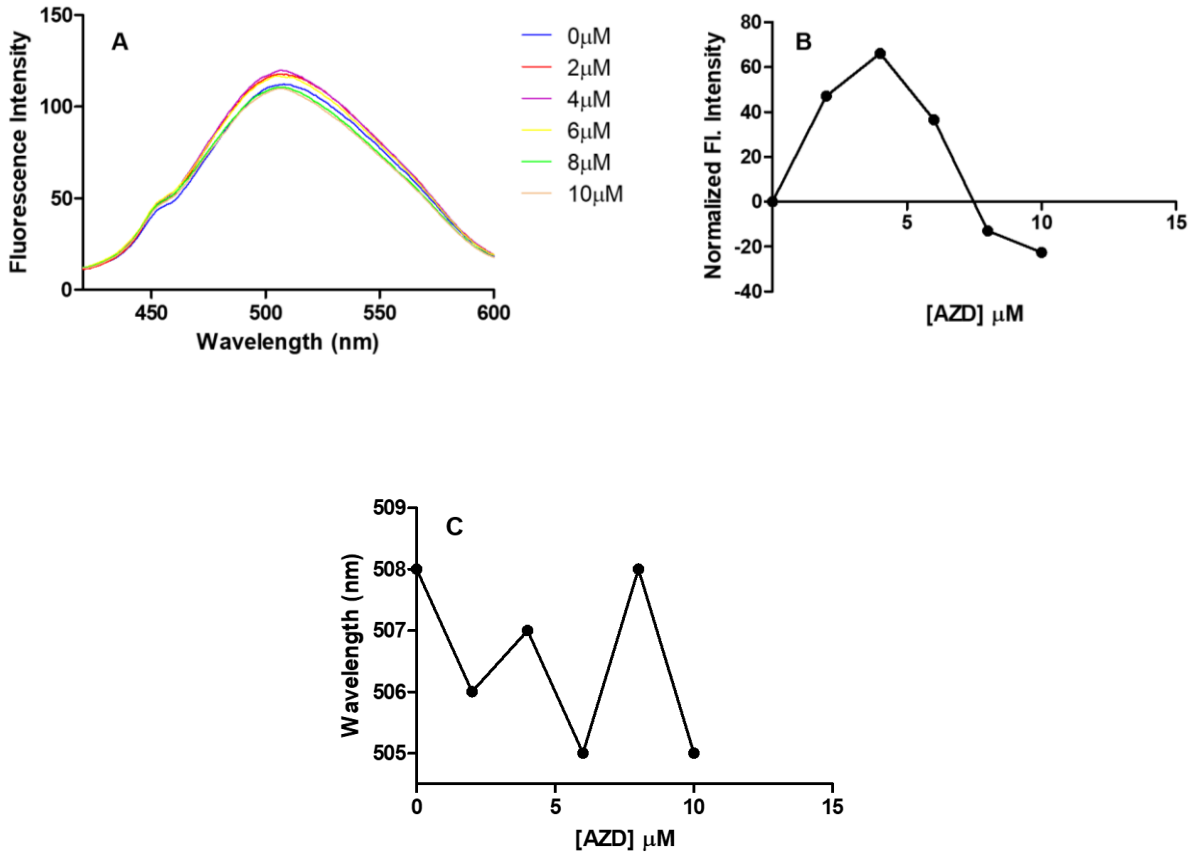

Figure 3.39: AZD exhibited a distinct effect on the fluorescence quantum yield of ANS upon incubation with HSF1-DBD.

A: ANS fluorescence emission spectra of HSF1-DBD at various concentrations of AZD as indicated obtained at 25°C.

B: ANS fluorescence intensity of HSF1-DBD at 508 nm with increasing concentrations of AZD as indicated.

C: ANS fluorescence emission maxima (λ_{max}) of HSF1-DBD as a function of varying AZD concentrations as indicated.

Azadiradione interacts with monomeric forms of HSF1 in the absence of DNA

The interaction of AZD (10 μM) with HSF1-WT monomer, HSF1-CM, and HSF1-DBD caused multimerization and stabilization of these proteins and increased their binding affinities for HSE (Figs. 3.21, 3.22 and 3.27). Thus, we were interested to know the binding affinities of these proteins for AZD in the absence of HSE. For this purpose, intrinsic fluorescence spectra of 0-10 μM AZD-equilibrated WT monomer, CM, and DBD were individually recorded as mentioned in 'Materials and Methods'. As revealed by the spectra, there was an increase in the intrinsic fluorescence intensity of all the proteins (obtained by excitation of the tryptophan and tyrosine residues) upon their interaction with AZD. The fluorescence intensity for all the proteins increased considerably from 0 to 2 μM AZD, after which saturation in fluorescence enhancement was observed from 2 to 10 μM (Figs. 3.40, 3.41 and 3.42). AZD showed negligible fluorescence emission under the conditions tested. The mean K_d values for all the above interactions were quite close to each other.

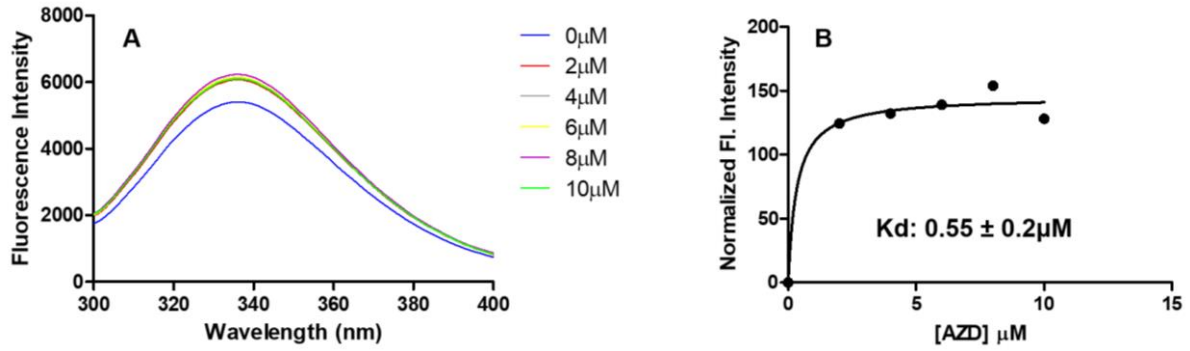

Figure 3.40: AZD interacts with HSF1-WT monomer as determined by protein intrinsic fluorescence assay.

A: Intrinsic fluorescence emission spectra of HSF1-WT monomer obtained after incubation with increasing concentrations of AZD as indicated.

B: Binding curve obtained by plotting normalized fluorescence emission intensity (at λ_{max}= 335 nm) versus AZD concentration.

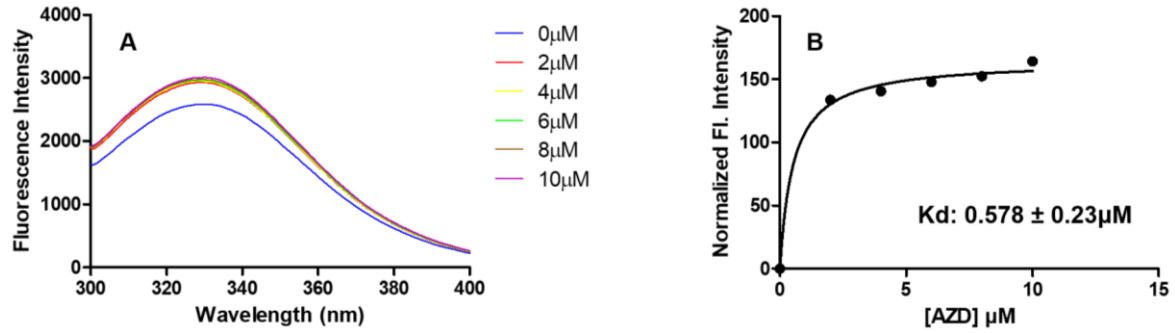

Figure 3.41: AZD interacts with HSF1-CM as determined by protein intrinsic fluorescence assay.

A: Intrinsic fluorescence emission spectra of HSF1-CM obtained after incubation with increasing concentrations of AZD as indicated.

B: Binding curve obtained by plotting normalized fluorescence emission intensity (at λ_{max}= 330 nm) versus AZD concentration as indicated.

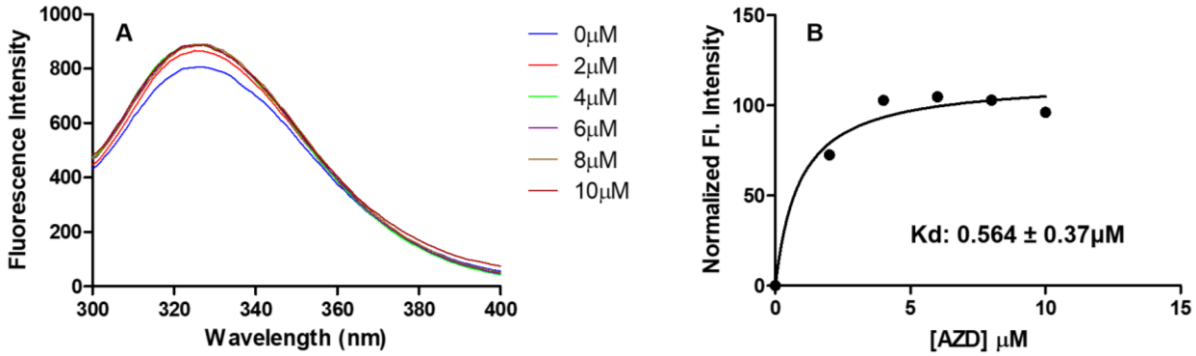

Figure 3.42: AZD interacts with HSF1-DBD as determined by protein intrinsic fluorescence assay.

A: Intrinsic fluorescence emission spectra of HSF1-DBD obtained after incubation with increasing concentrations of AZD as indicated.

B: Binding curve obtained by plotting normalized fluorescence emission intensity (at λ_{max}= 326 nm) versus AZD concentration.

Azadiradione-induced structural perturbation of HSF1-CT and HSF1-ΔTAD was probed by Thioflavin T fluorescence assay

Our DLS studies and ANS fluorescence assays have indicated the formation of protein aggregates upon treatment of HSF1-CT and HSF1-ΔTAD with AZD (Figs. 3.24, 3.25, 3.34, 3.35). We were interested in investigating the nature of these protein aggregates. For this purpose, we have studied the interaction of Thioflavin T (ThT), an extrinsic fluorescent dye, with these proteins in the absence and presence of AZD. ThT exhibits a substantial enhancement in its fluorescence intensity upon incubation with characteristic cross-β sheet structures and is thus a suitable probe to characterize amyloid aggregates (Hawe et. al. 2008). When the above-mentioned proteins were exposed to increasing concentrations of AZD and subsequently incubated with ThT, a considerable increase in the ThT fluorescence (at 485 nm) was observed (Figs. 3.43 and 3.44). Thus, exposure to AZD was shown to induce the formation of amyloid aggregates of HSF1-CT and HSF1-ΔTAD in a concentration-dependent manner.

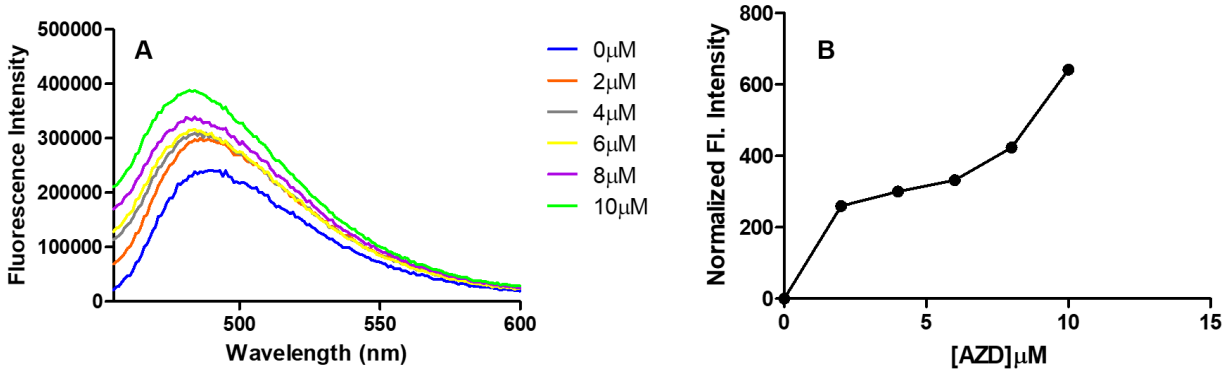

Figure 3.43: AZD increases cross-β sheet structures of HSF1-CT as probed by ThT fluorescence analysis.

A: Fluorescence emission spectra of ThT obtained upon binding with HSF1-CT exposed to various AZD concentrations as indicated.

B. Depiction of the change in ThT fluorescence emission intensity (at λ_{max}= 485 nm) with varying AZD concentration by plotting normalized fluorescence emission intensity versus AZD concentration.

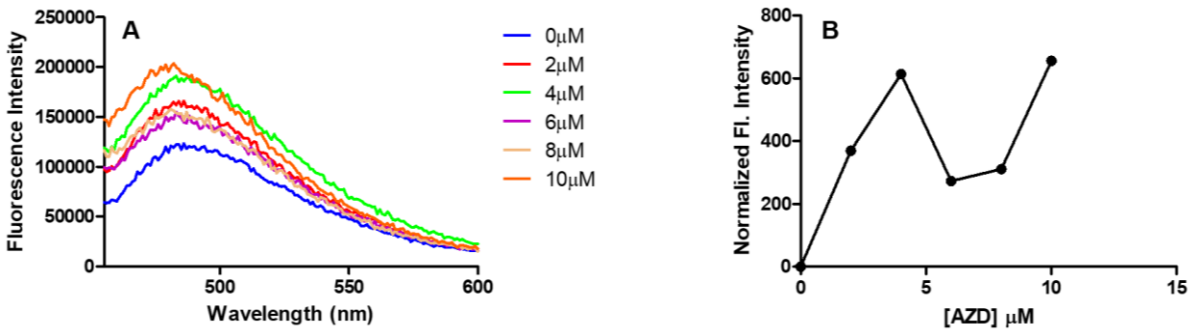

Figure 3.44: AZD increases cross-β sheet structures of HSF1-ΔTAD as probed by ThT fluorescence analysis.

A: Fluorescence emission spectra of ThT obtained upon binding with HSF1-ΔTAD exposed to various AZD concentrations as indicated.

B. Depiction of the change in ThT fluorescence emission intensity (at λ_{max}= 485 nm) with varying AZD concentration by plotting normalized fluorescence emission intensity versus AZD concentration.

Isothermal Titration Calorimetry (ITC) for determining the thermodynamic parameters of HSF1-AZD interaction

We attempted ITC as described in the 'Materials and Methods' section to determine the thermodynamic parameters pertaining to the interaction of HSF1-WT monomer with AZD. As shown in Fig. 3.45, the thermogram obtained did not show significant heat change. Moreover,

the spikes obtained with the corresponding injections of the ligand (AZD) into the reaction cell did not follow a definite pattern. It was noted that to obtain a reliable thermogram showing significant heat change, a relatively higher concentration of protein (~10 µM) with ligand concentration at 10-fold molar excess of that of the protein is required (Sinha et.al. 2021). In our case, the AZD stock solution (dissolved in DMSO) was diluted in the Dialysis Buffer to obtain a 100 µM AZD working solution. AZD, a compound with medium-range polarity (having both hydrophobic and hydrophilic properties), was phased out upon its dilution in Dialysis Buffer, yielding a turbid solution. This presumably interfered with the interaction of AZD with HSF1, producing inconsistent and inconclusive results.

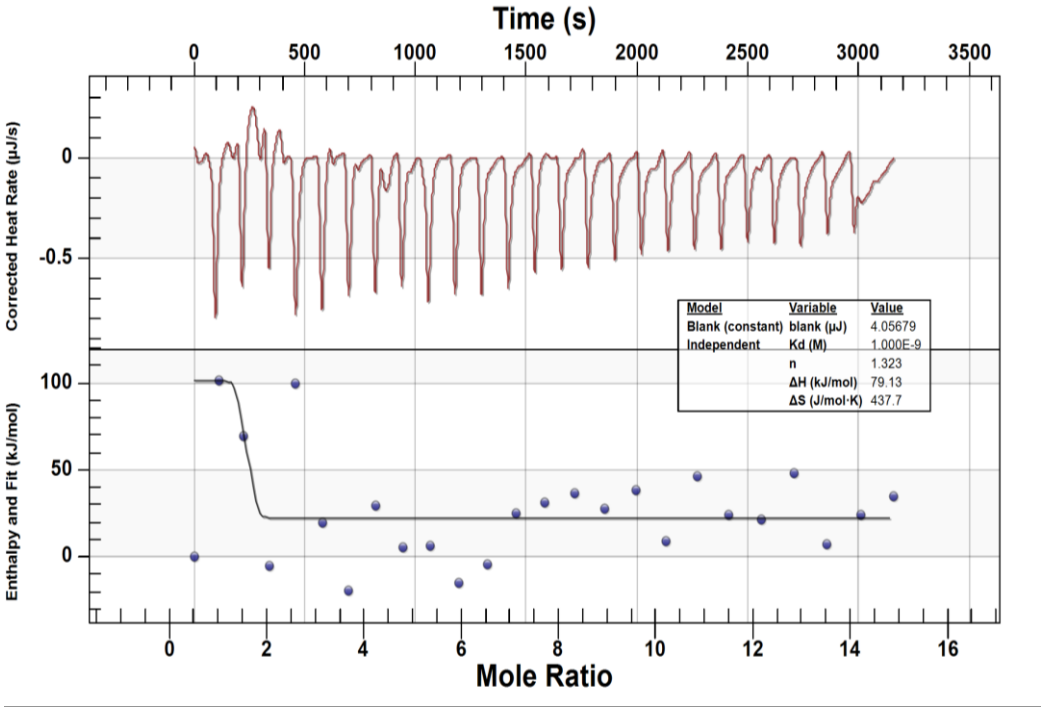

Figure 3.45: Analysis of the interaction of monomeric WT-HSF1 with AZD by Isothermal Titration Calorimetry (ITC). The upper panel shows the heat change involved upon each injection of the ligand into the reaction cell. The lower panel shows an analysis of the result by a one-site binding model using the machine's software.

CHAPTER 4

DISCUSSION

The present study explores the underlying basis of the functional enhancement of HSF1 activity by the phytochemical Azadiradione (AZD), a limonoid of MW 450.57 Da. AZD was identified by Nelson and colleagues as the only known direct activator of HSF1 to date (Nelson et. al. 2016). It was shown to interact directly with purified human HSF1 protein by an intrinsic tryptophan fluorescence assay (Nelson et. al. 2016). This interaction increased the ability of the purified protein to bind its cognate recognition element, the heat shock element (HSE). AZD also increased the affinity of the HSE-interacting cellular extract that contains HSF1 as shown by gel-shift assay (Nelson et. al. 2016). These findings were in good agreement with the studies on cell lines, *Drosophila,* and mouse models of neurodegenerative diseases, where AZD was found to enhance the activity of HSF1 as monitored by the increasing levels of its target gene products, such as molecular chaperones, thereby restoring the cellular protein homeostasis. Notably, HSF1 activation by AZD does not involve the generation of ROS (Nelson et. al. 2016, Singh et. al. 2018). AZD, interestingly, has been reported to serve as an antioxidant (Sakib et. al. 2023).

AZD was found to enhance the binding affinity of the monomeric form of wild-type HSF1 (obtained by size exclusion chromatography) for the canonical three-site HSE sequence appreciably in the absence of any stressful condition as determined by fluorescence polarization assay. This was shown to be mediated by the AZD-induced monomer to trimer/ multimer transition of the protein in the complete absence of HSE-DNA, as revealed by our DLS study (Fig. 3.21). This indicates that HSE binding plays no role in assisting the multimerization of HSF1-WT monomer by AZD; the fully formed trimer/ multimer binds HSE with high affinity. During our *in vitro* studies on protein-DNA interaction by fluorescence polarization (FP) assay, the labelled DNA was first added to the buffer, followed by the protein at various concentrations. AZD was the last component to be added, wherever necessary, before excitation of the reaction mixtures at 495 nm. Indeed, in unstressed cells, HSF1 remains as inactive monomers in the cytosol, and it is only after multimerization (induced by stress cues or AZD exposure) that they move to the nucleus to engage with the promoters of their target genes. The results of our *in vitro* studies are consistent with the spatiotemporal separation of HSF1 trimerization and HSE binding in the cells.

Most intriguing was our observation that AZD increased the binding affinity of the constitutively monomeric (CM) form of HSF1 for the canonical HSE sequence by ~75-fold [K_d value decreased from 490.99 ± 99.74 nM to 6.485 ± 2.77 nM] (Fig. 3.22). This derivative

of HSF1 completely lacks the oligomerization domain, which is known to be indispensable for the stress-induced multimerization of HSF1 (Figs. 3.6, 3.8, 3.13). AZD, however, was shown to cause multimerization of this protein efficiently in the absence of HSE; and the multimeric protein bound HSE with an affinity comparable to that of the multimerized monomeric wild-type HSF1 [Figs 3.21 & 3.22: (6.485 ± 2.77 nM vs. 7.8 ± 3 nM)]. Based on the published literature on the stress-induced multimerization mechanism of HSF1, this result was completely unanticipated and reveals a unique mechanism of HSF1 multimerization. A question thus naturally arises as to the point(s) of contact of the individual subunits in the multimeric form of HSF1-CM that hold the complex together.

The DNA binding domain (DBD) of HSF1 located at the protein's N-terminus is the only structurally characterized domain of HSF1 (Fig. 3.6) (Neudegger et.al. 2016, Feng et.al. 2021). Based on our observations described above, we were curious to study the interaction of purified DBD with AZD, as this domain is responsible for the binding of HSF1 with HSE. The DBD was found to exist predominantly in the monomeric form in solution in the absence of HSE, as suggested by a low hydrodynamic radius (R_h) in our DLS studies (Figs. 3.9, 3.17, 3.27). However, a dramatic monomer to multimer shift occurred upon incubation of the protein with AZD, suggested by a substantial increase in R_h (Fig. 3.27). Interestingly, DBD was shown to bind HSE in the presence of AZD with a ~4-fold higher affinity compared to the control condition (K_d value with AZD: 86.5 ± 11 nM; K_d value without AZD: 314.56 ± 91.9 nM). AZD seems to hold the individual DBD subunits in a multimeric complex, which binds HSE with a higher affinity (Fig. 3.27). The binding affinity, however, is low compared to those of the AZD-induced multimeric forms of HSF1-WT monomer (K_d: 7.8 ± 3 nM) and HSF1-CM (K_d: 6.485 ± 2.77 nM). Thus, the oligomerization domain may be dispensable for AZD-induced multimerization; however, the interaction of AZD with DBD may induce conformational changes in other domains of the protein, which enhances its binding affinity for HSE.

Our studies on the binding affinities of HSF1-WT monomer, HSF1-CM, and HSF1-DBD with AZD (in the absence of HSE) by protein intrinsic fluorescence spectroscopy revealed very close K_d values (Figs. 3.40-3.42). The K_d values for the binding of AZD with HSF1-WT monomer, HSF1-CM, and HSF1-DBD are 0.55 ± 0.2 μM, 0.578 ± 0.23 μM and 0.564 ± 0.37 μM respectively. These results are consistent with the idea that the DBD is the predominant site for the binding of AZD in HSF1.

Matthias Mayer's group has proposed the 'dimer activation model' to explain the stress-induced activation of HSF1 (Hentze et. al. 2016). In unstressed conditions, the LZ4 and LZ1-3 domains interact with each other to stabilize HSF1 protein in a monomeric form (Fig. 3.6). However, on account of the larger size of the LZ1-3 domain (75 amino acid residues) compared to the LZ4 domain (42 amino acid residues), monomeric HSF1 can form transient dimers via intermolecular interaction with the free region of LZ1-3 not involved in the intramolecular interaction. The intramolecular interaction tends to destabilize this intermolecular interaction, resulting in rapid dissociation of such dimers and a predominance of the monomeric form of the protein. Interestingly, the intermolecular LZ1-3-LZ1-3 interaction could also destabilize the intramolecular LZ1-3-LZ4 interaction. When the concentration of HSF1 is high, the chances of association of a third HSF1 monomer with the transient dimer are enhanced. This loosens the binding of LZ4 with LZ1-3, resulting in the formation of a stable trimeric structure via the LZ1-3 domains of the individual subunits. At low HSF1 concentration, an elevation of temperature would lead to the unfolding of LZ4 (and probably of LZ1-3 as well), leading to their detachment from each other. This would promote stabilization of the transient dimers and subsequent HSF1 trimerization.

Our studies have shown a specific interaction of AZD with HSF1-DBD and AZD-induced formation of DBD multimers. Thus, AZD possibly stabilizes the transient dimer described above by interacting with the DBDs in the dimeric structure. According to the 'dimer activation model', this stabilization could favour the destabilization of the intramolecular LZ1-3-LZ4 interaction of the individual monomers and give enough opportunity for the association of a third monomer with the AZD-stabilized transient dimer at low protein concentration and low temperature. This results in the displacement of LZ4 from LZ1-3 and the formation of a stable trimeric structure via the LZ1-3 domains (Fig. 4.1).

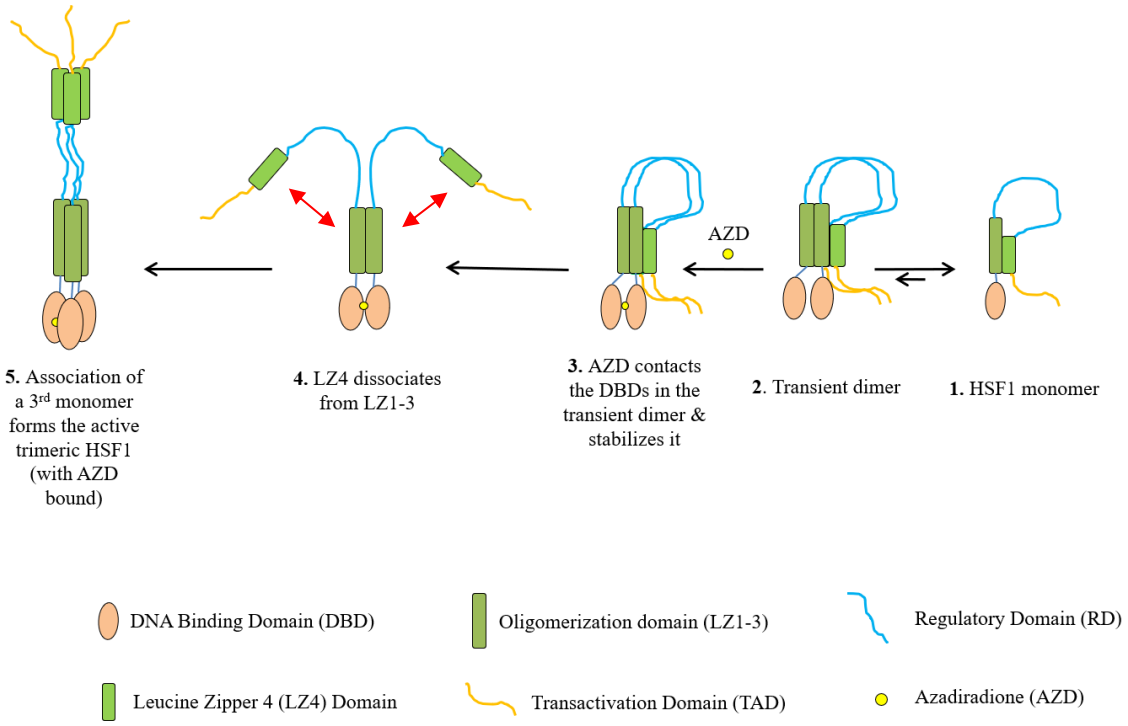

Figure 4.1: A plausible mechanism of the AZD-induced activation of monomeric HSF1.

(1) In the monomeric HSF1, LZ1-3 and LZ4 remain associated via an intramolecular interaction. (2) Two such monomers may transiently associate with each other to form a temporary dimeric structure, which tends to revert to the monomeric state. (3) When AZD contacts the DBDs in the transient dimer, the dimer gets stabilized and hence cannot revert to the monomeric state. (4) AZD-mediated stabilization of the transient dimer destabilizes the intramolecular LZ1-3-LZ4 interactions of the individual monomers (shown by red arrows). (5) This facilitates the association of a 3rd HSF1 monomer to the dimeric structure, resulting in the dissociation of LZ4 from LZ1-3 and the formation of an active trimeric HSF1, with AZD bound to the DBDs.

In our studies, the LZ1-3 domain plays no role in the recognition of AZD, as the binding affinity of ΔLZ1-3 mutant with AZD is comparable to that of WT monomer. Also, AZD forms a stable multimeric structure with the ΔLZ1-3 derivative i.e., HSF1-CM, which binds HSE with a very high affinity (Fig. 3.22). HSF1-ΔLZ1-3 is, however, non-existent in human cells, and we

sought to leverage the knowledge obtained from its study to gain insights into the activation mechanism of the WT monomer. Our results indicate that the AZD-induced HSF1-WT homo-trimeric/ -multimeric structure is stabilized in two ways: (a) by the inter-subunit LZ1-3 mediated interactions and (b) by AZD-mediated inter-subunit DBD-DBD interactions. AZD seems to orient the individual DBDs so that the trimeric/ multimeric structure can bind the HSE with maximum efficiency. Future studies are necessary to confirm this idea.

Another interesting aspect of our study is the revelation of an opposite effect of AZD on the pre-assembled homo-trimeric/ -oligomeric forms of HSF1. Both the trimeric/ oligomeric forms of HSF1: WT trimer/ oligomer (obtained by SEC of affinity-purified HSF1-WT protein) and the constitutively trimeric/ oligomeric mutant form of HSF1 (HSF1-CT) bound the HSE with lowered affinity in the presence of AZD in comparison to the compound's absence [Figs. 3.23, 3.24, 3.21: K_d of HSF1-WT trimer/ multimer and HSF-CT without AZD was 17.45 ± 15.35 nM and 25 ± 16.2 nM, respectively compared to 7.8 ± 3 nM for HSF1-WT monomer with AZD]. DLS analyses with these proteins in the absence of HSE revealed a slight increase in their hydrodynamic radii in the presence of AZD compared to the control conditions. This could be attributed to a partial destabilization of the HSF1 proteins' structure upon incubation with AZD (Figs. 3.23 & 3.24). Thus, AZD-induced structural destabilization of the proteins might be the reason for the decrease in their HSE-binding affinities. Our results suggest that the pre-assembled HSF1 homotrimer/ -multimer present in the cytoplasm/ nucleus is functionally inhibited by AZD, in contrast to the AZD-mediated functional activation of the monomeric form of HSF1.

It is well known that cancer cells need a constant supply of molecular chaperones to maintain proteostasis for supporting their survival, rapid proliferation, and metastasis, resulting in poor prognosis. HSF1 does not start the oncogenic transformation, but tumours become excessively dependent on HSF1 as their exposure to increasingly toxic microenvironments necessitates an enhanced level of molecular chaperones for maintaining protein homeostasis. Proteostatic imbalance in cancer cells keeps HSF1 in a constitutively active form, which ensures a sustained production of chaperones. This phenomenon is known as 'non-oncogenic addiction'(Dai et. al. 2007). Several proteins known to be critical in driving tumorigenesis, such as mutated or overexpressed kinases as well as transcription factors, are known to interact with the chaperone HSP90, which ensures their proper functioning (Alarcon et. al. 2012). Moreover, HSF1 has been shown to drive a unique cancer-specific transcriptional program exclusively in cancer cells which is distinct from the normal HSR (Mendillo et. al. 2012). This program targets

additional genes pertaining to core cellular functions that cater to the needs of such cells. As such, HSF1 inhibition has become a promising strategy in anticancer drug discovery, although transcription factors are not considered good drug targets. HSF1-targeting drugs are not expected to affect the survival of normal cells, since HSF1-target genes are supposed to be non-essential for their growth and survival under stress-free conditions. Indeed, *hsf1-/-* mice are viable under controlled laboratory conditions, and display a lower incidence of tumours (Dai et. al. 2007).

Several HSF1 inhibitors have been reported in the literature as direct interactors of HSF1. DTHIB, a synthetic compound, has been reported to interact with HSF1-DBD *in vitro* directly, but unlike AZD, it does not increase its affinity for HSE. Furthermore, DTHIB does not affect the HSE binding activity of homotrimeric HSF1 *in vitro*. It exerts its anticancer activity by causing E3 ligase-mediated selective degradation of nuclear HSF1 (Dong et. al. 2020). Another compound, I_{HSF1}115, also interacts with DBD and interferes with ATF1-containing complex assembly, thereby blocking HSF1's transcriptional activity (Vilaboa et. al. 2017). Peptide 14 (which mimics a discrete region of the LZ4 domain) interacts with the LZ1-3 domain and suppresses the DNA binding of HSF1 without altering its multimeric structure (Ran et. al. 2018). The inhibitory effect of AZD, however, seems to be directed only at the pre-assembled homomultimeric forms of HSF1, which is a possible intermediate in its activation pathway in the cell, and cancer cells supposedly carry abundant HSF1 activation pathway intermediates. In contrast, AZD's interaction with the monomeric forms of HSF1 (WT monomer, HSF1-CM, and DBD) stimulated their HSE-binding activities. Thus, AZD could be used as a double-edged sword: the same compound could have applications in the treatment of both neurodegenerative diseases (Singh et. al. 2018) and cancer. Indeed, the anticancer activity of AZD has been reported in the triple-negative breast cancer cell line MDA-MB 231, although the role of HSF1 has not been explored in this study (El-Senduny et. al. 2021).

How does the same compound enhance the activity of the monomeric forms of HSF1 and compromise the activity of its multimeric forms? The results of our DLS studies on the multimeric forms of full-length HSF1 rule out the possibility of dissociation of the multimeric structure into individual monomers; rather, it suggests the occurrence of such a conformational change of the homo-multimers which decreases their affinity for HSE. The hydrodynamic radii of the multimers were increased by AZD (Figs. 3.23, 3.24). To further explore the cause behind AZD-induced inhibition of multimeric HSF1, we studied the binding of the fluorescent probe ANS with these proteins treated with increasing concentrations of AZD. In the case of HSF1-

CT, an increase in AZD concentration caused a rise in the ANS fluorescence intensity signal with a concomitant shift of the fluorescence emission maxima to shorter wavelengths indicating a structural transition in the molecule. This indicates an AZD-induced increase in exposure of hydrophobic patches on the protein's surface (where ANS binds and shows enhanced fluorescence) which could be attributed to aggregation of the protein (Fig. 3.34). The binding of HSF1-CT with ThT at increasing concentrations of AZD was found to cause a substantial enhancement in the ThT fluorescence intensity, which is indicative of the AZD-induced formation of amyloid-like aggregates (Fig. 3.43). AZD was previously reported to completely destabilize Tau aggregates and inhibit the aggregation of Tau protein (Gorantla et.al. 2020). However, in our study, AZD exerts the opposite effect on HSF1-CT. In the case of the HSF1-WT trimer, surprisingly, a decrease in the ANS fluorescence intensity was observed upon incubation of the protein with increasing concentrations of AZD accompanied by a red shift of the spectral emission maxima. It should be remembered that both hydrophobic and electrostatic interactions have been implicated in the binding of ANS with proteins: the negatively charged sulfonate group interacting with positively charged amino acid residues and the aromatic rings with hydrophobic residues in an oriented manner (Hawe et. al. 2008). Thus, it is reasonable to infer that the destabilization of the protein induced by AZD causes a loss of complementarity of the positively charged and hydrophobic residues which is essential for the binding of ANS. As a result, ANS binds the protein loosely via only one form of interaction and hence gets detached easily, accounting for the decrease in quantum yield and the spectral redshift (Figs. 3.34, 3.36).

HSF1-ΔTAD, like HSF1-CT, showed a rise in the ANS quantum yield upon incubation with increasing concentrations of AZD accompanied by a spectral blueshift (Fig. 3.35). As mentioned earlier, the protein is essentially multimeric, and AZD was shown to decrease its binding affinity for HSE. AZD-induced structural reorganization/ destabilization of the protein, as demonstrated in our DLS studies, could be attributed to the presence of an aggregate-like structure which accounts for the ANS fluorescence enhancement. The nature of this aggregate-like structure was shown to be amyloid-like, as demonstrated by an AZD-induced increase in ThT fluorescence quantum yield (Fig. 3.44). Deleting the TAD from HSF1 was thus shown to render the protein susceptible to AZD-induced destabilization/ reorganization compared to the wild-type protein.

Recently, Sengupta et. al. (2023) reported that amyloid formation of the mutant as well as wild-type forms of p53 protein in cancer tissues is correlated with the loss of DNA binding and

transcriptional activities of this transcription factor and an increase in cancer grades. Misfolding and/ or aggregation and subsequent amyloid formation of the p53 protein compromise its function as a tumour suppressor. It is likely, therefore, that AZD-induced amyloid formation in HSF1-CT and HSF1-ΔTAD, as demonstrated in this study, is responsible for the observed decrease in their HSE-binding affinities. Amyloid formation of HSF1 caused by AZD in cancer cells and the consequent loss of its DNA-binding activity could be one of the reasons behind the demonstrated anticancer properties of AZD (El-Senduny et.al. 2021).

A transcription-independent anti-amyloid function of HSF1 has been demonstrated; HSF1 could neutralize soluble amyloid oligomers through physical interactions. As amyloids accumulate during cell overgrowth, HSF1 protects the mitochondrial proteome by safeguarding HSP60, a bona fide target of amyloid oligomers. This prevents HSP60 destabilization and consequent damage of the mitochondrial proteome, thereby rescuing the cells from mitophagy and apoptosis. This anti-amyloid action of HSF1 also protects human neurons against Aβ1–42–induced toxicity *in vitro* (Tang et. al. 2020). Future studies will address if AZD, which physically interacts with HSF1, can modulate this transcription-independent function of HSF1.

Studies on the interaction of ANS with HSF1-WT monomer and HSF1-CM treated with increasing concentrations of AZD revealed a startling fact: a gradual increase in the concentration of AZD led to an initial rise in the ANS fluorescence quantum yield followed by a decline of the same (Figs. 3.37 & 3.38). This was accompanied by a blue shift of the ANS spectral emission maxima at lower concentrations of AZD, followed by its redshift at higher concentrations. This indicates an initial destabilization of the proteins' structure (possible aggregation) at lower AZD concentrations followed by stabilization at higher concentrations. HSF1-DBD also showed similar behaviour, although the reason behind the changes in the ANS spectral emission maxima, in this case, is presently not clear (Fig. 3.39). Structural stabilization of the proteins at high AZD concentration is corroborated by the fact that 10 μM AZD (the highest AZD concentration used in the ANS binding assays) has been shown to increase their DNA binding ability appreciably. A similar kind of observation has been reported in a previous study, where maximal aggregation of the protein conalbumin has been shown at lower percentages of fluoroalcohols, while higher percentages caused an increase in the protein's helical propensity (Khan et. al. 2014).

Another interesting aspect of the present study is our observation of the specific and reversible interaction of AZD with the canonical 3X-HSE (cHSE) *in vitro* without any protein. This

naturally raises questions on the role of this interaction in the AZD-induced HSE recognition by monomeric HSF1. To address this issue, we studied the binding of AZD with mHSE sequence (to which both monomeric and oligomeric forms of HSF1 bind with extremely low affinity as reported by Jaeger et.al. 2014) under the same conditions as that of cHSE. No significant change was found in the binding affinities of AZD with cHSE and mHSE, suggesting a similar ligand binding mode with the two DNA sequences (Figs. 3.28, 3.31 & 3.32). The affinity of monomeric HSF1-mHSE interaction was raised appreciably in the presence of AZD (K_d: 84.77 ± 28.37 nM) compared to the control condition (K_d: 1172.33 ± 18.61 nM). The binding affinity still, however, remained appreciably lower than that of monomeric HSF1-cHSE interaction in the presence of AZD (K_d: 6.5 ± 2.77 nM) [Figs. 3.22 & 3.33]. This observation suggests that, apart from inducing multimerization of monomeric HSF1, AZD induces such a conformational alteration in the DNA molecule which increases its binding affinity for the multimerized protein. The fact that the binding affinity of multimerized HSF1 with mHSE is lower than that of multimerized HSF1 with cHSE reflects the effect of mutation of critical bases that are vital for HSF1-HSE binding.

Recently, the co-crystal structure of the DNA-bound HSF1 trimer consisting of three DBDs has been reported (Feng et.al. 2021). This study has suggested the preferential recognition and binding of a curved DNA molecule by HSF1. It thus seems possible that AZD induces curvature in both the cHSE and mHSE oligonucleotides, contributing to the enhanced binding affinity of monomeric HSF1 with these DNA oligonucleotides in the presence of AZD. Here, AZD-induced DNA bending seems to be sequence-independent.

A winged helix-turn-helix fold was identified in both NMR and X-ray crystal structures of DBD in heat shock factors from *Kluyveromyces lactis*, fruit fly, and human (Feng et. al. 2016; Littlefield and Nelson, 1999; Vuister et. al. 1994; Xiao et. al. 2020). Strikingly, unlike many transcription factors where the wing motif contacts the DNA, the wing motif of HSF-DBD does not contact the DNA. Rather, it mediates protein-protein interactions; within the same trimeric unit, the HSE-bound DBD molecules interact via this wing motif. The wing motif also mediates interactions between the HSE-bound DBD molecules from adjacent trimeric units, thereby facilitating a synergistic binding of DBDs to HSEs having multiple binding sites. (Feng et. al. 2021). Moreover, upon DNA binding, the recognition helix (α3, the second helix in the helix-turn-helix motif, formed of residues 66–75 in human HSF1-DBD) dips into the major groove and interacts with the 5'-nGAAn-3' motif of the HSE sequence (Neudegger et. al. 2016). The sequence specificity of this interaction was demonstrated by a pair of bidentate

hydrogen bonds established between a highly conserved arginine residue (Arg71 of human HSF1-DBD) and the guanine in the GAA motif (Feng et. al. 2021). Our results are consistent with the idea that AZD facilitates interactions among HSF1 monomers through this winged helix-turn-helix fold either directly or indirectly. Additional studies will be required to better understand this phenomenon.

REFERENCES

1. Agarwal S, Ganesh S. Perinuclear mitochondrial clustering, increased ROS levels, and HIF1 are required for the activation of HSF1 by heat stress. Journal of cell science. 2020 Jul 1;133(13):jcs245589.
2. Ahn SG, Thiele DJ. Redox regulation of mammalian heat shock factor 1 is essential for Hsp gene activation and protection from stress. Genes & development. 2003 Feb 15;17(4):516-28.
3. Ahn YH, Hwang Y, Liu H, Wang XJ, Zhang Y, Stephenson KK, Boronina TN, Cole RN, Dinkova-Kostova AT, Talalay P, Cole PA. Electrophilic tuning of the chemoprotective natural product sulforaphane. Proceedings of the National Academy of Sciences. 2010 May 25;107(21):9590-5.
4. Åkerfelt M, Henriksson E, Laiho A, Vihervaara A, Rautoma K, Kotaja N, Sistonen L. Promoter ChIP-chip analysis in mouse testis reveals Y chromosome occupancy by HSF2. Proceedings of the National Academy of Sciences. 2008 Aug 12;105(32):11224-9.
5. Åkerfelt M, Morimoto RI, Sistonen L. Heat shock factors: integrators of cell stress, development and lifespan. Nature reviews Molecular cell biology. 2010 Aug;11(8):545-55.
6. Alarcon SV, Mollapour M, Lee MJ, Tsutsumi S, Lee S, Kim YS, Prince T, Apolo AB, Giaccone G, Xu W, Neckers LM. Tumor-intrinsic and tumor-extrinsic factors impacting hsp90-targeted therapy. Current molecular medicine. 2012 Nov 1;12(9):1125-41.
7. Alemasova EE, Lavrik OI. Poly (ADP-ribosyl) ation by PARP1: reaction mechanism and regulatory proteins. Nucleic acids research. 2019 May 7;47(8):3811-27.
8. Ali A, Biswas A, Pal M. HSF1 mediated TNF-α production during proteotoxic stress response pioneers proinflammatory signal in human cells. The FASEB Journal. 2019 Feb;33(2):2621-35.
9. Anandhakumar J, Moustafa YW, Chowdhary S, Kainth AS, Gross DS. Evidence for multiple mediator complexes in yeast independently recruited by activated heat shock factor. Molecular and Cellular Biology. 2016 May 16.
10. Ananthan J, Goldberg AL, Voellmy R. Abnormal proteins serve as eukaryotic stress signals and trigger the activation of heat shock genes. Science. 1986 Apr 25;232(4749):522-4.

11. Anckar J, Sistonen L. Regulation of HSF1 function in the heat stress response: implications in aging and disease. Annual review of biochemistry. 2011 Jul 7;80:1089-115.
12. Andringa G, Jongenelen CA, Halfhide L, Drukarch B. The thiol antioxidant 1, 2-dithiole-3-thione stimulates the expression of heat shock protein 70 in dopaminergic PC12 cells. Neuroscience letters. 2007 Apr 6;416(1):76-81.
13. Antonietti P, Linder B, Hehlgans S, Mildenberger IC, Burger MC, Fulda S, Steinbach JP, Gessler F, Rödel F, Mittelbronn M, Kögel D. Interference with the HSF1/HSP70/BAG3 pathway primes glioma cells to matrix detachment and BH3 mimetic–induced apoptosis. Molecular cancer therapeutics. 2017 Jan 1;16(1):156-68.
14. Bali P, Pranpat M, Bradner J, Balasis M, Fiskus W, Guo F, Rocha K, Kumaraswamy S, Boyapalle S, Atadja P, Seto E. Inhibition of histone deacetylase 6 acetylates and disrupts the chaperone function of heat shock protein 90: a novel basis for antileukemia activity of histone deacetylase inhibitors. Journal of Biological Chemistry. 2005 Jul 22;280(29):26729-34.
15. Banerjee Mustafi S, Chakraborty PK, Dey RS, Raha S. Heat stress upregulates chaperone heat shock protein 70 and antioxidant manganese superoxide dismutase through reactive oxygen species (ROS), p38MAPK, and Akt. Cell Stress and Chaperones. 2009 Nov;14:579-89.
16. Banerjee S, Sangwan V, McGinn O, Chugh R, Dudeja V, Vickers SM, Saluja AK. Triptolide-induced cell death in pancreatic cancer is mediated by O-GlcNAc modification of transcription factor Sp1. Journal of Biological Chemistry. 2013 Nov 22;288(47):33927-38.
17. Brandt GE, Schmidt MD, Prisinzano TE, Blagg BS. Gedunin, a novel Hsp90 inhibitor: semisynthesis of derivatives and preliminary structure-activity relationships. Journal of medicinal chemistry. 2008 Oct 23;51(20):6495-502.
18. Brown CW, Chhoy P, Mukhopadhyay D, Karner ER, Mercurio AM. Targeting prominin2 transcription to overcome ferroptosis resistance in cancer. EMBO Molecular Medicine. 2021 Aug 9;13(8):e13792.
19. Bruce JL, Chen C, Xie Y, Zhong R, Wang YQ, Stevenson MA, Calderwood SK. Activation of heat shock transcription factor 1 to a DNA binding form during the G1 phase of the cell cycle. Cell stress & chaperones. 1999 Feb;4(1):36.

20. Budzyński MA, Puustinen MC, Joutsen J, Sistonen L. Uncoupling stress-inducible phosphorylation of heat shock factor 1 from its activation. Molecular and cellular biology. 2015 Jul 1;35(14):2530-40.
21. Calabrese EJ, Dhawan G, Kapoor R, Iavicoli I, Calabrese V. What is hormesis and its relevance to healthy aging and longevity?. Biogerontology. 2015 Dec;16:693-707.
22. Calabrese V, Bates TE, Mancuso C, Cornelius C, Ventimiglia B, Cambria MT, Di Renzo L, De Lorenzo A, Dinkova-Kostova AT. Curcumin and the cellular stress response in free radical-related diseases. Molecular nutrition & food research. 2008 Sep;52(9):1062-73.
23. Calabrese V, Butterfield DA, Stella AM. Nutritional antioxidants and the heme oxygenase pathway of stress tolerance: novel targets for neuroprotection in Alzheimer's disease. The Italian journal of biochemistry. 2003 Dec 1;52(4):177-81.
24. Calabrese V, Cornelius C, Dinkova-Kostova AT, Calabrese EJ, Mattson MP. Cellular stress responses, the hormesis paradigm, and vitagenes: novel targets for therapeutic intervention in neurodegenerative disorders. Antioxidants & redox signaling. 2010 Dec 1;13(11):1763-811.
25. Calamini B, Silva MC, Madoux F, Hutt DM, Khanna S, Chalfant MA, Saldanha SA, Hodder P, Tait BD, Garza D, Balch WE. Small-molecule proteostasis regulators for protein conformational diseases. Nature chemical biology. 2012 Feb;8(2):185-96.
26. Carpenter RL, Gökmen-Polar Y. HSF1 as a cancer biomarker and therapeutic target. Current cancer drug targets. 2019 Aug 1;19(7):515-24.
27. Carpenter RL, Paw I, Dewhirst MW, Lo HW. Akt phosphorylates and activates HSF-1 independent of heat shock, leading to Slug overexpression and epithelial–mesenchymal transition (EMT) of HER2-overexpressing breast cancer cells. Oncogene. 2015 Jan;34(5):546-57.
28. Chang Z, Lu M, Park SM, Park HK, Kang HS, Pak Y, Park JS. Functional HSF1 requires aromatic-participant interactions in protecting mouse embryonic fibroblasts against apoptosis via G2 cell cycle arrest. Molecules and cells. 2012 May;33:465-70.
29. Cheeseman MD, Chessum NE, Rye CS, Pasqua AE, Tucker MJ, Wilding B, Evans LE, Lepri S, Richards M, Sharp SY, Ali S. Discovery of a chemical probe bisamide (CCT251236): an orally bioavailable efficacious pirin ligand from a heat shock transcription factor 1 (HSF1) phenotypic screen. Journal of Medicinal Chemistry. 2017 Jan 12;60(1):180-201.
30. Cheeseman MD, Chessum NE, Rye CS, Pasqua AE, Tucker MJ, Wilding B, Evans LE, Lepri S, Richards M, Sharp SY, Ali S. Discovery of a chemical probe bisamide

(CCT251236): an orally bioavailable efficacious pirin ligand from a heat shock transcription factor 1 (HSF1) phenotypic screen. Journal of Medicinal Chemistry. 2017 Jan 12;60(1):180-201.

31. Chen BC, Tu SL, Zheng BA, Dong QJ, Wan ZA, Dai QQ. Schizandrin A exhibits potent anticancer activity in colorectal cancer cells by inhibiting heat shock factor 1. Bioscience Reports. 2020 Mar;40(3):BSR20200203.
32. Chen F, Fan Y, Cao P, Liu B, Hou J, Zhang B, Tan K. Pan-cancer analysis of the prognostic and immunological role of HSF1: a potential target for survival and immunotherapy. Oxidative medicine and cellular longevity. 2021 Jun 18;2021.
33. Chen R, Wierda WG, Chubb S, Hawtin RE, Fox JA, Keating MJ, Gandhi V, Plunkett W. Mechanism of action of SNS-032, a novel cyclin-dependent kinase inhibitor, in chronic lymphocytic leukemia. Blood, The Journal of the American Society of Hematology. 2009 May 7;113(19):4637-45.
34. Chou SD, Prince T, Gong J, Calderwood SK. mTOR is essential for the proteotoxic stress response, HSF1 activation and heat shock protein synthesis. PloS one. 2012 Jun 29;7(6):e39679.
35. Da Costa R, De Almeida S, Chevarin M, Hadj-Rabia S, Leclerc-Mercier S, Thauvin-Robinet C, Garrido C, Faivre L, Vabres P, Duplomb L, Jego G. Neutralization of HSF1 in cells from PIK3CA-related overgrowth spectrum patients blocks abnormal proliferation. Biochemical and biophysical research communications. 2020 Sep 24;530(3):520-6.
36. Dai C, Whitesell L, Rogers AB, Lindquist S. Heat shock factor 1 is a powerful multifaceted modifier of carcinogenesis. Cell. 2007 Sep 21;130(6):1005-18.
37. Dai S, Tang Z, Cao J, Zhou W, Li H, Sampson S, Dai C. Suppression of the HSF 1-mediated proteotoxic stress response by the metabolic stress sensor AMPK. The EMBO journal. 2015 Feb 3;34(3):275-93.
38. Dayalan Naidu S, Dinkova-Kostova AT. Regulation of the mammalian heat shock factor 1. The FEBS journal. 2017 Jun;284(11):1606-27.
39. Dayalan Naidu S, Sutherland C, Zhang Y, Risco A, de la Vega L, Caunt CJ, Hastie CJ, Lamont DJ, Torrente L, Chowdhry S, Benjamin IJ. Heat shock factor 1 is a substrate for p38 mitogen-activated protein kinases. Molecular and cellular biology. 2016 Sep 1;36(18):2403-17.
40. Desai S, Liu Z, Yao J, Patel N, Chen J, Wu Y, Ahn EE, Fodstad O, Tan M. Heat shock factor 1 (HSF1) controls chemoresistance and autophagy through transcriptional

regulation of autophagy-related protein 7 (ATG7). Journal of Biological Chemistry. 2013 Mar 29;288(13):9165-76.

41. Diane Marsolini SS. A Phase 1 Clinical Study of NXP800 in Subjects with Advanced Cancers. ClinicalTrials.gov. 2022.
42. Dinkova-Kostova AT, Massiah MA, Bozak RE, Hicks RJ, Talalay P. Potency of Michael reaction acceptors as inducers of enzymes that protect against carcinogenesis depends on their reactivity with sulfhydryl groups. Proceedings of the National Academy of Sciences. 2001 Mar 13;98(6):3404-9.
43. Dinkova-Kostova AT, Talalay P, Sharkey J, Zhang Y, Holtzclaw WD, Wang XJ, David E, Schiavoni KH, Finlayson S, Mierke DF, Honda T. An exceptionally potent inducer of cytoprotective enzymes: elucidation of the structural features that determine inducer potency and reactivity with Keap1. Journal of Biological Chemistry. 2010 Oct 29;285(44):33747-55.
44. Dinkova-Kostova AT. The role of sulfhydryl reactivity of small molecules for the activation of the KEAP1/NRF2 pathway and the heat shock response. Scientifica. 2012 Jan 1;2012.
45. Dokladny K, Myers OB, Moseley PL. Heat shock response and autophagy—cooperation and control. Autophagy. 2015 Feb 1;11(2):200-13.
46. Dong B, Jaeger AM, Hughes PF, Loiselle DR, Hauck JS, Fu Y, Haystead TA, Huang J, Thiele DJ. Targeting therapy-resistant prostate cancer via a direct inhibitor of the human heat shock transcription factor 1. Science translational medicine. 2020 Dec 16;12(574):eabb5647.
47. Dong B, Jaeger AM, Thiele DJ. Inhibiting heat shock factor 1 in cancer: a unique therapeutic opportunity. Trends in pharmacological sciences. 2019 Dec 1;40(12):986-1005.
48. Dong Q, Xiu Y, Wang Y, Hodgson C, Borcherding N, Jordan C, Buchanan J, Taylor E, Wagner B, Leidinger M, Holman C. HSF1 is a driver of leukemia stem cell self-renewal in acute myeloid leukemia. Nature communications. 2022 Oct 16;13(1):6107.
49. El-Senduny FF, Altouhamy M, Zayed G, Harsha C, Jalaja R, Somappa SB, Nair MS, Kunnumakkara AB, Alsharif FM, Badria FA. Azadiradione-loaded liposomes with improved bioavailability and anticancer efficacy against triple negative breast cancer. Journal of Drug Delivery Science and Technology. 2021 Oct 1;65:102665.

50. Eroglu B, Pang J, Jin X, Xi C, Moskophidis D, Mivechi NF. HSF1-mediated control of cellular energy metabolism and mTORC1 activation drive acute T-cell lymphoblastic leukemia progression. Molecular Cancer Research. 2020 Mar 1;18(3):463-76.
51. Feng H, Wang S, Guo L, Punekar AS, Ladenstein R, Wang DC, Liu W. MD simulation of high-resolution X-ray structures reveals post-translational modification dependent conformational changes in HSF-DNA interaction. Protein & Cell. 2016 Dec;7(12):916-20.
52. Feng N, Feng H, Wang S, Punekar AS, Ladenstein R, Wang DC, Zhang Q, Ding J, Liu W. Structures of heat shock factor trimers bound to DNA. Iscience. 2021 Sep 24;24(9).
53. Fok JH, Hedayat S, Zhang L, Aronson LI, Mirabella F, Pawlyn C, Bright MD, Wardell CP, Keats JJ, De Billy E, Rye CS. HSF1 is essential for myeloma cell survival and a promising therapeutic target. Clinical Cancer Research. 2018 May 15;24(10):2395-407.
54. Fujimoto M, Takaki E, Takii R, Tan K, Prakasam R, Hayashida N, Iemura SI, Natsume T, Nakai A. RPA assists HSF1 access to nucleosomal DNA by recruiting histone chaperone FACT. Molecular cell. 2012 Oct 26;48(2):182-94.
55. Fujimoto M, Takii R, Takaki E, Katiyar A, Nakato R, Shirahige K, Nakai A. The HSF1–PARP13–PARP1 complex facilitates DNA repair and promotes mammary tumorigenesis. Nature communications. 2017 Nov 21;8(1):1638.
56. Gan N, Wu YC, Brunet M, Garrido C, Chung FL, Dai C, Mi L. Sulforaphane activates heat shock response and enhances proteasome activity through up-regulation of Hsp27. Journal of Biological Chemistry. 2010 Nov 1;285(46):35528-36.
57. Ganguly S, Home T, Yacoub A, Kambhampati S, Shi H, Dandawate P, Padhye S, Saluja AK, McGuirk J, Rao R. Targeting HSF1 disrupts HSP90 chaperone function in chronic lymphocytic leukemia. Oncotarget. 2015 Oct 10;6(31):31767.
58. Gibbs A, Schwartzman J, Deng V, Alumkal J. Sulforaphane destabilizes the androgen receptor in prostate cancer cells by inactivating histone deacetylase 6. Proceedings of the National Academy of Sciences. 2009 Sep 29;106(39):16663-8.
59. Goetzl EJ, Boxer A, Schwartz JB, Abner EL, Petersen RC, Miller BL, Carlson OD, Mustapic M, Kapogiannis D. Low neural exosomal levels of cellular survival factors in Alzheimer's disease. Annals of clinical and translational neurology. 2015 Jul;2(7):769-73.
60. Gomez-Pastor R, Burchfiel ET, Neef DW, Jaeger AM, Cabiscol E, McKinstry SU, Doss A, Aballay A, Lo DC, Akimov SS, Ross CA. Abnormal degradation of the neuronal stress-protective transcription factor HSF1 in Huntington's disease. Nature communications. 2017 Feb 13;8(1):14405

61. Gomez-Pastor R, Burchfiel ET, Thiele DJ. Regulation of heat shock transcription factors and their roles in physiology and disease. Nature reviews Molecular cell biology. 2018 Jan;19(1):4-19.
62. Gorantla NV, Das R, Chidambaram H, Dubey T, Mulani FA, Thulasiram HV, Chinnathambi S. Basic Limonoid modulates Chaperone-mediated Proteostasis and dissolve Tau fibrils. Scientific Reports. 2020 Mar 4;10(1):4023.
63. Grover A, Shandilya A, Agrawal V, Pratik P, Bhasme D, Bisaria VS, Sundar D. Hsp90/Cdc37 chaperone/co-chaperone complex, a novel junction anticancer target elucidated by the mode of action of herbal drug Withaferin A. BMC bioinformatics. 2011 Dec;12(1):1-3.
64. Grunberg N, Pevsner-Fischer M, Goshen-Lago T, Diment J, Stein Y, Lavon H, Mayer S, Levi-Galibov O, Friedman G, Ofir-Birin Y, Syu LJ. Cancer-associated fibroblasts promote aggressive gastric cancer phenotypes via heat shock factor 1–mediated secretion of extracellular vesicles. Cancer research. 2021 Apr 1;81(7):1639-53.
65. Guo R, Xu Q, Liu L, Liu H, Liu Y, Wei W, Qin Y. Bioactive hexapeptide reduced the resistance of ovarian cancer cells to DDP by affecting HSF1/HSP70 signaling pathway. Journal of Cancer. 2021;12(20):6081.
66. Guo Y, Guettouche T, Fenna M, Boellmann F, Pratt WB, Toft DO, Smith DF, Voellmy R. Evidence for a mechanism of repression of heat shock factor 1 transcriptional activity by a multichaperone complex. Journal of Biological Chemistry. 2001 Dec 7;276(49):45791-9.
67. Hamilton KL, Gupta S, Knowlton AA. Estrogen and regulation of heat shock protein expression in female cardiomyocytes: cross-talk with NFκB signaling. Journal of Molecular and Cellular Cardiology. 2004 Apr 1;36(4):577-84.
68. Harrison CJ, Bohm AA, Nelson HC. Crystal structure of the DNA binding domain of the heat shock transcription factor. Science. 1994 Jan 14;263(5144):224-7.
69. Hartl FU, Bracher A, Hayer-Hartl M. Molecular chaperones in protein folding and proteostasis. Nature. 2011 Jul 21;475(7356):324-32.
70. Hartl FU, Hayer-Hartl M. Molecular chaperones in the cytosol: from nascent chain to folded protein. Science. 2002 Mar 8;295(5561):1852-8.
71. Hawe A, Sutter M, Jiskoot W. Extrinsic fluorescent dyes as tools for protein characterization. Pharmaceutical research. 2008 Jul;25:1487-99.
72. Heimberger T, Andrulis M, Riedel S, Stühmer T, Schraud H, Beilhack A, Bumm T, Bogen B, Einsele H, Bargou RC, Chatterjee M. The heat shock transcription factor 1 as a

potential new therapeutic target in multiple myeloma. British journal of haematology. 2013 Feb;160(4):465-76.

73. Hentze N, Le Breton L, Wiesner J, Kempf G, Mayer MP. Molecular mechanism of thermosensory function of human heat shock transcription factor Hsf1. elife. 2016 Jan 19;5:e11576.
74. Hieronymus H, Lamb J, Ross KN, Peng XP, Clement C, Rodina A, Nieto M, Du J, Stegmaier K, Raj SM, Maloney KN. Gene expression signature-based chemical genomic prediction identifies a novel class of HSP90 pathway modulators. Cancer cell. 2006 Oct 1;10(4):321-30.
75. Hietakangas V, Ahlskog JK, Jakobsson AM, Hellesuo M, Sahlberg NM, Holmberg CI, Mikhailov A, Palvimo JJ, Pirkkala L, Sistonen L. Phosphorylation of serine 303 is a prerequisite for the stress-inducible SUMO modification of heat shock factor 1. Molecular and cellular biology. 2003 Apr 1;23(8):2953-68.
76. Hietakangas V, Anckar J, Blomster HA, Fujimoto M, Palvimo JJ, Nakai A, Sistonen L. PDSM, a motif for phosphorylation-dependent SUMO modification. Proceedings of the National Academy of Sciences. 2006 Jan 3;103(1):45-50.
77. Himanen SV, Puustinen MC, Da Silva AJ, Vihervaara A, Sistonen L. HSFs drive transcription of distinct genes and enhancers during oxidative stress and heat shock. Nucleic Acids Research. 2022 Jun 24;50(11):6102-15.
78. Holmes B, Benavides-Serrato A, Freeman RS, Landon KA, Bashir T, Nishimura RN, Gera J. mTORC2/AKT/HSF1/HuR constitute a feed-forward loop regulating Rictor expression and tumor growth in glioblastoma. Oncogene. 2018 Feb;37(6):732-43.
79. Home T, Jensen RA, Rao R. Heat shock factor 1 in protein homeostasis and oncogenic signal integration. Cancer research. 2015 Mar 15;75(6):907-12.
80. Hou Y, Wei H, Luo Y, Liu G. Modulating expression of brain heat shock proteins by estrogen in ovariectomized mice model of aging. Experimental gerontology. 2010 May 1;45(5):323-30.
81. Hu R, Xu C, Shen G, Jain MR, Khor TO, Gopalkrishnan A, Lin W, Reddy B, Chan JY, Kong AN. Gene expression profiles induced by cancer chemopreventive isothiocyanate sulforaphane in the liver of C57BL/6J mice and C57BL/6J/Nrf2 (−/−) mice. Cancer letters. 2006 Nov 18;243(2):170-92.
82. Hu R, Xu C, Shen G, Jain MR, Khor TO, Gopalkrishnan A, Lin W, Reddy B, Chan JY, Kong AN. Identification of Nrf2-regulated genes induced by chemopreventive

isothiocyanate PEITC by oligonucleotide microarray. Life sciences. 2006 Oct 12;79(20):1944-55.

83. Huang CY, Kuo WW, Lo JF, Ho TJ, Pai PY, Chiang SF, Chen PY, Tsai FJ, Tsai CH. Doxorubicin attenuates CHIP-guarded HSF1 nuclear translocation and protein stability to trigger IGF-IIR-dependent cardiomyocyte death. Cell death & disease. 2016 Nov;7(11):e2455-.
84. Huang M, Dong W, Xie R, Wu J, Su Q, Li W, Yao K, Chen Y, Zhou Q, Zhang Q, Li W. HSF1 facilitates the multistep process of lymphatic metastasis in bladder cancer via a novel PRMT5-WDR5-dependent transcriptional program. Cancer Communications. 2022 May;42(5):447-70.
85. Iakoucheva LM, Kimzey AL, Masselon CD, Smith RD, Dunker AK, Ackerman EJ. Aberrant mobility phenomena of the DNA repair protein XPA. Protein Science. 2001 Jul;10(7):1353-62
86. Inouye S, Katsuki K, Izu H, Fujimoto M, Sugahara K, Yamada SI, Shinkai Y, Oka Y, Katoh Y, Nakai A. Activation of heat shock genes is not necessary for protection by heat shock transcription factor 1 against cell death due to a single exposure to high temperatures. Molecular and cellular biology. 2003 Aug 1;23(16):5882-95.
87. Ishtikhar M, Khan MV, Khan S, Chaturvedi SK, Badr G, Mahmoud MH, Khan RH. Biophysical and molecular docking insight into interaction mechanism and thermal stability of human serum albumin isoforms with a semi-synthetic water-soluble camptothecin analog irinotecan hydrochloride. Journal of Biomolecular Structure and Dynamics. 2016 Jul 2;34(7):1545-60.
88. Iwasaki S, Floor SN, Ingolia NT. Rocaglates convert DEAD-box protein eIF4A into a sequence-selective translational repressor. Nature. 2016 Jun 23;534(7608):558-61.
89. Jacobs AT, Marnett LJ. Heat shock factor 1 attenuates 4-Hydroxynonenal-mediated apoptosis: critical role for heat shock protein 70 induction and stabilization of Bcl-XL. Journal of Biological Chemistry. 2007 Nov 16;282(46):33412-20.
90. Jacobs AT, Marnett LJ. HSF1-mediated BAG3 expression attenuates apoptosis in 4-hydroxynonenal-treated colon cancer cells via stabilization of anti-apoptotic Bcl-2 proteins. Journal of Biological Chemistry. 2009 Apr 3;284(14):9176-83.
91. Jaeger AM, Makley LN, Gestwicki JE, Thiele DJ. Genomic heat shock element sequences drive cooperative human heat shock factor 1 DNA binding and selectivity. Journal of Biological Chemistry. 2014 Oct 31;289(44):30459-69.

92. Jaeger AM, Pemble IV CW, Sistonen L, Thiele DJ. Structures of HSF2 reveal mechanisms for differential regulation of human heat-shock factors. Nature structural & molecular biology. 2016 Feb;23(2):147-54.
93. Jiang X, Stockwell BR, Conrad M. Ferroptosis: mechanisms, biology and role in disease. Nature reviews Molecular cell biology. 2021 Apr;22(4):266-82.
94. Joutsen J, Sistonen L. Tailoring of proteostasis networks with heat shock factors. Cold Spring Harbor perspectives in biology. 2019 Apr 1;11(4):a034066.
95. Kang H, Oh T, Bahk YY, Kim GH, Kan SY, Shin DH, Kim JH, Lim JH. HSF1 regulates mevalonate and cholesterol biosynthesis pathways. Cancers. 2019 Sep 13;11(9):1363.
96. Kang MJ, Yun HH, Lee JH. KRIBB11 accelerates Mcl-1 degradation through an HSF1-independent, Mule-dependent pathway in A549 non-small cell lung cancer cells. Biochemical and biophysical research communications. 2017 Oct 21;492(3):304-9.
97. Kanitkar M, Bhonde RR. Curcumin treatment enhances islet recovery by induction of heat shock response proteins, Hsp70 and heme oxygenase-1, during cryopreservation. Life sciences. 2008 Jan 16;82(3-4):182-9.
98. Kansanen E, Jyrkkänen HK, Volger OL, Leinonen H, Kivelä AM, Häkkinen SK, Woodcock SR, Schopfer FJ, Horrevoets AJ, Ylä-Herttuala S, Freeman BA. Nrf2-dependent and-independent responses to nitro-fatty acids in human endothelial cells. Journal of Biological Chemistry. 2009 Nov 27;284(48):33233-41.
99. Katiyar A, Fujimoto M, Tan K, Kurashima A, Srivastava P, Okada M, Takii R, Nakai A. HSF1 is required for induction of mitochondrial chaperones during the mitochondrial unfolded protein response. FEBS Open bio. 2020 Jun;10(6):1135-48.
100. Khan MV, Rabbani G, Ahmad E, Khan RH. Fluoroalcohols-induced modulation and amyloid formation in conalbumin. International journal of biological macromolecules. 2014 Sep 1;70:606-14.
101. Kijima T, Prince TL, Tigue ML, Yim KH, Schwartz H, Beebe K, Lee S, Budzynski MA, Williams H, Trepel JB, Sistonen L. HSP90 inhibitors disrupt a transient HSP90-HSF1 interaction and identify a noncanonical model of HSP90-mediated HSF1 regulation. Scientific reports. 2018 May 3;8(1):6976.
102. Kil YS, Choi SK, Lee YS, Jafari M, Seo EK. Chalcones from Angelica keiskei: evaluation of their heat shock protein inducing activities. Journal of natural products. 2015 Oct 23;78(10):2481-7.

103. Kim E, Wang B, Sastry N, Masliah E, Nelson PT, Cai H, Liao FF. NEDD4-mediated HSF1 degradation underlies α-synucleinopathy. Human molecular genetics. 2016 Jan 15;25(2):211-22.

104. Kim JA, Kim Y, Kwon BM, Han DC. The natural compound cantharidin induces cancer cell death through inhibition of heat shock protein 70 (HSP70) and Bcl-2-associated athanogene domain 3 (BAG3) expression by blocking heat shock factor 1 (HSF1) binding to promoters. Journal of Biological Chemistry. 2013 Oct 4;288(40):28713-26.

105. Kim SH, Han SI, Oh SY, Chung HY, Do Kim H, Kang HS. Activation of heat shock factor 1 by pyrrolidine dithiocarbamate is mediated by its activities as pro-oxidant and thiol modulator. Biochemical and Biophysical Research Communications. 2001 Feb 23;281(2):367-72.

106. Kim SJ, Tsukiyama T, Lewis MS, Wu C. Interaction of the DNA-binding domain of Drosophila heat shock factor with its cognate DNA site: A thermodynamic analysis using analytical ultracentrifugation. Protein Science. 1994 Jul;3(7):1040-51.

107. Kim SY, Lee HJ, Nam JW, Seo EK, Lee YS. Coniferyl aldehyde reduces radiation damage through increased protein stability of heat shock transcriptional factor 1 by phosphorylation. International Journal of Radiation Oncology* Biology* Physics. 2015 Mar 15;91(4):807-16.

108. Kmiecik SW, Mayer MP. Molecular mechanisms of heat shock factor 1 regulation. Trends in biochemical sciences. 2022 Mar 1;47(3):218-34.

109. Kourtis N, Moubarak RS, Aranda-Orgilles B, Lui K, Aydin IT, Trimarchi T, Darvishian F, Salvaggio C, Zhong J, Bhatt K, Chen EI. FBXW7 modulates cellular stress response and metastatic potential through HSF1 post-translational modification. Nature cell biology. 2015 Mar;17(3):322-32.

110. Krakowiak J, Zheng X, Patel N, Feder ZA, Anandhakumar J, Valerius K, Gross DS, Khalil AS, Pincus D. Hsf1 and Hsp70 constitute a two-component feedback loop that regulates the yeast heat shock response. Elife. 2018 Feb 2;7:e31668.

111. Kunnumakkara AB, Bordoloi D, Padmavathi G, Monisha J, Roy NK, Prasad S, Aggarwal BB. Curcumin, the golden nutraceutical: multitargeting for multiple chronic diseases. British journal of pharmacology. 2017 Jun;174(11):1325-48.

112. Lakowicz JR, editor. Principles of fluorescence spectroscopy. Boston, MA: springer US; 2006 Sep 15.

113. Lee S, Jung J, Lee YJ, Kim SK, Kim JA, Kim BK, Park KC, Kwon BM, Han DC. Targeting HSF1 as a therapeutic strategy for multiple mechanisms of EGFR inhibitor resistance in EGFR mutant non-small-cell lung cancer. Cancers. 2021 Jun 15;13(12):2987.

114. Lee YJ, Kim EH, Lee JS, Jeoung D, Bae S, Kwon SH, Lee YS. HSF1 as a mitotic regulator: phosphorylation of HSF1 by Plk1 is essential for mitotic progression. Cancer research. 2008 Sep 15;68(18):7550-60.

115. Lee YY, Gil ES, Jeong IH, Kim H, Jang JH, Choung YH. Heat shock factor 1 prevents age-related hearing loss by decreasing endoplasmic reticulum stress. Cells. 2021 Sep 17;10(9):2454.

116. Leong SS, Ng WM, Lim J, Yeap SP. Dynamic light scattering: effective sizing technique for characterization of magnetic nanoparticles. Handbook of materials characterization. 2018:77-111.

117. Li G, Kryczek I, Nam J, Li X, Li S, Li J, Wei S, Grove S, Vatan L, Zhou J, Du W. LIMIT is an immunogenic lncRNA in cancer immunity and immunotherapy. Nature cell biology. 2021 May;23(5):526-37.

118. Li J, Chauve L, Phelps G, Brielmann RM, Morimoto RI. E2F coregulates an essential HSF developmental program that is distinct from the heat-shock response. Genes & development. 2016 Sep 15;30(18):2062-75.

119. Li J, Labbadia J, Morimoto RI. Rethinking HSF1 in stress, development, and organismal health. Trends in cell biology. 2017 Dec 1;27(12):895-905.

120. Li J, Song P, Jiang T, Dai D, Wang H, Sun J, Zhu L, Xu W, Feng L, Shin VY, Morrison H. Heat shock factor 1 epigenetically stimulates glutaminase-1-dependent mTOR activation to promote colorectal carcinogenesis. Molecular Therapy. 2018 Jul 5;26(7):1828-39.

121. Li K, Deng X, Feng G, Chen Y. Knockdown of Bcl-2-Associated Athanogene-3 Can Enhance the Efficacy of BGJ398 via Suppressing Migration and Inducing Apoptosis in Gastric Cancer. Digestive Diseases and Sciences. 2021 Sep;66:3036-44.

122. Li N, Wang T, Li Z, Ye X, Deng B, Zhuo S, Yao P, Yang M, Mei H, Chen X, Zhu T. Dorsomorphin induces cancer cell apoptosis and sensitizes cancer cells to HSP90 and proteasome inhibitors by reducing nuclear heat shock factor 1 levels. Cancer Biology & Medicine. 2019 May;16(2):220.

123. Li Q, Martinez JD. Loss of HSF1 results in defective radiation-induced G2 arrest and DNA repair. Radiation research. 2011 Jul 1;176(1):17-24.

124. Li Y, Wang D, Ping X, Zhang Y, Zhang T, Wang L, Jin L, Zhao W, Guo M, Shen F, Meng M. Local hyperthermia therapy induces browning of white fat and treats obesity. Cell. 2022 Mar 17;185(6):949-66.

125. Li Y, Zhang T, Schwartz SJ, Sun D. Sulforaphane potentiates the efficacy of 17-allylamino 17-demethoxygeldanamycin against pancreatic cancer through enhanced abrogation of Hsp90 chaperone function. Nutrition and cancer. 2011 Oct 1;63(7):1151-9.

126. Liang W, Liao Y, Zhang J, Huang Q, Luo W, Yu J, Gong J, Zhou Y, Li X, Tang B, He S. Heat shock factor 1 inhibits the mitochondrial apoptosis pathway by regulating second mitochondria-derived activator of caspase to promote pancreatic tumorigenesis. Journal of Experimental & Clinical Cancer Research. 2017 Dec;36:1-4.

127. Liao Y, Xue Y, Zhang L, Feng X, Liu W, Zhang G. Higher heat shock factor 1 expression in tumor stroma predicts poor prognosis in esophageal squamous cell carcinoma patients. Journal of translational medicine. 2015 Dec;13:1-3.

128. Littlefield O, Nelson H. A new use for the'wing'of the'winged'helix-turn-helix motif in the HSF–DNA cocrystal. Nature structural biology. 1999 May;6(5):464-70.

129. Liu Y, Chang A. Heat shock response relieves ER stress. The EMBO journal. 2008 Apr 9;27(7):1049-59.

130. Lu M, Kim HE, Li CR, Kim S, Kwak IJ, Lee YJ, Kim SS, Moon JY, Kim CH, Kim DK, Kang HS. Two distinct disulfide bonds formed in human heat shock transcription factor 1 act in opposition to regulate its DNA binding activity. Biochemistry. 2008 Jun 3;47(22):6007-15.

131. Lu M, Lee YJ, Park SM, Kang HS, Kang SW, Kim S, Park JS. Aromatic-participant interactions are essential for disulfide-bond-based trimerization in human heat shock transcription factor 1. Biochemistry. 2009 May 12;48(18):3795-7.

132. Luft JC, Benjamin IJ, Mestril R, Dix DJ. Heat shock factor 1–mediated thermotolerance prevents cell death and results in G2/M cell cycle arrest. Cell Stress & Chaperones. 2001 Oct;6(4):326.

133. Ma X, Xu L, Alberobello AT, Gavrilova O, Bagattin A, Skarulis M, Liu J, Finkel T, Mueller E. Celastrol protects against obesity and metabolic dysfunction through activation of a HSF1-PGC1α transcriptional axis. Cell metabolism. 2015 Oct 6;22(4):695-708.

134. Mahat DB, Salamanca HH, Duarte FM, Danko CG, Lis JT. Mammalian heat shock response and mechanisms underlying its genome-wide transcriptional regulation. Molecular cell. 2016 Apr 7;62(1):63-78.

135. Mancuso C, Bates TE, Butterfield DA, Calafato S, Cornelius C, Lorenzo AD, Dinkova Kostova AT, Calabrese V. Natural antioxidants in Alzheimer's disease. Expert opinion on investigational drugs. 2007 Dec 1;16(12):1921-31.

136. Martínez-Ruiz A, Villanueva L, de Orduña CG, López-Ferrer D, Higueras MÁ, Tarín C, Rodríguez-Crespo I, Vázquez J, Lamas S. S-nitrosylation of Hsp90 promotes the inhibition of its ATPase and endothelial nitric oxide synthase regulatory activities. Proceedings of the National Academy of Sciences. 2005 Jun 14;102(24):8525-30.

137. Masser AE, Ciccarelli M, Andréasson C. Hsf1 on a leash–controlling the heat shock response by chaperone titration. Experimental Cell Research. 2020 Nov 1;396(1):112246.

138. McConnell JR, Buckton LK, McAlpine SR. Regulating the master regulator: Controlling heat shock factor 1 as a chemotherapy approach. Bioorganic & medicinal chemistry letters. 2015 Sep 1;25(17):3409-14.

139. Meisel H. Biochemical properties of peptides encrypted in bovine milk proteins. Current medicinal chemistry. 2005 Aug 1;12(16):1905-19.

140. Mendillo ML, Santagata S, Koeva M, Bell GW, Hu R, Tamimi RM, Fraenkel E, Ince TA, Whitesell L, Lindquist S. HSF1 drives a transcriptional program distinct from heat shock to support highly malignant human cancers. Cell. 2012 Aug 3;150(3):549-62.

141. Menezes K, Aram G, Mirabella F, Johnson DC, Sherborne AL, Houlston RS, Cheeseman MD, Pasqua E, Clarke P, Workman P, Jones K. The novel protein HSF1 stress pathway inhibitor bisamide CCT361814 demonstrates pre-clinical anti-tumor activity in myeloma. Blood. 2017 Dec 8;130:3072.

142. Meng L, Gabai VL, Sherman MY. Heat-shock transcription factor HSF1 has a critical role in human epidermal growth factor receptor-2-induced cellular transformation and tumorigenesis. Oncogene. 2010 Sep;29(37):5204-13.

143. Metzler B, Abia R, Ahmad M, Wernig F, Pachinger O, Hu Y, Xu Q. Activation of heat shock transcription factor 1 in atherosclerosis. The American journal of pathology. 2003 May 1;162(5):1669-76.

144. Myzak MC, Dashwood WM, Orner GA, Ho E, Dashwood RH. Sulforaphane inhibits histone deacetylase in vivo and suppresses tumorigenesis in Apcmin mice. The FASEB journal: official publication of the Federation of American Societies for Experimental Biology. 2006 Mar;20(3):506.

145. Myzak MC, Hardin K, Wang R, Dashwood RH, Ho E. Sulforaphane inhibits histone deacetylase activity in BPH-1, LnCaP and PC-3 prostate epithelial cells. Carcinogenesis. 2006 Apr 1;27(4):811-9.

146. Myzak MC, Karplus PA, Chung FL, Dashwood RH. A novel mechanism of chemoprotection by sulforaphane: inhibition of histone deacetylase. Cancer research. 2004 Aug 15;64(16):5767-74.

147. Neef DW, Jaeger AM, Gomez-Pastor R, Willmund F, Frydman J, Thiele DJ. A direct regulatory interaction between chaperonin TRiC and stress-responsive transcription factor HSF1. Cell reports. 2014 Nov 6;9(3):955-66.

148. Neef DW, Jaeger AM, Gomez-Pastor R, Willmund F, Frydman J, Thiele DJ. A direct regulatory interaction between chaperonin TRiC and stress-responsive transcription factor HSF1. Cell reports. 2014 Nov 6;9(3):955-66.

149. Neef DW, Turski ML, Thiele DJ. Modulation of heat shock transcription factor 1 as a therapeutic target for small molecule intervention in neurodegenerative disease. PLoS biology. 2010 Jan 19;8(1):e1000291.

150. Nelson VK, Ali A, Dutta N, Ghosh S, Jana M, Ganguli A, Komarov A, Paul S, Dwivedi V, Chatterjee S, Jana NR. Azadiradione ameliorates polyglutamine expansion disease in Drosophila by potentiating DNA binding activity of heat shock factor 1. Oncotarget. 2016 Nov 11;7(48):78281.

151. Neudegger T, Verghese J, Hayer-Hartl M, Hartl FU, Bracher A. Structure of human heat-shock transcription factor 1 in complex with DNA. Nature structural & molecular biology. 2016 Feb;23(2):140-6.

152. Oommen D, Prise KM. KNK437, abrogates hypoxia-induced radioresistance by dual targeting of the AKT and HIF-1α survival pathways. Biochemical and Biophysical Research Communications. 2012 May 11;421(3):538-43.

153. Östling P, Björk JK, Roos-Mattjus P, Mezger V, Sistonen L. Heat shock factor 2 (HSF2) contributes to inducible expression of hsp genes through interplay with HSF1. Journal of Biological Chemistry. 2007 Mar 9;282(10):7077-86.

154. Park JM, Werner J, Kim JM, Lis JT, Kim YJ. Mediator, not holoenzyme, is directly recruited to the heat shock promoter by HSF upon heat shock. Molecular cell. 2001 Jul 1;8(1):9-19.

155. Patwardhan CA, Fauq A, Peterson LB, Miller C, Blagg BS, Chadli A. Gedunin Inactivates the Co-chaperone p23 Protein Causing Cancer Cell Death by Apoptosis. Journal of Biological Chemistry. 2013 Mar 8;288(10):7313-25.

156. Peffer S, Gonçalves D, Morano KA. Regulation of the Hsf1-dependent transcriptome via conserved bipartite contacts with Hsp70 promotes survival in yeast. Journal of Biological Chemistry. 2019 Aug 9;294(32):12191-202.

157. Pelham HR. A regulatory upstream promoter element in the Drosophila hsp 70 heat-shock gene. Cell. 1982 Sep 1;30(2):517-28.

158. Pledgie-Tracy A, Sobolewski MD, Davidson NE. Sulforaphane induces cell type–specific apoptosis in human breast cancer cell lines. Molecular cancer therapeutics. 2007 Mar 1;6(3):1013-21.

159. Qiao A, Jin X, Pang J, Moskophidis D, Mivechi NF. The transcriptional regulator of the chaperone response HSF1 controls hepatic bioenergetics and protein homeostasis. Journal of Cell Biology. 2017 Mar 6;216(3):723-41.

160. Ran X, Burchfiel ET, Dong B, Rettko NJ, Dunyak BM, Shao H, Thiele DJ, Gestwicki JE. Rational design and screening of peptide-based inhibitors of heat shock factor 1 (HSF1). Bioorganic & medicinal chemistry. 2018 Oct 15;26(19):5299-306.

161. Ray Chaudhuri A, Nussenzweig A. The multifaceted roles of PARP1 in DNA repair and chromatin remodelling. Nature reviews Molecular cell biology. 2017 Oct;18(10):610-21.

162. Raychaudhuri S, Loew C, Körner R, Pinkert S, Theis M, Hayer-Hartl M, Buchholz F, Hartl FU. Interplay of acetyltransferase EP300 and the proteasome system in regulating heat shock transcription factor 1. Cell. 2014 Feb 27;156(5):975-85.

163. Retzlaff M, Stahl M, Eberl HC, Lagleder S, Beck J, Kessler H, Buchner J. Hsp90 is regulated by a switch point in the C-terminal domain. EMBO reports. 2009 Oct;10(10):1147-53.

164. Rokavec M, Wu W, Luo JL. IL6-mediated suppression of miR-200c directs constitutive activation of inflammatory signaling circuit driving transformation and tumorigenesis. Molecular cell. 2012 Mar 30;45(6):777-89.

165. Roos-Mattjus P, Sistonen L. Interplay between mammalian heat shock factors 1 and 2 in physiology and pathology. The FEBS Journal. 2022 Dec;289(24):7710-25.

166. Roy M, Bhakta K, Bhowmick A, Gupta S, Ghosh A, Ghosh A. Archaeal Hsp14 drives substrate shuttling between small heat shock proteins and thermosome: insights into a novel substrate transfer pathway. The FEBS Journal. 2022 Feb;289(4):1080-104.

167. Rye CS, Chessum NE, Lamont S, Pike KG, Faulder P, Demeritt J, Kemmitt P, Tucker J, Zani L, Cheeseman MD, Isaac R. Discovery of 4, 6-disubstituted pyrimidines as potent inhibitors of the heat shock factor 1 (HSF1) stress pathway and CDK9. Medchemcomm. 2016;7(8):1580-6.

168. Sakib R, Caruso F, Belli S, Rossi M. Azadiradione, a Component of Neem Oil, Behaves as a Superoxide Dismutase Mimic When Scavenging the Superoxide Radical, as

Shown Using DFT and Hydrodynamic Voltammetry. Biomedicines. 2023 Nov 18;11(11):3091.

169. Salminen A, Lehtonen M, Paimela T, Kaarniranta K. Celastrol: molecular targets of thunder god vine. Biochemical and biophysical research communications. 2010 Apr 9;394(3):439-42.

170. Sandqvist A, Björk JK, Åkerfelt M, Chitikova Z, Grichine A, Vourc'h C, Jolly C, Salminen TA, Nymalm Y, Sistonen L. Heterotrimerization of heat-shock factors 1 and 2 provides a transcriptional switch in response to distinct stimuli. Molecular biology of the cell. 2009 Mar 1;20(5):1340-7.

171. Sangle GV, Zhao R, Mizuno TM, Shen GX. Involvement of RAGE, NADPH oxidase, and Ras/Raf-1 pathway in glycated LDL-induced expression of heat shock factor-1 and plasminogen activator inhibitor-1 in vascular endothelial cells. Endocrinology. 2010 Sep 1;151(9):4455-66.

172. Sangwan V, Banerjee S, Jensen KM, Chen Z, Chugh R, Dudeja V, Vickers SM, Saluja AK. Primary and Liver Metastasis–Derived Cell Lines From KrasG12D; Trp53R172H; Pdx-1 Cre Animals Undergo Apoptosis in Response to Triptolide. Pancreas. 2015 May 1;44(4):583-9.

173. Sano R, Reed JC. ER stress-induced cell death mechanisms. Biochimica et Biophysica Acta (BBA)-Molecular Cell Research. 2013 Dec 1;1833(12):3460-70.

174. Santagata S, Mendillo ML, Tang YC, Subramanian A, Perley CC, Roche SP, Wong B, Narayan R, Kwon H, Koeva M, Amon A. Tight coordination of protein translation and HSF1 activation supports the anabolic malignant state. Science. 2013 Jul 19;341(6143):1238303.

175. Santagata S, Xu YM, Wijeratne EK, Kontnik R, Rooney C, Perley CC, Kwon H, Clardy J, Kesari S, Whitesell L, Lindquist S. Using the heat-shock response to discover anticancer compounds that target protein homeostasis. ACS chemical biology. 2012 Feb 17;7(2):340-9.

176. Sarkar C, Chaudhary P, Jamaddar S, Janmeda P, Mondal M, Mubarak MS, Islam MT. Redox activity of flavonoids: Impact on human health, therapeutics, and chemical safety. Chemical Research in Toxicology. 2022 Jan 19;35(2):140-62.

177. Sasaya T, Kubo T, Murata K, Mizue Y, Sasaki K, Yanagawa J, Imagawa M, Kato H, Tsukahara T, Kanaseki T, Tamura Y. Cisplatin-induced HSF1-HSP90 axis enhances the expression of functional PD-L1 in oral squamous cell carcinoma. Cancer Medicine. 2023 Feb;12(4):4605-15.

178. Satoh T, Rezaie T, Seki M, Sunico CR, Tabuchi T, Kitagawa T, Yanagitai M, Senzaki M, Kosegawa C, Taira H, McKercher SR. Dual neuroprotective pathways of a pro-electrophilic compound via HSF-1-activated heat-shock proteins and Nrf2-activated phase 2 antioxidant response enzymes. Journal of neurochemistry. 2011 Nov;119(3):569-78.

179. Satyal SH, Morimoto RI. Biochemical events in the activation and attenuation of the heat shock transcriptional response. Journal of biosciences. 1998 Oct;23:303-11.

180. Scherz-Shouval R, Santagata S, Mendillo ML, Sholl LM, Ben-Aharon I, Beck AH, Dias-Santagata D, Koeva M, Stemmer SM, Whitesell L, Lindquist S. The reprogramming of tumor stroma by HSF1 is a potent enabler of malignancy. Cell. 2014 Jul 31;158(3):564-78.

181. Schilling D, Kühnel A, Konrad S, Tetzlaff F, Bayer C, Yaglom J, Multhoff G. Sensitizing tumor cells to radiation by targeting the heat shock response. Cancer letters. 2015 May 1;360(2):294-301.

182. Schilling D, Kühnel A, Tetzlaff F, Konrad S, Multhoff G. NZ28-induced inhibition of HSF1, SP1 and NF-κB triggers the loss of the natural killer cell-activating ligands MICA/B on human tumor cells. Cancer Immunology, Immunotherapy. 2015 May;64:599-608.

183. Schulz R, Streller F, Scheel AH, Rueschoff J, Reinert MC, Dobbelstein M, Marchenko ND, Moll UM. HER2/ErbB2 activates HSF1 and thereby controls HSP90 clients including MIF in HER2-overexpressing breast cancer. Cell death & disease. 2014 Jan;5(1):e980-.

184. Seal S, Banerjee N, Mahato R, Kundu T, Sinha D, Chakraborty T, Sinha D, Sau K, Chatterjee S, Sau S. Serine 106 preserves the tertiary structure, function, and stability of a cyclophilin from Staphylococcus aureus. Journal of Biomolecular Structure and Dynamics. 2023 Mar 4;41(4):1479-94.

185. Sengupta S, Singh N, Paul A, Datta D, Chatterjee D, Mukherjee S, Gadhe L, Devi J, Mahesh Y, Jolly MK, Maji SK. p53 amyloid pathology is correlated with higher cancer grade irrespective of the mutant or wild-type form. Journal of cell science. 2023 Sep 1;136(17):jcs261017.

186. Shaashua L, Ben-Shmuel A, Pevsner-Fischer M, Friedman G, Levi-Galibov O, Nandakumar S, Barki D, Nevo R, Brown LE, Zhang W, Stein Y. BRCA mutational status shapes the stromal microenvironment of pancreatic cancer linking clusterin expression in

cancer associated fibroblasts with HSF1 signaling. Nature communications. 2022 Oct 31;13(1):6513.

187. Sharma C, Seo YH. Small molecule inhibitors of HSF1-activated pathways as potential next-generation anticancer therapeutics. Molecules. 2018 Oct 24;23(11):2757.

188. Sharma R, Sharma A, Chaudhary P, Pearce V, Vatsyayan R, Singh SV, Awasthi S, Awasthi YC. Role of lipid peroxidation in cellular responses to D, L-sulforaphane, a promising cancer chemopreventive agent. Biochemistry. 2010 Apr 13;49(14):3191-202.

189. Shen Z, Yin L, Zhou H, Ji X, Jiang C, Zhu X, He X. Combined inhibition of AURKA and HSF1 suppresses proliferation and promotes apoptosis in hepatocellular carcinoma by activating endoplasmic reticulum stress. Cellular Oncology. 2021 Oct;44(5):1035-49.

190. Shi Y, Mosser DD, Morimoto RI. Molecular chaperones as HSF1-specific transcriptional repressors. Genes & development. 1998 Mar 1;12(5):654-66.

191. Shi Y, Sun L, Zhang R, Hu Y, Wu Y, Dong X, Dong D, Chen C, Geng Z, Li E, Fan Y. Thrombospondin 4/integrin α2/HSF1 axis promotes proliferation and cancer stem-like traits of gallbladder cancer by enhancing reciprocal crosstalk between cancer-associated fibroblasts and tumor cells. Journal of Experimental & Clinical Cancer Research. 2021 Dec;40(1):1-9.

192. Sinclair DA, Guarente L. Small-molecule allosteric activators of sirtuins. Annual review of pharmacology and toxicology. 2014 Jan 6;54:363-80.

193. Singh BK, Vatsa N, Nelson VK, Kumar V, Kumar SS, Mandal SC, Pal M, Jana NR. Azadiradione restores protein quality control and ameliorates the disease pathogenesis in a mouse model of Huntington's disease. Molecular neurobiology. 2018 Aug;55:6337-46.

194. Sinha D, Sinha D, Dutta A, Chakraborty T, Mondal R, Seal S, Poddar A, Chatterjee S, Sau S. Alternative sigma factor of Staphylococcus aureus interacts with the cognate Antisigma factor primarily using its domain 3. Biochemistry. 2021 Jan 6;60(2):135-51.

195. Smith RS, Takagishi SR, Amici DR, Metz K, Gayatri S, Alasady MJ, Wu Y, Brockway S, Taiberg SL, Khalatyan N, Taipale M. HSF2 cooperates with HSF1 to drive a transcriptional program critical for the malignant state. Science Advances. 2022 Mar 16;8(11):eabj6526.

196. Solís EJ, Pandey JP, Zheng X, Jin DX, Gupta PB, Airoldi EM, Pincus D, Denic V. Defining the essential function of yeast Hsf1 reveals a compact transcriptional program for maintaining eukaryotic proteostasis. Molecular cell. 2016 Jul 7;63(1):60-71.

197. Sonawane SK, Uversky VN, Chinnathambi S. Baicalein inhibits heparin-induced Tau aggregation by initializing non-toxic Tau oligomer formation. Cell Communication and Signaling. 2021 Dec;19:1-6.
198. Sorger PK, Pelham HR. Purification and characterization of a heat-shock element binding protein from yeast. The EMBO journal. 1987 Oct;6(10):3035-41.
199. Sreeramulu S, Gande SL, Göbel M, Schwalbe H. Molecular mechanism of inhibition of the human protein complex Hsp90–Cdc37, a kinome chaperone–cochaperone, by triterpene celastrol. Angewandte Chemie International Edition. 2009 Jul 27;48(32):5853-5.
200. Studier FW, Moffatt BA. Use of bacteriophage T7 RNA polymerase to direct selective high-level expression of cloned genes. Journal of molecular biology. 1986 May 5;189(1):113-30.
201. Su KH, Cao J, Tang Z, Dai S, He Y, Sampson SB, Benjamin IJ, Dai C. HSF1 critically attunes proteotoxic stress sensing by mTORC1 to combat stress and promote growth. Nature cell biology. 2016 May;18(5):527-39.
202. Sun X, Ou Z, Xie M, Kang R, Fan Y, Niu X, Wang H, Cao L, Tang D. HSPB1 as a novel regulator of ferroptotic cancer cell death. Oncogene. 2015 Nov;34(45):5617-25.
203. Sun X, Ou Z, Xie M, Kang R, Fan Y, Niu X, Wang H, Cao L, Tang D. HSPB1 as a novel regulator of ferroptotic cancer cell death. Oncogene. 2015 Nov;34(45):5617-25.
204. Szopa A, Ekiert R, Ekiert H. Current knowledge of Schisandra chinensis (Turcz.) Baill.(Chinese magnolia vine) as a medicinal plant species: a review on the bioactive components, pharmacological properties, analytical and biotechnological studies. Phytochemistry Reviews. 2017 Apr;16:195-218.
205. Takii R, Fujimoto M, Matsumoto M, Srivastava P, Katiyar A, Nakayama KI, Nakai A. The pericentromeric protein shugoshin 2 cooperates with HSF 1 in heat shock response and RNA Pol II recruitment. The EMBO Journal. 2019 Dec 16;38(24):e102566.
206. Takii R, Fujimoto M, Tan K, Takaki E, Hayashida N, Nakato R, Shirahige K, Nakai A. ATF1 modulates the heat shock response by regulating the stress-inducible heat shock factor 1 transcription complex. Molecular and cellular biology. 2015 Jan 1;35(1):11-25.
207. Tan K, Fujimoto M, Takii R, Takaki E, Hayashida N, Nakai A. Mitochondrial SSBP1 protects cells from proteotoxic stresses by potentiating stress-induced HSF1 transcriptional activity. Nature communications. 2015 Mar 12;6(1):6580.

208. Tang Z, Dai S, He Y, Doty RA, Shultz LD, Sampson SB, Dai C. MEK guards proteome stability and inhibits tumor-suppressive amyloidogenesis via HSF1. Cell. 2015 Feb 12;160(4):729-44.

209. Thompson CA, Burcham PC. Genome-wide transcriptional responses to acrolein. Chemical Research in Toxicology. 2008 Dec 15;21(12):2245-56.

210. Toma-Jonik A, Vydra N, Janus P, Widłak W. Interplay between HSF1 and p53 signaling pathways in cancer initiation and progression: non-oncogene and oncogene addiction. Cellular Oncology. 2019 Oct;42:579-89.

211. Velayutham M, Cardounel AJ, Liu Z, Ilangovan G. Discovering a reliable heat-shock factor-1 inhibitor to treat human cancers: potential opportunity for phytochemists. Frontiers in Oncology. 2018 Apr 6;8:97.

212. Venkatakrishnan CD, Dunsmore K, Wong H, Roy S, Sen CK, Wani A, Zweier JL, Ilangovan G. HSP27 regulates p53 transcriptional activity in doxorubicin-treated fibroblasts and cardiac H9c2 cells: p21 upregulation and G2/M phase cell cycle arrest. American Journal of Physiology-Heart and Circulatory Physiology. 2008 Apr;294(4):H1736-44.

213. Vihervaara A, Sergelius C, Vasara J, Blom MA, Elsing AN, Roos-Mattjus P, Sistonen L. Transcriptional response to stress in the dynamic chromatin environment of cycling and mitotic cells. Proceedings of the National Academy of Sciences. 2013 Sep 3;110(36):E3388-97.

214. Vilaboa N, Boré A, Martin-Saavedra F, Bayford M, Winfield N, Firth-Clark S, Kirton SB, Voellmy R. New inhibitor targeting human transcription factor HSF1: effects on the heat shock response and tumor cell survival. Nucleic acids research. 2017 Jun 2;45(10):5797-817.

215. Vuister GW, Kim SJ, Orosz A, Marquardt J, Wu C, Bax A. Solution structure of the DNA-binding domain of Drosophila heat shock transcription factor. Nature structural biology. 1994 Sep 1;1(9):605-14.

216. Vydra N, Toma A, Glowala-Kosinska M, Gogler-Piglowska A, Widlak W. Overexpression of heat shock transcription factor 1 enhances the resistance of melanoma cells to doxorubicin and paclitaxel. BMC cancer. 2013 Dec;13:1-1.

217. Wang G, Cao P, Fan Y, Tan K. Emerging roles of HSF1 in cancer: cellular and molecular episodes. Biochimica et Biophysica Acta (BBA)-Reviews on Cancer. 2020 Aug 1;1874(1):188390.

218. Wang H, Wang X, Zhang H, Deng T, Liu R, Liu Y, Li H, Bai M, Ning T, Wang J, Ge S. The HSF1/miR-135b-5p axis induces protective autophagy to promote oxaliplatin resistance through the MUL1/ULK1 pathway in colorectal cancer. Oncogene. 2021 Jul 15;40(28):4695-708.

219. Watanabe Y, Tsujimura A, Taguchi K, Tanaka M. HSF1 stress response pathway regulates autophagy receptor SQSTM1/p62-associated proteostasis. Autophagy. 2017 Jan 2;13(1):133-48.

220. West JD, Wang Y, Morano KA. Small molecule activators of the heat shock response: chemical properties, molecular targets, and therapeutic promise. Chemical research in toxicology. 2012 Oct 15;25(10):2036-53.

221. Westerheide SD, Anckar J, Stevens Jr SM, Sistonen L, Morimoto RI. Stress-inducible regulation of heat shock factor 1 by the deacetylase SIRT1. Science. 2009 Feb 20;323(5917):1063-6.

222. Westerheide SD, Bosman JD, Mbadugha BN, Kawahara TL, Matsumoto G, Kim S, Gu W, Devlin JP, Silverman RB, Morimoto RI. Celastrols as Inducers of the Heat Shock Response and Cytoprotection*[boxs]. Journal of Biological Chemistry. 2004 Dec 31;279(53):56053-60.

223. Whitesell L, Lindquist S. Inhibiting the transcription factor HSF1 as an anticancer strategy. Expert opinion on therapeutic targets. 2009 Apr 1;13(4):469-78.

224. Whitesell L, Lindquist SL. HSP90 and the chaperoning of cancer. Nature Reviews Cancer. 2005 Oct;5(10):761-72.

225. Wittig I, Braun HP, Schägger H. Blue native PAGE. Nature protocols. 2006 Jun;1(1):418-28.

226. Wood JG, Rogina B, Lavu S, Howitz K, Helfand SL, Tatar M, Sinclair D. Sirtuin activators mimic caloric restriction and delay ageing in metazoans. Nature. 2004 Aug 5;430(7000):686-9.

227. Workman P, Clarke PA, Te Poele R, Powers M, Box G, De Billy E, Brandon AD, Hallsworth A, Hayes A, McCann H, Sharp S. Discovery and validation of biomarkers to support clinical development of NXP800: A first-in-class orally active, small-molecule HSF1 pathway inhibitor. European Journal of Cancer. 2022 Oct 1;174:S35.

228. WU LX, XU JH, HUANG XW, ZHANG KZ, WEN CX, CHEN YZ. Down-regulation of p210bcr/abl by curcumin involves disrupting molecular chaperone functions of Hsp90 1. Acta Pharmacologica Sinica. 2006 Jun;27(6):694-9.

229. Wu Y, Chen C, Sun X, Shi X, Jin B, Ding K, Yeung SC, Pan J. Cyclin-dependent kinase 7/9 inhibitor SNS-032 abrogates FIP1-like-1 platelet-derived growth factor receptor α and bcr-abl oncogene addiction in malignant hematologic cells. Clinical Cancer Research. 2012 Apr 1;18(7):1966-78.

230. Xia Y, Wang M, Beraldi E, Cong M, Zoubeidi A, Gleave M, Peng L. A novel triazole nucleoside suppresses prostate cancer cell growth by inhibiting heat shock factor 1 and androgen receptor. Anti-Cancer Agents in Medicinal Chemistry (Formerly Current Medicinal Chemistry-Anti-Cancer Agents). 2015 Dec 1;15(10):1333-40.

231. Xiao H, Lis JT. Germline transformation used to define key features of heat-shock response elements. Science. 1988 Mar 4;239(4844):1139-42.

232. Xiao Z, Guo L, Zhang Y, Cui L, Dai Y, Lan Z, Zhang Q, Wang S, Liu W. Structural analysis of missense mutations occurring in the DNA-binding domain of HSF4 associated with congenital cataracts. Journal of Structural Biology: X. 2020 Jan 1;4:100015.

233. Xu J, Shi Q, Xu W, Zhou Q, Shi R, Ma Y, Chen D, Zhu L, Feng L, Cheng AS, Morrison H. Metabolic enzyme PDK3 forms a positive feedback loop with transcription factor HSF1 to drive chemoresistance. Theranostics. 2019;9(10):2999.

234. Xu Q, Hu Y, Kleindienst R, Wick G. Nitric oxide induces heat-shock protein 70 expression in vascular smooth muscle cells via activation of heat shock factor 1. The Journal of clinical investigation. 1997 Sep 1;100(5):1089-97.

235. Yallowitz A, Ghaleb A, Garcia L, Alexandrova EM, Marchenko N. Heat shock factor 1 confers resistance to lapatinib in ERBB2-positive breast cancer cells. Cell death & disease. 2018 May 24;9(6):621.

236. Yang T, Ren C, Lu C, Qiao P, Han X, Wang L, Wang D, Lv S, Sun Y, Yu Z. Phosphorylation of HSF1 by PIM2 induces PD-L1 expression and promotes tumor growth in breast cancer. Cancer research. 2019 Oct 15;79(20):5233-44.

237. Yang W, Cui M, Lee J, Gong W, Wang S, Fu J, Wu G, Yan K. Heat shock protein inhibitor, quercetin, as a novel adjuvant agent to improve radiofrequency ablation-induced tumor destruction and its molecular mechanism. Chinese journal of cancer research. 2016 Feb;28(1):19.

238. Yang X, Wang J, Liu S, Yan Q. HSF1 and Sp1 regulate FUT4 gene expression and cell proliferation in breast cancer cells. Journal of cellular biochemistry. 2014 Jan;115(1):168-78.

239. Yang Z, Klionsky DJ. Mammalian autophagy: core molecular machinery and signaling regulation. Current opinion in cell biology. 2010 Apr 1;22(2):124-31.

240. Yoon T, Kang GY, Han AR, Seo EK, Lee YS. 2, 4-Bis (4-hydroxybenzyl) phenol inhibits heat shock transcription factor 1 and sensitizes lung cancer cells to conventional anticancer modalities. Journal of natural products. 2014 May 23;77(5):1123-9.

241. Yoon YJ, Kim JA, Shin KD, Shin DS, Han YM, Lee YJ, Lee JS, Kwon BM, Han DC. KRIBB11 inhibits HSP70 synthesis through inhibition of heat shock factor 1 function by impairing the recruitment of positive transcription elongation factor b to the hsp70 promoter. Journal of Biological Chemistry. 2011 Jan 21;286(3):1737-47.

242. Yu Y, Hamza A, Zhang T, Gu M, Zou P, Newman B, Li Y, Gunatilaka AL, Zhan CG, Sun D. Withaferin A targets heat shock protein 90 in pancreatic cancer cells. Biochemical pharmacology. 2010 Feb 15;79(4):542-51.

243. Zaarur N, Gabai VL, Porco Jr JA, Calderwood S, Sherman MY. Targeting heat shock response to sensitize cancer cells to proteasome and Hsp90 inhibitors. Cancer research. 2006 Feb 1;66(3):1783-91.

244. Zaman M, Chaturvedi SK, Zaidi N, Qadeer A, Chandel TI, Nusrat S, Alam P, Khan RH. DNA induced aggregation of stem bromelain; a mechanistic insight. RSC advances. 2016;6(44):37591-9.

245. Zelin E, Freeman BC. Lysine deacetylases regulate the heat shock response including the age-associated impairment of HSF1. Journal of molecular biology. 2015 Apr 10;427(7):1644-54.

246. Zelin E, Zhang Y, Toogun OA, Zhong S, Freeman BC. The p23 molecular chaperone and GCN5 acetylase jointly modulate protein-DNA dynamics and open chromatin status. Molecular cell. 2012 Nov 9;48(3):459-70.

247. Zhai Z, Ren Y, Shu C, Chen D, Liu X, Liang Y, Li A, Zhou J. JAC1 targets YY1 mediated JWA/p38 MAPK signaling to inhibit proliferation and induce apoptosis in TNBC. Cell Death Discovery. 2022 Apr 5;8(1):169.

248. Zhang B, Au Q, Yoon IS, Tremblay MH, Yip G, Zhou Y, Barber JR, Ng SC. Identification of small-molecule HSF1 amplifiers by high content screening in protection of cells from stress induced injury. Biochemical and biophysical research communications. 2009 Dec 18;390(3):925-30.

249. Zhang D, Zhang B. Selective killing of cancer cells by small molecules targeting heat shock stress response. Biochemical and biophysical research communications. 2016 Sep 30;478(4):1509-14.

250. Zhang Y, Ahn YH, Benjamin IJ, Honda T, Hicks RJ, Calabrese V, Cole PA, Dinkova-Kostova AT. HSF1-dependent upregulation of Hsp70 by sulfhydryl-reactive inducers of the KEAP1/NRF2/ARE pathway. Chemistry & biology. 2011 Nov 23;18(11):1355-61.

251. Zhang Y, Dayalan Naidu S, Samarasinghe K, Van Hecke GC, Pheely A, Boronina TN, Cole RN, Benjamin IJ, Cole PA, Ahn YH, Dinkova-Kostova AT. Sulphoxythiocarbamates modify cysteine residues in HSP90 causing degradation of client proteins and inhibition of cancer cell proliferation. British journal of cancer. 2014 Jan;110(1):71-82.

252. Zhao R, Le K, Moghadasian MH, Shen GX. Regulatory role of NADPH oxidase in glycated LDL-induced upregulation of plasminogen activator inhibitor-1 and heat shock factor-1 in mouse embryo fibroblasts and diabetic mice. Free Radical Biology and Medicine. 2013 Aug 1;61:18-25.

253. Zhao R, Ma X, Shen GX. Transcriptional regulation of plasminogen activator inhibitor-1 in vascular endothelial cells induced by oxidized very low density lipoproteins. Molecular and cellular biochemistry. 2008 Oct;317:197-204.

254. Zhao R, Shen GX. Involvement of Heat Shock Factor-1 in Glycated LDL–Induced Upregulation of Plasminogen Activator Inhibitor-1 in Vascular Endothelial Cells. Diabetes. 2007 May 1;56(5):1436-44.

255. Zhao Y, Liu H, Liu Z, Ding Y, LeDoux SP, Wilson GL, Voellmy R, Lin Y, Lin W, Nahta R, Liu B. Overcoming trastuzumab resistance in breast cancer by targeting dysregulated glucose metabolism. Cancer research. 2011 Jul 1;71(13):4585-97.

256. Zhao YH, Zhou M, Liu H, Ding Y, Khong HT, Yu D, Fodstad O, Tan M. Upregulation of lactate dehydrogenase A by ErbB2 through heat shock factor 1 promotes breast cancer cell glycolysis and growth. Oncogene. 2009 Oct;28(42):3689-701.

257. Zheng X, Krakowiak J, Patel N, Beyzavi A, Ezike J, Khalil AS, Pincus D. Dynamic control of Hsf1 during heat shock by a chaperone switch and phosphorylation. elife. 2016 Nov 10;5:e18638.

258. Zhu BT, Conney AH. Functional role of estrogen metabolism in target cells: review and perspectives. Carcinogenesis. 1998 Jan 1;19(1):1-27.

259. Zingarelli B, Hake PW, O'Connor M, Denenberg A, Wong HR, Kong S, Aronow BJ. Differential regulation of activator protein-1 and heat shock factor-1 in myocardial ischemia and reperfusion injury: role of poly (ADP-ribose) polymerase-1. American Journal of Physiology-Heart and Circulatory Physiology. 2004 Apr;286(4):H1408-15.

260. Zou J, Guo Y, Guettouche T, Smith DF, Voellmy R. Repression of heat shock transcription factor HSF1 activation by HSP90 (HSP90 complex) that forms a stress-sensitive complex with HSF1. Cell. 1998 Aug 21;94(4):471-80.

SUMMARY

The stress-inducible transcription activator, heat shock factor 1 (HSF1), helps to maintain protein homeostasis in stress-exposed cells by upregulating the expression of proteins responsible for the refolding and/ or degradation of misfolded/aggregated proteins. This phenomenon is known as the cellular heat shock response (HSR) or proteotoxic stress response (PSR). In its activation pathway, HSF1 undergoes a monomer-to-trimer/ multimer transition, as well as several post-translational modifications before it engages with the DNA binding sequence, called the heat shock element (HSE) located in its target gene promoters to regulate their expression. The HSEs are inverted repeats of the 5'-nGAAn-3' sequence. In aged individuals and patients suffering from protein misfolding disorders, HSF1 activity is supposedly compromised. Forceful activation of HSF1 is, therefore, thought to be a promising strategy to ameliorate toxicity associated with protein misfolding and aggregation in Parkinson's, Alzheimer's, Huntington's, and similar diseases.

Numerous small molecule activators (having natural and synthetic origins) of HSF1 are reported in the literature. However, none of them boost the activity of HSF1 directly. HSF1 activation is achieved by these molecules through the functional inhibition of cellular Hsp90 or the proteasome, which are essential for normal cellular functions, thereby exerting toxic effects. In contrast, Azadiradione (AZD), a limonoid of MW 450.6 Da was isolated from the seeds of *Azadirachta indica* as a direct activator of HSF1. AZD is the only direct activator of HSF1 reported so far. This compound was shown to enhance the activity of HSF1 via direct interaction with the protein, without significantly compromising the activities of cellular Hsp90 and the proteasome. Notably, AZD does not cause oxidative stress, rather, it has been reported to serve as an antioxidant. It has already demonstrated promising results in fruit fly and mouse models of neurodegenerative diseases. In this study, we aimed to understand the molecular basis of the AZD-mediated activation of human HSF1.

We prepared various truncation derivatives of the human HSF1 protein by sequentially deleting stretches of amino acids (domains) from its C-terminus. A trimerization domain-deficient constitutively monomeric (CM) form of HSF1, a constitutively trimeric (CT) mutant form of HSF1, and the wild-type (WT) HSF1, were also procured. All these proteins were isolated from an overexpressing *E. coli* strain and purified by high-resolution gel filtration chromatography.

Various biophysical methods were employed to study how AZD modulates HSF1's binding to its recognition sequence, the heat shock element (HSE).

Our study has brought to light a unique mechanism of AZD-mediated HSF1 activation. We performed a fluorescence polarization (FP) assay and dynamic light scattering (DLS) to reveal that AZD increases the binding affinity of WT monomeric HSF1 for the HSE sequence (HSE-DNA) by inducing its oligomerization (possibly trimerization). AZD mediates this oligomerization by interacting with the DNA Binding Domain of HSF1 (HSF1-DBD). Notably, the DBD appears to be the predominant AZD-binding site on HSF1; HSF1-DBD undergoes oligomerization and binds HSE with greater affinity in the presence of AZD. The trimerization/ oligomerization domain of HSF1, known to be indispensable for the protein's stress-induced trimerization/oligomerization and DNA binding, appears to be non-essential in AZD-induced multimerization and HSE-DNA recognition. Interestingly, AZD decreases the DNA binding affinity of both the WT trimeric and constitutively trimeric forms of HSF1. HSF1 with its C-terminal Transactivation Domain deleted (HSF1-ΔTAD), binds HSE with reduced affinity upon AZD exposure. 1-Anilinonaphthalene-8-sulfonic acid (ANS) and Thioflavin T (ThT) fluorescence assays reveal that the HSF1-CT and HSF1-ΔTAD form aggregates upon exposure to AZD, explaining the inhibitory effect of AZD on their binding to HSE. ANS and ThT are routinely used as extrinsic fluorescent probes for detecting the surface-exposed hydrophobic patches and cross-β sheet (amyloid-like) conformation in proteins, respectively. HSF1-WT trimer, however, does not form aggregates upon AZD exposure, as revealed by ANS fluorescence assay. These results reveal the potential of AZD as an anticancer agent, as cancer cells heavily depend on HSF1 for their survival, proliferation, invasion, and metastasis, and supposedly carry HSF1 in the active trimeric/ oligomeric state. AZD appears to bind the HSE sequence specifically and reversibly in the absence of protein. AZD also interacts with the mutant HSE [mHSE] sequence with similar affinity. Our results imply that, apart from the AZD-induced oligomerization of monomeric HSF1, conformational alterations in the HSE-DNA and its mutant form caused by AZD also play a role in facilitating the binding of monomeric HSF1 with these sequences. We also analyzed our results in light of published X-ray crystal structures of HSF1-DBD in complex with HSE to understand possible interaction site(s) of AZD on the HSF1-HSE complex. In this structure, HSF1-DBD subunits interact with each other through their winged helix-turn-helix folds (WHTHF). Our results are consistent with the idea that AZD facilitates this WHTHF-mediated intermolecular interaction either directly or indirectly, enhancing the binding affinity of HSF1 with HSE.

PUBLICATION(S)

1. De S, Paul S, Manna A, Majumder C, Pal K, Casarcia N, Mondal A, Banerjee S, Nelson VK, Ghosh S, Hazra J. Phenolic phytochemicals for prevention and treatment of colorectal cancer: A critical evaluation of in vivo studies. Cancers. 2023 Feb 3;15(3):993.